DOPAMINE IN THE RAT NUCLEUS ACCUMBENS CORE: PATCHWORK OF DOMAINS AND PREFERENTIAL EFFECTS OF NOMIFENSINE

by

Zhan Shu

B.S. Chemistry, Wuhan University, 2009

Submitted to the Graduate Faculty of the

Kenneth P. Dietrich School of Arts and Sciences in partial fulfillment

of the requirements for the degree of

Doctor of Philosophy

University of Pittsburgh

2014

UNIVERSITY OF PITTSBURGH

KENNETH P. DIETRICH SCHOOL OF ARTS AND SCIENCES

This dissertation is presented

by

Zhan Shu

It was defended on

August 13th, 2014

and approved by

Shigeru Amemiya, Associate Professor, Department of Chemistry

Stephen G. Weber, Professor, Department of Chemistry

Michael J. Zigmond, Professor, Department of Neurology

Dissertation Advisor: Adrian C. Michael, Professor, Department of Chemistry

DOPAMINE IN THE RAT NUCLEUS ACCUMBENS CORE: PATCHWORK OF DOMAINS AND PREFERENTIAL EFFECTS OF NOMIFENSINE

Zhan Shu, PhD

University of Pittsburgh, 2014

Dopamine (DA) is critically important in numerous aspects of normal central nervous system (CNS) function and the etiology of several CNS disorders, including Parkinson's disease, substance abuse, and attention deficit hyperactive disorder. The diversity of DA function and dysfunction means an understanding of the mechanisms that control extracellular DA concentrations and their spatiotemporal dynamics is highly significant. Such mechanisms have been extensively studied in the subregions of the striatum, e.g. the dorsal striatum and nucleus accumbens that play central roles in motor control and reword-addiction.

To measure DA concentration changes in extracellular space, two techniques have been heavily used in the *in vivo* studies: microdialysis and electrochemistry. Microdialysis sampling of the brain is straightforward and has numerous applications. But implanting microdialysis probe into brain tissue causes a penetration injury. Thus, the probe samples injured tissue. In Chapter I, we used dexamethasone, a potent anti-inflammatory and immunosuppressant drug, to mitigate the effect of the penetration injury and examined its effects using fluorescence imaging and no-net-flux measurement. We conclude that dexamethasone is highly effective at suppressing gliosis and ischemia but is limited in its neuroprotective activity.

In vivo electrochemistry, using carbon fiber microelectrodes with single-digit micrometer diameter and 100-400 micrometer in detecting length coupled with fast-scan cyclic voltammetry, offers high spatial and temporal resolution with minimal tissue damage. Taking these

advantages, our group has demonstrated that DA in the rat dorsal striatum is organized as a patchwork of domains that show distinct DA kinetics. In Chapter II, we demonstrated that a patchwork of domains exists in the rat nucleus accumbens core (NAcc), but shows substantial differences between the NAcc domains and those of the dorsal striatum. There are no signs of short-term plasticity during multiple consecutive stimuli nor a domain-dependent autoinhibitory tone in NAcc. In Chapter III, we examine the domain-dependent actions of nomifensine, a competitive DA transport inhibitor, in NAcc and demonstrated that it preferentially enhance evoked DA overflow in slow domains compared with fast domains. We quantified the apparent K_M of DA clearance and concluded that nomifensine preferentially increases the apparent K_M in NAcc compared with dorsal striatum.

TABLE OF CONTENTS

LIST OF TABLES

LIST OF FIGURES

PREFACE

First, I would like to thank my research advisor Dr. Adrian Michael. He is a good teacher in the classroom, a good mentor in the lab and a good friend in everyday life. He taught me the fundamentals of Electrochemistry, showed me how to run microdialysis and guided me into the amazing dopamine world, and most importantly he set an example of balanced work and life. I have learned a lot from him, not only in science and research, but also in sailing and skiing.

Next, I would like to thank my committee members: Dr. Steve Weber, Dr. Shigeru Amemiya, and Dr. Michael Zigmond. Dr. Weber gave me a lot of help on my first project – a microdialysis project involves two graduate students, two post-docs and tow PIs. Dr. Amemiya has advised my original proposal. Dr. Zigmond has supported my last project collaborated with his lab for over a year.

I would like to thank all the Michal lab members as well. Former members Keith Moquin and Yuexiang (Mary) Wang taught me how to make electrodes and how to perform animal surgeries. Andrea Jaquins-Gerstl showed me how to perfuse and slice brains. Seth Walters, Katy Nesbitt and Erika Varner provided a lot of thought-provoking discussions. And the honorary member Dr. Kat Salerno brought lots of neuroscience knowledge and loud laugh to our lab. Most of all, I'd like to thank Mitch Taylor, my buddy in the lab. We teamed together even before we both joined Michael lab and worked together all the way to our graduation.

Last but not least, I must thank my family. My parents gave me huge amount of support emotionally and financially. They let me – their only child, go abroad to pursue my dreams five years ago, but their encouragement and love just followed me across the Pacific from Wuhan to Pittsburgh. Finally, I want to say thank you to Keling, my beloved wife and Hope, my adorable daughter. Keling, without you I can never accomplish this. You maintain a sweet home for me and take care of Hope all by yourself almost everyday. Hope, you just bring so much fun and laugh to my life and make me a much better person too. This is for both of you.

INTRODUCTION

Dopamine (DA) in central neuronal systems (CNS) plays an important role in many of body's vital functions, such as planning and modulation of pathways, reward, mood regulation and attention (Schultz 2007). And dysfunction in dopaminergic systems has been found involving in many pathologies, including Parkinson's disease, schizophrenia, attention deficit hyperactivity disorder and substance abuse (Grace 1991, Swanson 2000, Lotharius & Brundin 2002). However, the mechanisms of dopamine signaling in CNS are not well defined in both functions and dysfunctions. Take attention deficit hyperactivity disorder (ADHD) for instance. ADHD is the most commonly studied and diagnosed psychiatric disorder in children, which has three subtypes: predominantly hyperactive-impulsive, predominantly inattentive and combined hyperactive-impulsive and inattentive (Porcerelli et al. 2011). According to the current dopamine models, hyperactive is associated with elevated dopamine levels (Grace 2000). However, in practice, ADHD symptoms in all subtypes can be alleviated with the treatment of methylphenidate, a reuptake inhibitor of dopamine transporter, which increases dopamine levels (Wender et al. 2011). So, how did further increasing dopamine level in patients with predominantly hyperactive-impulsive subtype relieve the symptoms, if high dopamine level is the cause? The paradox here is a matter of longstanding interest.

Dopamine neurological system is a network of neurons that communicate through the released dopamine molecules in extracellular space as neurotransmitters. In central neuronal

systems, cell bodies of dopamine neurons are mainly located in two areas: substantial nigra and ventral tegmental area. Their axons are crossing the medial forebrain bundle and project their terminals in striatum and nucleus accumbens at high density. Dopamine molecules packed in vesicles inside pre-synaptic terminals are released into the synaptic cleft, which is approximately 300 nm in length and 15 nm in width, and quickly diffused into extracellular space (Garris & Wightman 1994). The release has been further regulated by two families of dopamine autoreceptors, D1-like and D2-like, which primarily located outside cleft (Garris & Wightman 1994, Sesack et al. 1994). In extracellular space, released dopamine molecules can activates pre-synaptic receptors until removed back into terminals by the dopamine transporters (DAT). Thus, the spatiotemporal dynamics of DA's extracellular concentration, and therefore the extent and duration of DA receptor stimulation, are intricately determined by the kinetics of DA release and clearance as well as the mass transport of DA through the extracellular space (Wightman et al., 1988; Garris et al., 1994; Cragg & Rice, 2004; Taylor et al., 2012; Taylor et al., 2013).

In order to measure dopamine concentration changes in extracellular space, two techniques have been heavily used in the *in vivo* studies: microdialysis and electrochemistry. Microdialysis is a widely and frequently used sampling technique (Chaurasia et al. 2007). Small molecules such as dopamine and serotonin are recovered from extracellular space in central neuron system by diffusing into a perfusate through a semi-permeable membrane on a microdialysis probe. Samples of the dialysate are usually analyzed by HPLC or capillary electrophoresis coupled with a variety of detection methods. The benefit of microdialysis is that dialysate is carrying the analyte out of the living system so it can be easily analyzed with separation and detection steps that provide extremely high selectivity. For *in vivo* electrochemistry, on the order hand, analyte separation and detection processes are self-

contained and *in situ*, and chemical identification is relied on voltammograms (Wightman et al. 1988b). Although in vivo electrochemical technique is limited in chemical selectivity comparing to microdialysis, it can provide information that are not presently accessible by microdialysis or any other measurements, as it offers high spatial and temporal resolution (Borland & Michael 2007). Carbon fibers with single-digit micrometer diameter are constructed as chemical microsensors with 100 to 400 μm in detecting length, which are more than then thousand times smaller than typical microdialysis probes in volume. One of the advantages of their small dimensions is that minimal damage can be achieved when implanting microsensors into living brain tissues, which ensures the information collected are not biased by presence of the sensor (Peters et al. 2004, Jaquins-Gerstl & Michael 2009). Another advantage is that minimal damage will allow the carbon fiber electrode to be placed within micrometer distance of normal neuronal terminals (Venton et al. 2003, Peters et al. 2004, Taylor et al. 2012). So it can reveal the highly localized activities such as heterogeneity of evoked dopamine release (Garris et al. 1994b, Moquin & Michael 2009, Taylor et al. 2012) and evaluate kinetics of dopamine transporter (Garris et al. 1994a, Wu et al. 2001, Wu et al. 2002, Michael et al. 2005, Shu et al. 2013, Shu et al. 2014, Walters et al. 2014) suffering little diffusional distortion. The high temporal resolution can also benefit electrochemical recordings on detecting dopamine concentration change within subsecond time frame: monitoring dopamine release and clearance triggered by brief electrical stimulation such as 12 pulses stimulus or even recording the non-evoked dopamine transients in the brain of freely moving animals (Robinson et al. 2002, Robinson & Wightman 2004, Wightman et al. 2007). None of them above are visible in the microdialysis because of the temporal blurring associated with diffusion across the dialysis membrane and spatial averaging associated with large sampling area. Thus, it is clear that high spatial and temporal resolution of

electrochemical techniques can provide unique information about the characteristics of dopamine systems in the living brain tissue.

In Chapter I, we examined and mitigated the penetration injury associated with brain microdialysis. Microdialysis sampling of the brain is an analytical technique with numerous applications in neuroscience and the neurointensive care of brain-injured human patients. Even so, implanting microdialysis probes into brain tissue causes a penetration injury that triggers gliosis (the activation and proliferation of glial cells) and ischemia (the interruption of blood flow). Thus, the probe samples injured tissue. Mitigating the effects of the penetration injury might refine the technique. The synthetic glucocorticoid, dexamethasone, is a potent anti-inflammatory and immunosuppressant substance. We performed microdialysis in the rat brain for 5 days, with and without dexamethasone in the perfusion fluid (10 μM for the first 24 hrs and 2 μM thereafter). On the 1st and 4th day of the perfusion, we performed dopamine no-net-flux measurements. On the 5th day, we sectioned and stained the brain tissue and examined it by fluorescence microscopy. Although dexamethasone profoundly inhibited gliosis and ischemia around the probe tracks it had only modest effects on dopamine no-net-flux results. These findings show that dexamethasone is highly effective at suppressing gliosis and ischemia but is limited in its neuroprotective activity.

In Chapter II, we addressed the hypothesis that a domain patchwork might also exist in the nucleus accumbens core (NAcc), a DA terminal field involved deeply in reward processing and the mechanisms underlying substance abuse. The dopamine (DA) terminal field in rat dorsal striatum is organized as a patchwork of domains that exhibit distinct DA kinetics. The rate and short-term plasticity of evoked DA release, the rate of DA clearance, and the actions of several dopaminergic drugs are all domain-dependent. The patchwork arises in part from local

variations in DA's basal extracellular concentration, which establishes an autoinhibitory tone in slow but not fast domains. DA recordings in the NAcc by fast-scan voltammetry during electrical stimulation of the medial forebrain bundle confirm that the NAcc contains a patchwork of fast and slow domains exhibiting significantly different rates of evoked DA release and DA clearance. Moreover, the NAcc domains are substantially different from those in the dorsal striatum. There are no signs in the NAcc of short-term plasticity of DA release during multiple consecutive stimuli and no signs of a domain-dependent autoinhibitory tone. Thus, the NAcc domains are distinct from each other and from the domains of the dorsal striatum.

In Chapter III, we used fast-scan cyclic voltammetry recordings of electrically evoked DA overflow to test the hypothesis that nomifensine might exhibit domain-dependent actions within the NAcc, as we previously found to be the case within the DS. Within the NAcc, nomifensine preferentially enhanced evoked dopamine overflow in the slow compared to the fast domains. To seek a kinetic explanation for nomifensine's selective actions, we quantified the apparent K_M of DA clearance by numerically evaluating the derivative of the descending phase of the DA signal after the end of the stimulus. For comparison, we likewise quantified apparent K_M in the domains of the DS. As expected because it is a competitive inhibitor, nomifensine significantly increased the apparent K_M in both the fast and slow domains of both the NAcc and DS. However, our analysis also leads to the novel finding that nomifensine preferentially increases the apparent K_M in the NAcc compared to the DS: apparent K_M increased by ~500% in the NAcc and ~200% in the DS.

CHAPTER I. EFFECT OF DEXAMETHASONE ON GLIOSIS, ISCHEMIA, AND DOPAMINE EXTRACTION DURING MICRODIALYSIS SAMPLING IN BRAIN TISSUE

Adapted with revision from Andrea Jaquins-Gerstl, Zhan Shu, Jing Zhang, Yansheng Liu, Stephen G. Weber, and Adrian C. Michael, (2011) *Analytical Chemistry*, 83, 7662-7667.

Zhan Shu's contribution to this published article is the dopamine no-net-flux microdialysis measurement, mainly presented as Figure I.8 and Table 1 in this chapter.

A. INTRODUCTION

The significance of brain microdialysis as an analytical technique in neuroscience is well-established and its application as a tool for the neurointensive care of brain-injured human patients continues to be explored (Dreier et al., 2000; Meixensberger et al., 2001; Sakowitz et al., 2001; Bosche et al., 2003; Dreier et al., 2006; Sakowitz et al., 2007; Fabricius et al., 2008; Schlenk et al., 2008; Nordstrom, 2009; Feuerstein. et al., 2010). The power of microdialysis is attributable to its several beneficial attributes: the dialysate samples contain a plethora of interesting and important small molecules (Westerink & Cremers, 2007; Perry et al., 2009) (for an extensive review see Westerink and Cremers, 2007), the technique is relatively simple to perform and compatible with the constraints of intensive care, the probes are commercially

available or easily built in-house, and the dialysis process prepares the samples for direct, often times on-line, analysis by a broad array of techniques, such as HLPC, CE, and MS. Microdialysis has contributed significantly to the understanding of normal brain function, the pathology of brain disorders and injuries, and the actions of neuroactive drugs, both therapeutic and illicit (Benveniste & Diemer, 1987; Benveniste et al., 1989; Bradberry et al., 1993; Bradberry et al., 2000; Rittenhouse & Pollack, 2000; Berger et al., 2002; Sarrafzadeh et al., 2002; Parkin et al., 2005; Sakowitz & Unterberg, 2006; Hashemi et al., 2009).

Although microdialysis provides valuable insights into brain chemistry, implanting the probes causes a penetration injury to the brain tissue (Clapp-Lilly et al., 1999; Zhou et al., 2002; Mitala et al., 2008; Hascup et al., 2009; Jaquins-Gerstl & Michael, 2009) that triggers gliosis (the activation and proliferation of glial cells) (Zhou et al., 2002; Mitala et al., 2008; Stroncek & Reichert, 2008; Jaquins-Gerstl & Michael, 2009) and ischemia (interruption of blood flow). Consequently, the tissue sampled by the probe is perturbed from its normal state (Stroncek & Reichert, 2008). Understanding, and possibly mitigating, the effects of the penetration injury could be a path to enhancing the technique, refining its accuracy and precision, extending the viable microdialysis sampling time window, and enabling deeper insights into the neurochemical aspects of brain function. Given that many neurological disorders, while treatable, are neither preventable nor curable and that the therapies for brain trauma remain limited, enhancing the chemical information output from brain microdialysis procedures stands to be highly significant.

In the present study, we examined the effect of dexamethasone on the probe-induced penetration injury of the rat brain. Dexamethasone is a synthetic, highly potent glucocorticoid with anti-inflammatory and immunosuppressant activity. Several studies have demonstrated that gliosis at brain implants is inhibited by dexamethasone-releasing coatings (Shain et al., 2003;

Spataro et al., 2005; Zhong & Bellamkonda, 2007). Furthermore, Stenken's group recently reported that dexamethasone inhibits the immune response to subcutaneous microdialysis probes (Mou et al., 2011). We performed microdialysis in the rat brain for 5 days with and without dexamethasone in the perfusion fluid. On the 1st and 4th day of the perfusion we performed dopamine no-net-flux measurements and at the end of the perfusion we sectioned, stained, and examined the brain tissue by fluorescence microscopy to assess gliosis and ischemia.

B. MATERIALS AND METHODS

1. Reagents

All reagents were used as-received from the indicated supplier. All solutions were prepared in ultrapure water (Nanopure, Barnstead Inc, Dubuque, IA) and filtered with Iso-Disc TM filters, (N-25-2 Nylon 25mm x 0.2μm, Supelco, Bellefonte; PA). Bovine serum albumin (BSA), paraformaldehyde, polyvinyl alcohol, glycerol, 1,4-diazabicyclo [2.2.2] octane (DABCO), Triton-X 100, dopamine (DA) and ascorbic acid were from Sigma (St. Louis; MO); 2-methybutane was from Alfa Aesar (Ward Hill, MA); fluorescent beads were from Molecular Probes (0.1 μm diameter, FluoSpheres® carboxylate-modified polystyrene microspheres suspended (2% solids) in water with 2 mM sodium azide; Eugene, OR); primary antibody for glial fibrillary acidic protein (GFAP) in 0.5% BSA was from BD Biosciences Pharmingen (San Diego, CA); secondary antibody (goat anti-mouse IgG, CY3 in 0.5% BSA) was from Jackson Immunoresearch (West Grove, PA); isoflurane was from Halocarbon Products Corporation (North Augusta, SC); dexamethasone sodium phosphate (9-fluoro-11β,17,21-trihydroxy-16α-

methylpregna-1,4-diene-3,20-dione-21-(dihydrogen phosphate) disodium salt, 20mg/5ml, American Regent Incorporated, Shirley, NY) was purchased from the University of Pittsburgh Presbyterian Hospital Pharmacy. All other salts and reagents were from Fisher Scientific (Pittsburgh, PA). Phosphate buffered saline (PBS) contained 155 mM NaCl and 100 mM phosphate adjusted to pH 7.4. Artificial cerebrospinal fluid (aCSF) contained 144 mM Na^{+}, 1.2 mM Ca^{2+}, 2.7 mM K^{+}, 152 mM Cl^{-}, 1.0 mM Mg^{2+}, and 2.0 M PO_4^{3-} and was adjusted to pH 7.4.

2. Animals and surgical procedures

All procedures involving animals were approved by the Institutional Animal Care and Use Committee of the University of Pittsburgh. Male Sprague-Dawley rats (Hilltop; Scottsdale, PA) were anesthetized with isoflurane and wrapped in a 37 °C homoeothermic blanket (EKEG Electronics; Vancouver, BC, Canada) during an aseptic stereotaxic surgical procedure to position a guide cannula (MD-2251, Bioanalytical Systems, Inc. (BASi), West Lafayette, IN) over the striatum. The guide cannula was anchored in place with bone screws and acrylic cement and animals were given four days for post-operative recovery before experiments continued. All animals regained or exceeded their pre-surgical body weight by the end of the post-operative recovery period.

3. Microdialysis procedures

Prior to use, microdialysis probes (BASi MD-2204) were sterilized with ethylene oxide and flushed for 1 hr with aCSF. The probes were connected via FEP tubing (MF-5164, BASi) to a 1.0 ml gas-tight syringe (Hamilton). Rats were re-anesthetized briefly with isoflurane and

returned to the stereotax while the stereotaxic carrier was used to slowly (~30 min) lower the probes through the guide cannula and into the striatum. The probes were perfused with aCSF at a flow rate of 0.610 µL/min for 5 days by means of a syringe pump (Harvard Apparatus). In one group of rats, the probes were perfused with plain aCSF. In a second group of rats, the aCSF contained dexamethasone. The dexamethasone concentration was 10 µM for the first 24 hrs of the perfusion and 2 µM for the remainder of the experiment: preliminary experiments showed that continued perfusion with 10-µM dexamethasone profoundly agitated the rats causing them to damage the probe or connecting tubing and, in one instance, injuring themselves. The biological half-life of dexamethasone is 36-54 hrs (Marcus HJ, 2010), so it is likely that the continuous perfusion led to a cumulative dosing effect.

4. HPLC analysis

The microdialysis samples were analyzed by capillary HPLC coupled to a highly sensitive electrochemical detector. The mobile phase was delivered with a NanoLC Ultra pump (Eksigent Technologies, Dublin, CA) at 2 µL/min without the use of a splitter. The sample injection valve (VICI Valco Instruments, Houston, TX) had a 500-nL fused silica capillary sample loop. The fused silica capillary columns (5.5-6.5 cm long, 100 µm i.d., and 365 µm o.d.) were packed in-house with Waters 2.6 µm XTerra C18 MS stationary phase (Waters, Milford MA) by the slurry method. Mobile phases were prepared by mixing acetonitrile (4%) with aqueous buffer (96%) containing 100 mM sodium acetate, 0.15 mM disodium EDTA, and 18 mM sodium octyl sulfate adjusted to pH 4 with acetic acid. The mobile phase was passed through a 0.20 µm Nylon filter prior to use (Fisher Scientific, Pittsburgh, PA). A short length of 25 µm i.d. fused silica capillary acted as a connecter between the column and a radial-flow electrochemical detector with a BASi

radial style auxiliary electrode, a thin (13 μm) Teflon spacer and a lab-made glassy carbon working electrode block. A BASi Epsilon potentiostat controlled the detection potential at +0.7 V vs. Ag/AgCl (3 M NaCl). This system separated dopamine from other electroactive species in less than 3 minutes (Figure I.1). Detection limit is 1.0 nM (three times signal to noise) and quantification limit is 3.2 nM (ten times signal to noise). Calibration curves were established on the same day as analysis with freshly prepared standard solutions (Figure I.1, inset).

5. Dopamine extraction curves

Dopamine extraction curves were obtained by perfusing the probes with 0, 100, 250, or 1000 nM dopamine and 50 μM ascorbate as a preservative. This range of dopamine concentrations is wider than typically used: most studies of dopamine extraction are confined to the 0-200 nM range (Smith & Justice, 1994; Bungay et al., 2007), although serotonin and norepinephrine have been studied over the 0-400 nM range (Cosford et al., 1996). The selection of a wider concentration range here was based on preliminary results that indicated the non-linear character of the dopamine extraction curves obtained in the presence of dexamethasone (see Results and Discussion). The wider concentration range allowed a more thorough investigation of the nonlinear character of the extraction curves. After changing the composition of the perfusion fluid, probes were perfused for 1 hr, after which a 1 hr sample was collected into a glass microvial containing 4 μL of 0.5 M acetic acid (the acetic acid acidified the samples and protected the dopamine from air-oxidation during the 1-hr collection). Samples were stored on dry ice and analyzed in triplicate by HPLC as soon as possible after sample collection, usually on the same day as collection. The results were used to construct dopamine extraction curves, as

explained in the following paper. The extraction curves were analyzed by linear or quadratic regression with OriginPro 7.5 (OriginLabs, Northampton, MA).

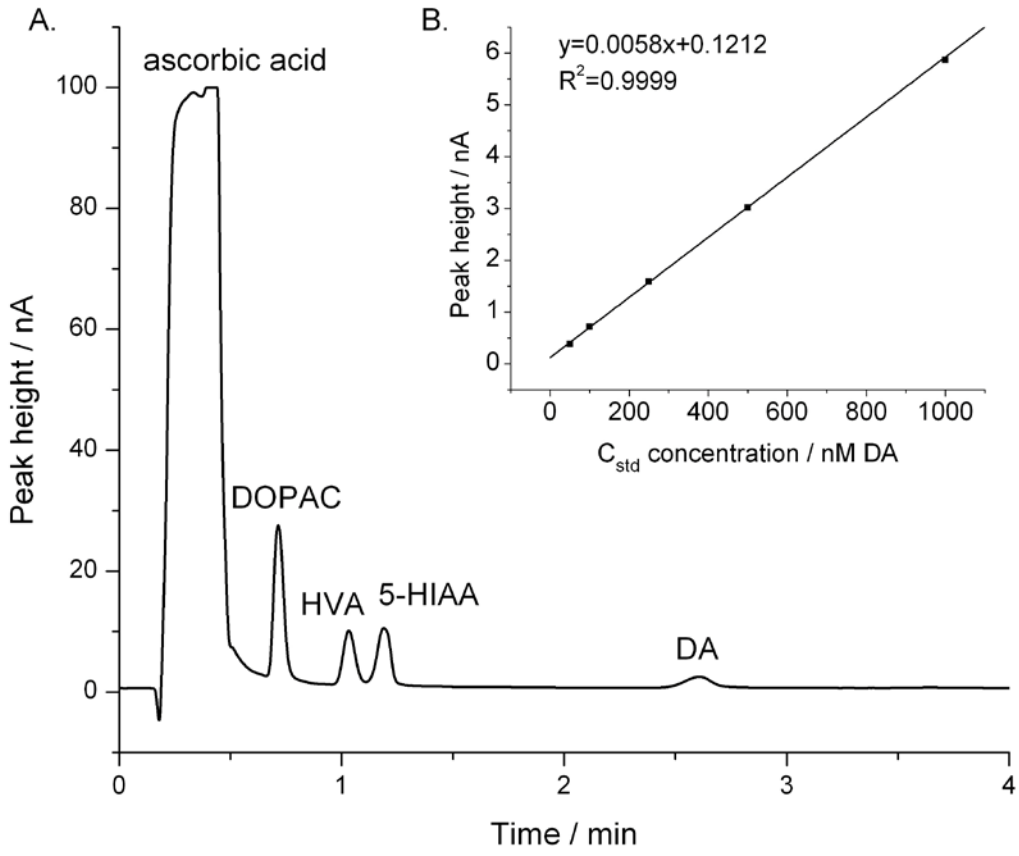

Figure I.1 A) A typical chromatogram of a brain dialysate sample obtained by capillary HPLC coupled to a radial-flow electrochemical detector with a thin (13 µm) Teflon spacer. This sample was obtained 1 day after probe implantation: the probe was perfused with dexamethasone and dopamine (1000 nM). B) A typical calibration curve for dopamine.

6. Tissue fixation and processing

After 5 days of continuous microdialysis, rats underwent transcardial perfusion with 160 ml PBS, 160 ml of 4% paraformaldehyde in PBS, and 50 ml of a 0.1% suspension of fluorescent beads (0.1 μm diameter) in PBS. The brain was submerged in 4% paraformaldehyde for 2 hours and then in 30% sucrose overnight. The brain was frozen by dipping in liquid nitrogen-cooled 2-methylbutane and stored at -80°C until sliced horizontally in a cryostat into 30-μm thick sections. The sections were mounted onto glass slides and stored at -20°C until further use.

7. Immunofluorescence protocol and fluorescence microscopy

Standard protocols were used to label the thin tissue sections with antibodies for glial fibrillary acidic protein, GFAP, a well-known marker for astocytes, one type of glial cell involved in gliosis. Sections were also treated with DAPI to aide in the visualization of neuronal and glial nuclei. Fluorescence microscopy (Olympus BX61, Olympus; Melville, NY) was performed with a 10X or 20X objective and appropriate filter sets (Chroma Technology; Rockingham, VT) for visualization of the beads, GFAP antibody, and DAPI-labeled nuclei. The images were analyzed with the Metamorph/Fluor 7.1 software package (Universal Imaging Corporation; Molecular Devices) and quantified with Metamorph and OriginPro.

C. RESULTS AND DISCUSSION

1. Microdialysis probes induce gliosis

GFAP immunofluorescence reveals profound gliosis at the tracks of microdialysis probes after 5-day perfusions in the rat brain (Figure I.2). The GFAP image from the non-implanted brain hemisphere (Figure I.2A) resembles that from non-implanted rats (Supplementary Figure I.9). Glia surrounding the probe tracks exhibit enlarged cell bodies and thickened and elongated processes (Figure I.2B). The images in Figure I.1 extend our previous report that gliosis is evident after 24-hr perfusions (Hascup et al., 2009). These longer perfusions are relevant to the neurointensive care applications of microdialysis (Fabricius et al., 2008; Feuerstein et al., 2010).

2. Dexamethasone inhibits gliosis

After 5-day perfusions without dexamethasone microdialysis probes are fully engulfed by a glial barrier (Figure I.3). The glial barriers were continuous around the entire circumference of the tracks, which maintained their symmetrical shape even when the probes were withdrawn to section the tissue (Figure I.3B). The rigidity of the glial barrier is attributable to the proteoglycan secretions of activated glia (Laabs et al., 2007). Dexamethasone inhibited the gliosis resulting in a residual, discontinuous, non-rigid glial barrier (Figure I.3C). Dexamethasone-perfused tracks showed more GFAP labeling than non-implanted tissues (Figure I.3A) but less than tracks perfused without dexamethasone (Figure I.3B). After perfusion with dexamethasone, the tracks did not maintain their open circular shape during tissue processing, so they appear distorted and non-symmetric in the images.

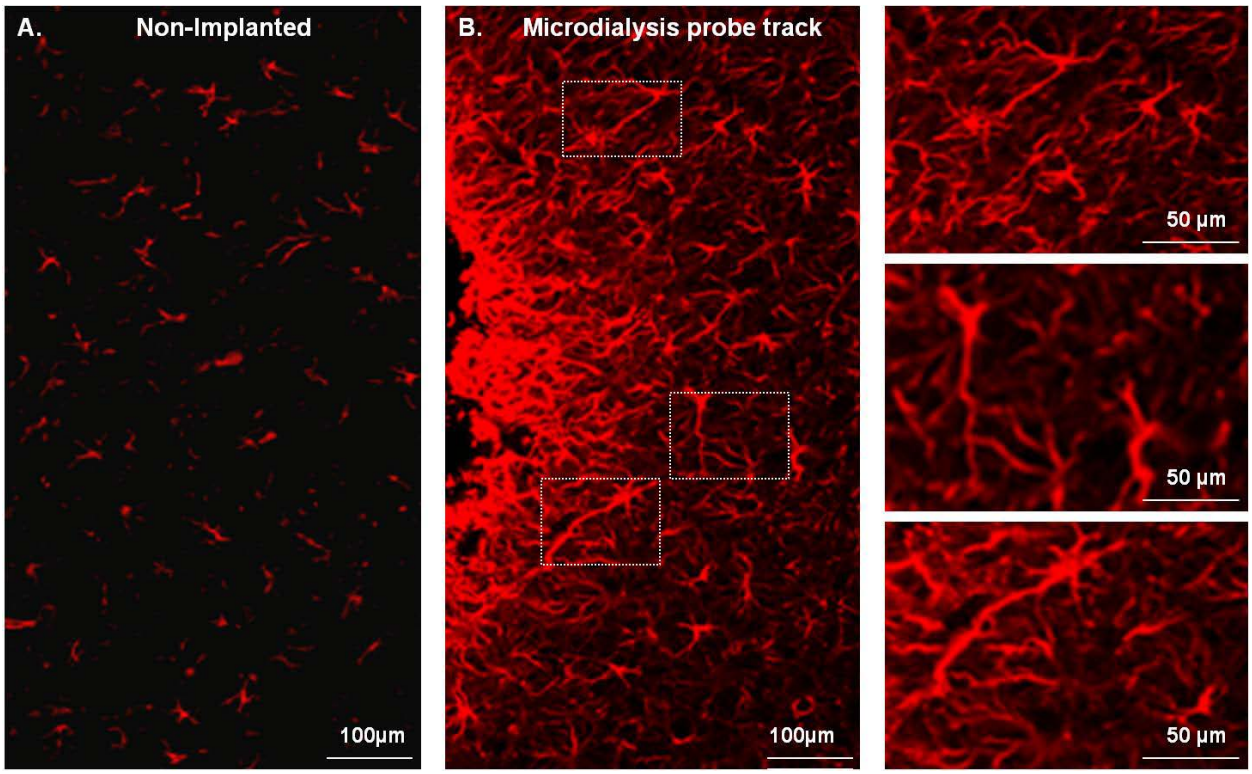

Figure I.2 The effect of a microdialysis probe on striatal glial cells labeled with GFAP antibody. A) Striatal tissue from a non-implanted brain hemisphere (contralateral to the probe). B) Striatal tissue next to a microdialysis probe track: the edge of the track is on the left side of the image. The right-hand column shows enlargements of the white boxes in panel B.

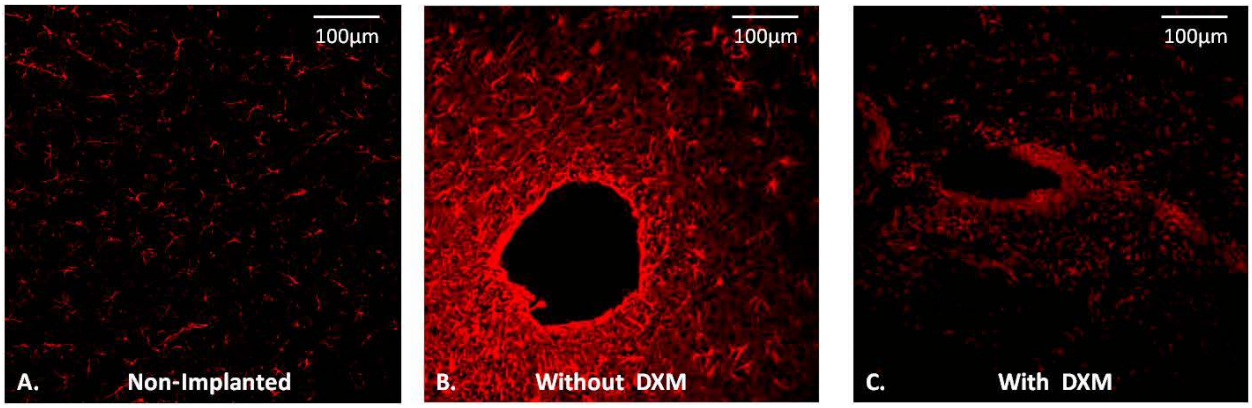

Figure I.3 Retrodialysis of dexamethasone inhibits gliosis. A) GFAP image of striatal tissue from a non-implanted hemisphere contralateral to a microdialysis probe. B) GFAP image of a glial barrier formed after 5 days of microdialysis without dexamethasone. C) GFAP image of a probe track after 5 days of retrodialysis of dexamethasone.

3. Dexamethasone prevents ischemia

5-day perfusions without dexamethasone caused profound ischemia, as evidenced by a near-total absence of bead-labeled blood vessels near the probe tracks (Figure I.4, right panel). However, after 5-day perfusions with dexamethasone bead-laden vessels near the tracks appear essentially normal (Figure I.4, left panel). Thus, dexamethasone, in addition to inhibiting gliosis, also prevented ischemia at the probe tracks.

4. Objective analysis of GFAP images

Using Metamorph, we converted 9 images (3 non-implanted, 3 without dexamethasone, and 3 with dexamethasone) to color-coded surface intensity plots (see Supplementary Figure I.10) and then to binned intensity histograms (Figure I.5). In control images (blue, Figure I.5), the majority of pixels are in the lowest intensity bin (0-43) because GFAP labeling is sparse in these tissues. Perfusion without dexamethasone decreases the number pixels in the lowest intensity bin (0-43) and increases the number of pixels in all higher intensity bins (44-255), reflecting the increased GFAP labeling in these tissues (red, Figure I.5). Dexamethasone returned the number of pixels in the higher intensity bins (>129) to control levels and increased the number of pixels in the low intensity bins (<128), providing a quantitative measure of the inhibition of gliosis by perfusion with dexamethasone.

We also used Metamorph to construct line-scan intensity profiles of the GFAP images (Figure I.6). The lines were arranged like “spokes” surrounding a “hub” (Figure I.6B) centered on the probe track (in non-implanted control tissue, the hub was centered within the striatum). The line-scans from non-implanted tissues (blue, Figure I.6C) exhibit only minor variations in

intensity with distance from the hub. The line-scans from probe tracks (red and green, Figure I.6C) show a region of low intensity near the center of the track where there is no GFAP labeling: the size of this region is affected by the asymmetry of the tracks (see Figure I.3). The line-scans from tissues perfused with (green) and without (red) dexamethasone show the profiles of the respective glial barriers. Dexamethasone substantially diminished the height and width of the glial barrier profile.

5. Objective analysis of blood vessel images

We also used Metamorph software to compare the number of fluorescent pixels in the blood vessel images from implanted and non-implanted tissues. The images were centered on the striatum (non-implanted controls) or the probe tracks (implanted tissues). The results, normalized to the average pixel count from six non-implanted controls, show that in tissues from rats perfused for 5 days without dexamethasone, the number of fluorescent pixels was reduced to 4.4% (red, Figure I.7), reflecting profound probe-induced ischemia. In tissues from rats perfused for 5 days with dexamethasone, the number of fluorescent pixels was reduced to 42.8% (green, Figure I.7), mainly because the images contained the probe track where blood vessels are completely absent. Thus, Figure I.7 confirms quantitatively that dexamethasone inhibited probe-induced ischemia.

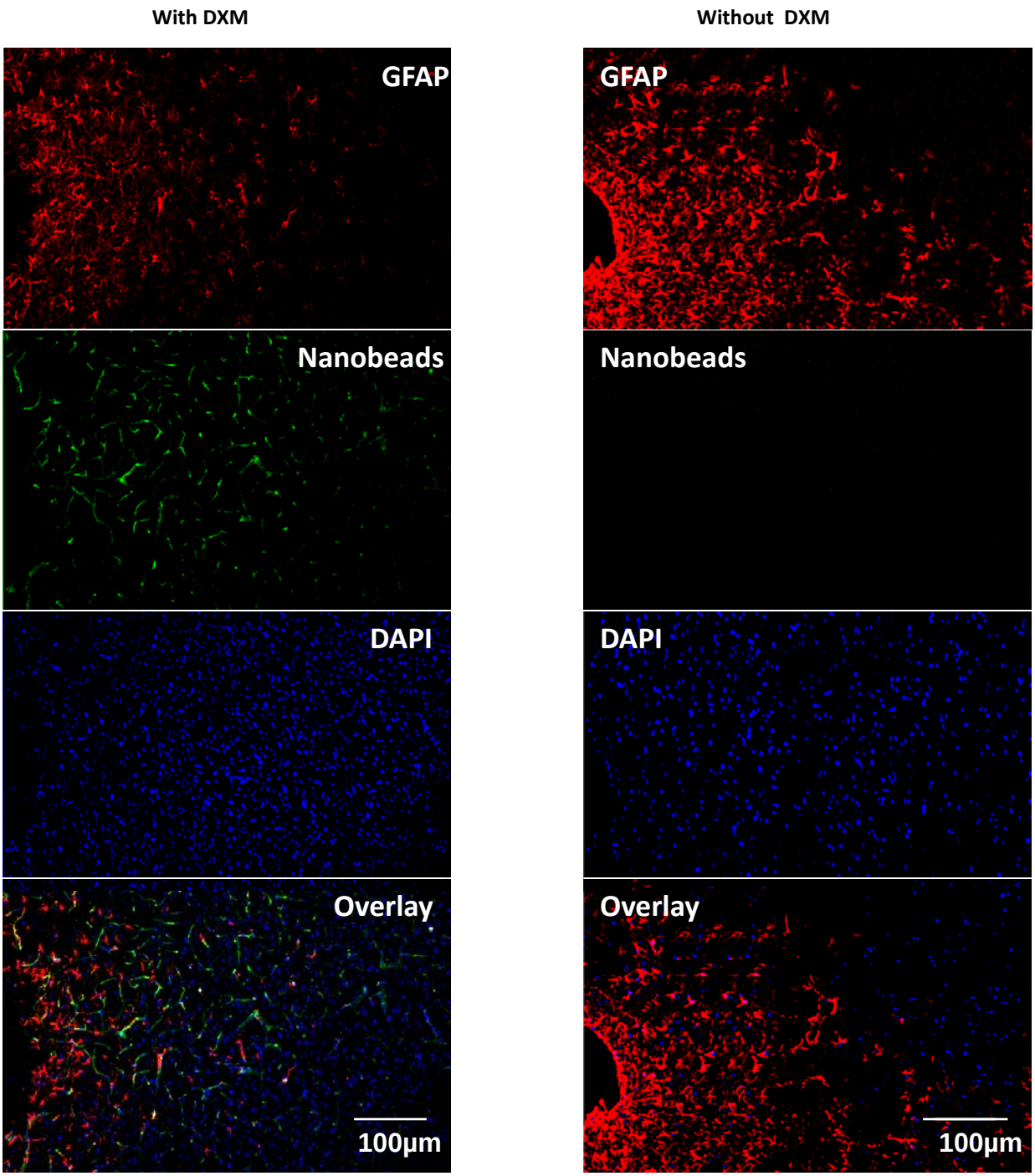

Figure I.4 A montage of the tissue response after 5 days of microdialysis with (left) and without (right) of dexamethasone. Note the complete absence of nanobeads in the right hand column, indicating profound ischemia in this tissue. The position of the microdialysis probe track is at the far left in both panels.

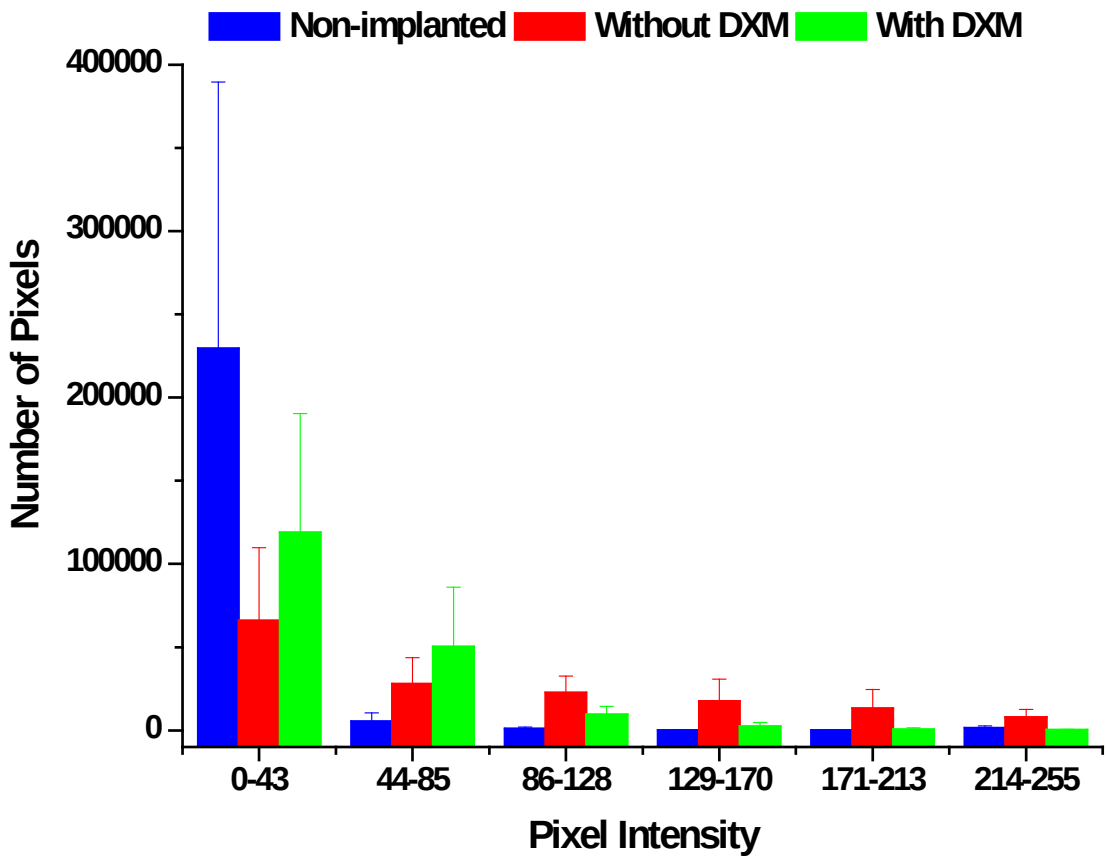

Figure I.5 Comparison of the pixel intensity distribution in images of non-implanted (control) tissue (blue) and tissue dialyzed without (red) and with (green) dexamethasone. The data are reported as the mean and standard deviation of the number of pixels in each intensity bin from three images.

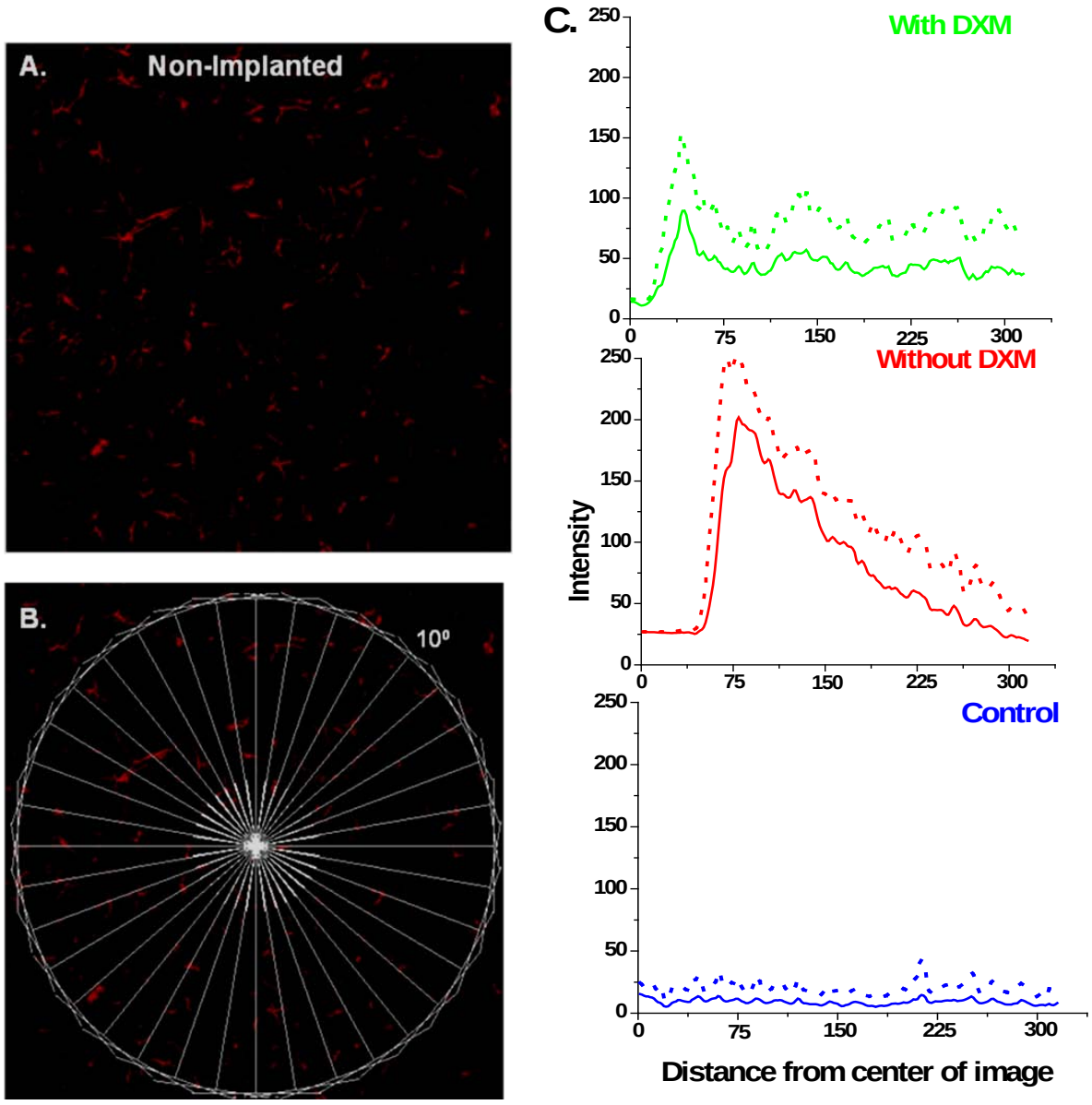

Figure I.6 Line scan analysis of GFAP images. A) Non-Implanted control tissue. B) The same image overlaid with the spoke pattern of lines used to construct the line-scans in C. C) Line scan intensity profiles obtained from non-implanted control tissue (blue) and from tissue dialyzed without (red) and with (green) dexamethasone. Data are reported as the mean (solid line) and the standard deviation (dotted line) of 36 lines per image.

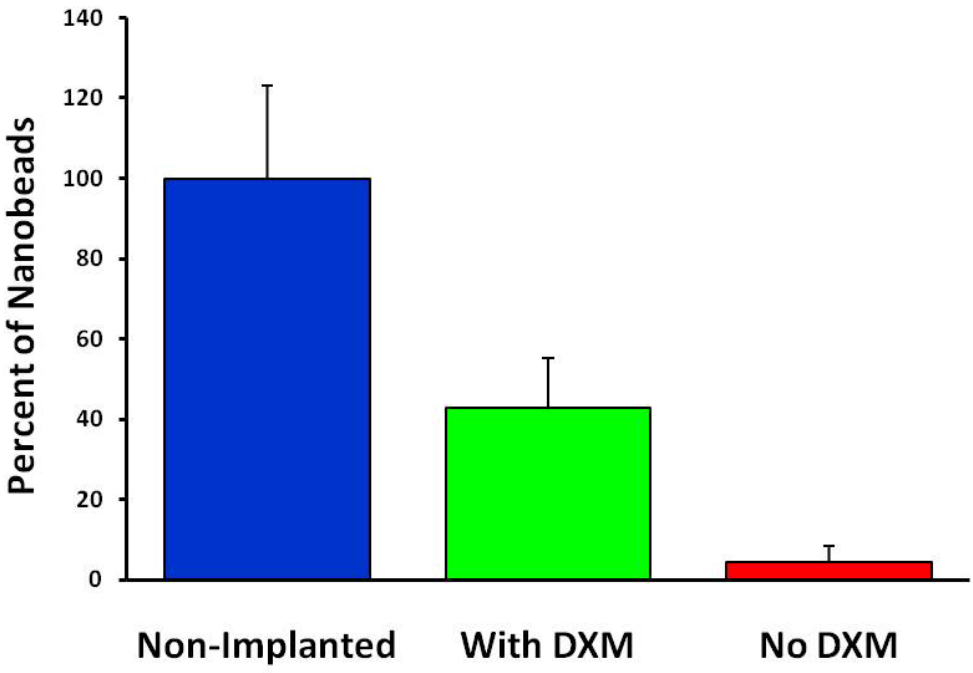

Figure I.7 The number of fluorescent pixels in blood vessel images from non-implanted control tissues (blue) and implanted tissues perfused with (green) and without (red) dexamethasone: the data are normalized with respect to the average pixel count from the non-implanted controls. Tissue with and without dexamethasone were significantly different from one another and from non-Implanted tissue (ANOVA and Tukey posthoc test: $F_{(2,12)} = 57.1$; $p < 0.00001$).

6. The effect of dexamethasone on dopamine no-net-flux

Because the impact of dexamethasone on gliosis and ischemia is readily apparent, we became interested in knowing how the drug might affect microdialysis results. To investigate this, we measured no-net-flux curves for dopamine, an important neurotransmitter and the subject of prior microdialysis studies (Justice, 1993; Yang et al., 1998; Bungay et al., 2003; Borland & Michael, 2004; Borland et al., 2005; Perry et al., 2009).

Microdialysis extraction curves (see Supplementary Information) are usually linear and aptly described by the following equation (Michael et al., 2005):

$$C_{in} - C_{out} = E \cdot C_{in} - R \cdot C_{ext} \quad \text{(Equation 1)}$$

where C_{in} and C_{out} are the concentrations at the inlet and outlet of the probe, C_{ext} is the concentration outside the probe, R is the recovery factor, and E is the extraction factor. Since R and C_{ext} are not separable during in vivo experiments, it is practical to replace $R \cdot C_{ext}$ with C_{out} measured when C_{in} is zero, which is known as the conventional microdialysis result, $C_{out,c}$:

$$C_{in} - C_{out} = E \cdot C_{in} - C_{out,c} \quad \text{(Equation 2)}$$

According to Equation 2, $C_{out,c}$ is the inverse of the y-intercept of the extraction curve and E is its slope. The x-intercept of the extraction curve corresponds to the condition that C_{in} and C_{out} are equal to each other: their common value is called the no-net-flux concentration, C_{nnf} (Bungay et al., 2003; Michael et al., 2005; Chefer et al., 2006; Bungay et al., 2007).

Using probes perfused without dexamethasone, the dopamine extraction curves measured on day 1 and day 4 (red, Figure I.8) exhibited typical features: the curves were linear with $C_{out,c}$ and C_{nnf} values near 10 nM (Kulagina et al., 2001) (see also Table 1). Dexamethasone had no significant effect on the values of $C_{out,c}$ and C_{nnf} (Table 1). To us, this came as a surprise, as we had anticipated that inhibiting gliosis and ischemia might increase $C_{out,c}$ and C_{nnf} towards the

higher in vivo dopamine concentrations we have measured with microelectrodes (Peters & Michael, 1998; Borland & Michael, 2004; Wang et al., 2010). This suggests that even though dexamethasone inhibited gliosis and ischemia, it did not protect dopamine terminals from the penetration injury.

Interestingly, however, the extraction curves measured in the presence of dexamethasone appear to be non-linear (green, Figure I.8 and Table 1). The most likely explanation for this involves the Michaelis-Menten kinetics of the dopamine transporter, the protein responsible for the uptake of dopamine by brain tissue. The transporter aids the extraction of dopamine from the microdialysis probe by enabling nearby brain tissue to take up dopamine after it diffuses out of the probe, as originally explained by Smith and Justice (Smith & Justice, 1994). Since the transporter has a K_M value near 200 nM, it is surprising that the extraction curves are linear, as we observed in the absence of dexamethasone, even when the C_{in} values substantially exceed K_M. This indicates that the dopamine is diluted by the time it diffuses to the transporter, such that the transporter does not become saturated with dopamine. The non-linear extraction curve observed with dexamethasone, then, suggests that dopamine more readily diffuses to the transporter, consistent with a reduction of the glial barrier next to the probe, making it easier to saturate the transporter.

Previous microdialysis studies have concluded that steroid use inhibits dopamine uptake, (Becker & Cha, 1989; Castner et al., 1993; Pacak et al., 2002; Sadri-Vakili et al., 2003) prompting speculation that steroids possess a cocaine-like activity that exacerbates their abuse by some users. However, the authors of those prior studies were likely unaware that steroids might have indirect effects on dopamine uptake due to alterations in the tissue reaction to the

microdialysis probe. This illustrates that hidden subtleties can impact the interpretation of in vivo analytical measurements.

D. CONCLUSION

The results of this study support the conclusion that dexamethasone is highly effective at preventing the gliosis and ischemia triggered by the penetration injury that accompanies the implantation of microdialysis probes into brain tissue, while offering relatively little neuroprotection per se to the dopamine terminals. Nevertheless, we speculate that inhibiting gliosis and ischemia is likely a necessary component of an overall neuroprotective strategy, as activated glia destroy neurons and their processes and prevent their regrowth (Goritz et al., 2002; Stroncek & Reichert, 2008). So, we expect that dexamethasone will contribute to mitigating probe-induced injury, especially if combined with complementary neuroprotective measures (e.g. the use of glutamate antagonists, antioxidants, or radical scavengers, etc.). In closing, we note that there may be restrictions on the uses of dexamethasone, which has failed human trials as a therapeutic agent for traumatic brain injury: human trials were terminated early because dexamethasone increased mortality (Alderson & Roberts, 1997).

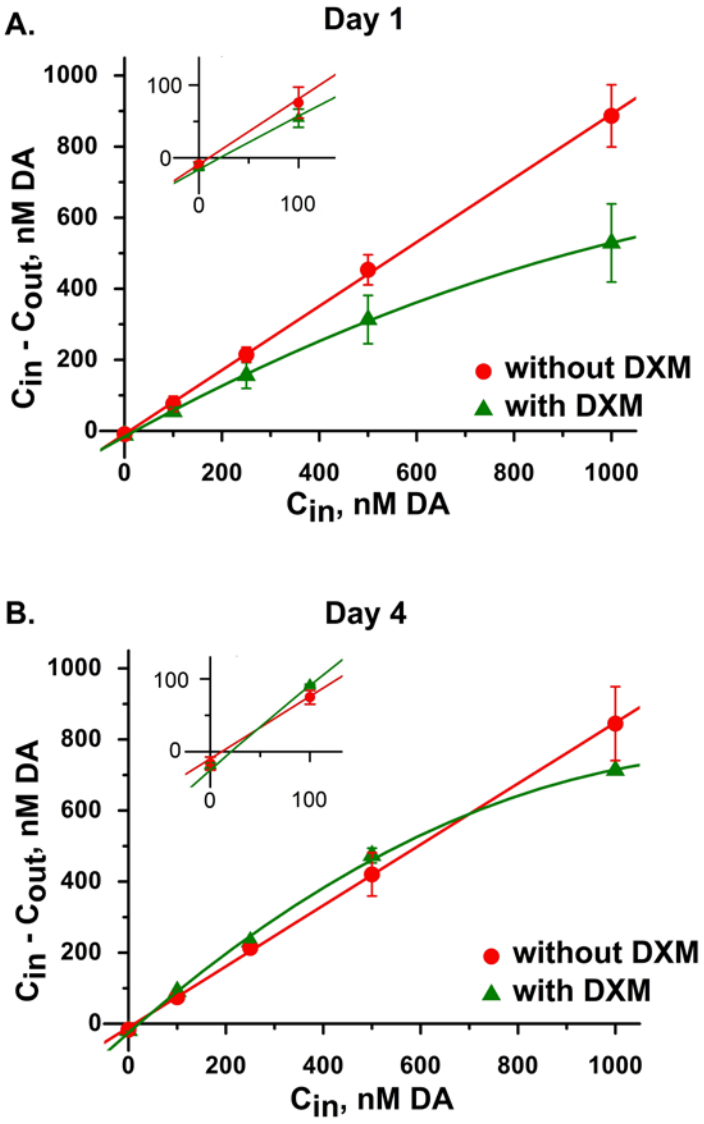

Figure I.8 Dopamine concentration difference plots obtained in the rat striatum on day 1 (A) and day 4 (B) of microdialysis with (green) and without (red) dexamethasone. The data points represent the mean ± the standard error. The solid lines show the linear regression of the data obtained without dexamethasone (red) and the quadratic regression of the data obtained with dexamethasone (green). Insets expand the region near the origin to visualize $C_{out,c}$ and C_{nnf}.

Table 1 Dopamine no-net-flux measurement.

Parameter	Day 1		Day 4	
	Without DXM N = 3	With DXM N = 6	Without DXM N = 3	With DXM N = 3
Conventional Microdialysis Concentration ($C_{out, c}$), nM[a]	9.19 ± 3.49	11.94 ± 5.36	16.49 ± 8.85	19.11 ± 3.41
No-net-flux Concentration (C_{nnf}), nM[b]	9.34 ± 7.17	16.26 ± 1.54	19.07 ± 4.19	19.37 ± 1.61
Extraction Fraction (E)[c]	0.901 ± 0.010		0.858 ± 0.008	
Regression Equation[c] $Y = C_{in} - C_{out}$ $X = C_{in}$	Y = 0.901X – 9.02	$Y = -2.1\times10^{-4}X^2 + 0.76X - 15.78$	Y = 0.858X − 10.02	$Y = -4.6\times10^{-4}X^2 + 1.20X - 25.07$
Coefficient of Determination (r^2)[c]	0.9996	0.9997	0.9997	0.9987

a: Determined by direct measurement.
b: Determined by regression of data from individual animal.
c: Determined by regression of averages across animals.

E. SUPPLEMENTARY INFORMATION

1. Microscopy of non-implanted control tissues

Images of 30-μm thick horizontally-cut sections of the non-implanted rat striatum (control tissue) exhibit the normal structure and morphology of this brain region (Supplementary Figure I.9). DAPI-labeled nuclei (blue, Supplementary Figure I.9A) are distributed uniformly with no obvious voids or clusters. Bead-laden blood vessels (green, Supplementary Figure I.9B) are spaced on-average 60 μm apart, with some vessels appearing in profile and some appearing in cross-section. Most vessels are capillaries but larger vessels are observed occasionally. The beads are confined to the vessels and do not reach the interstitial spaces, because brain endothelial cells form tight junctions. GFAP-labeled glial cells (red, Supplementary Figure I.9C) appear star-like, hence the name astrocyte, are sparsely distributed, and exhibit numerous fine processes. An overlay image of the blood vessels and astrocytes shows points of contact (yellow, Supplementary Figure I.9D), consistent with the role glia play in transporting substances from vessels to brain cells. The differential interference contrast (DIC) image (Supplementary Figure I.9F) shows that the tissue is uniform and free of defects.

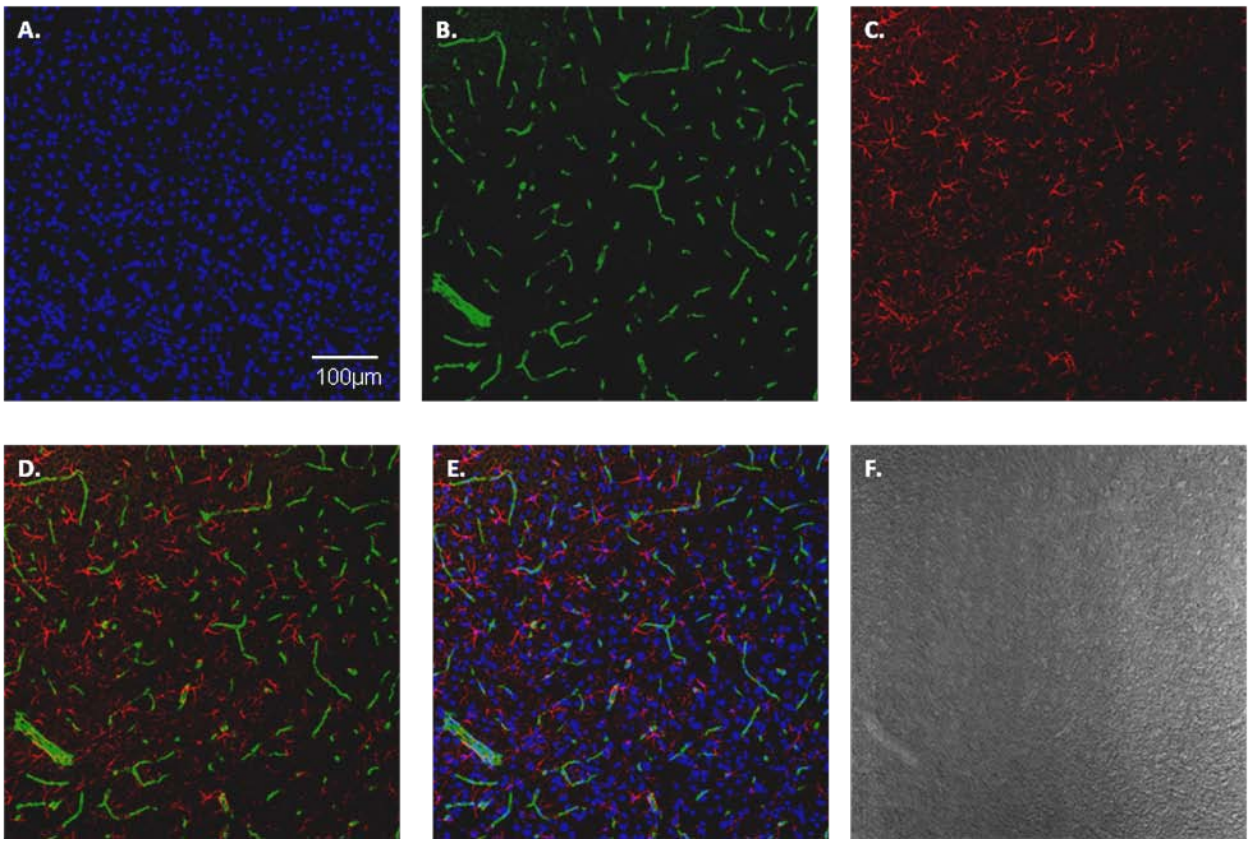

Figure I.9 Microscopy of non-implanted striatal tissue. A) nuclei labeled with DAPI, B) blood vessels labeled with fluorescent beads, C) glial cells (astrocytes) labeled with GFAP antibody, D) overlay of B and C (note yellow pixels indicating contact between glial cells and blood vessels), E) overlay of A, B, and C, F) DIC image.

2. Color-coded intensity plots

For quantitative image analysis, we used Metamorph software to convert the fluorescent GFAP images to color-coded surface intensity plots (Supplementary Figure I.10): the intensity range was 0-255 (low-high). In non-implanted tissues (Supplementary Figure I.10A) occasional spots of medium intensity (yellow) correspond to normal glial cells. In tissues perfused without dexamethasone (Supplementary Figure I.10B), the increased number and intensity of the GFAP spots reflect both the proliferation and enlargement of the glial cells. These features are absent in the tissues perfused with dexamethasone (Supplementary Figure I.10C).

3. Dopamine extraction curves

Table 1 reports the numerical values of $C_{out,c}$ and C_{nnf} for dopamine measured in the rat striatum. $C_{out,c}$ was determined by HPCL analysis of dialysate samples collected when C_{in} was zero. C_{nnf} was determined by regression analysis of the extraction curves. Linear regression of the results obtained without dexamethasone produced r^2 values greater than 0.999. However, in the case of the results obtained with dexamethasone, high regression coefficients required quadratic regression.

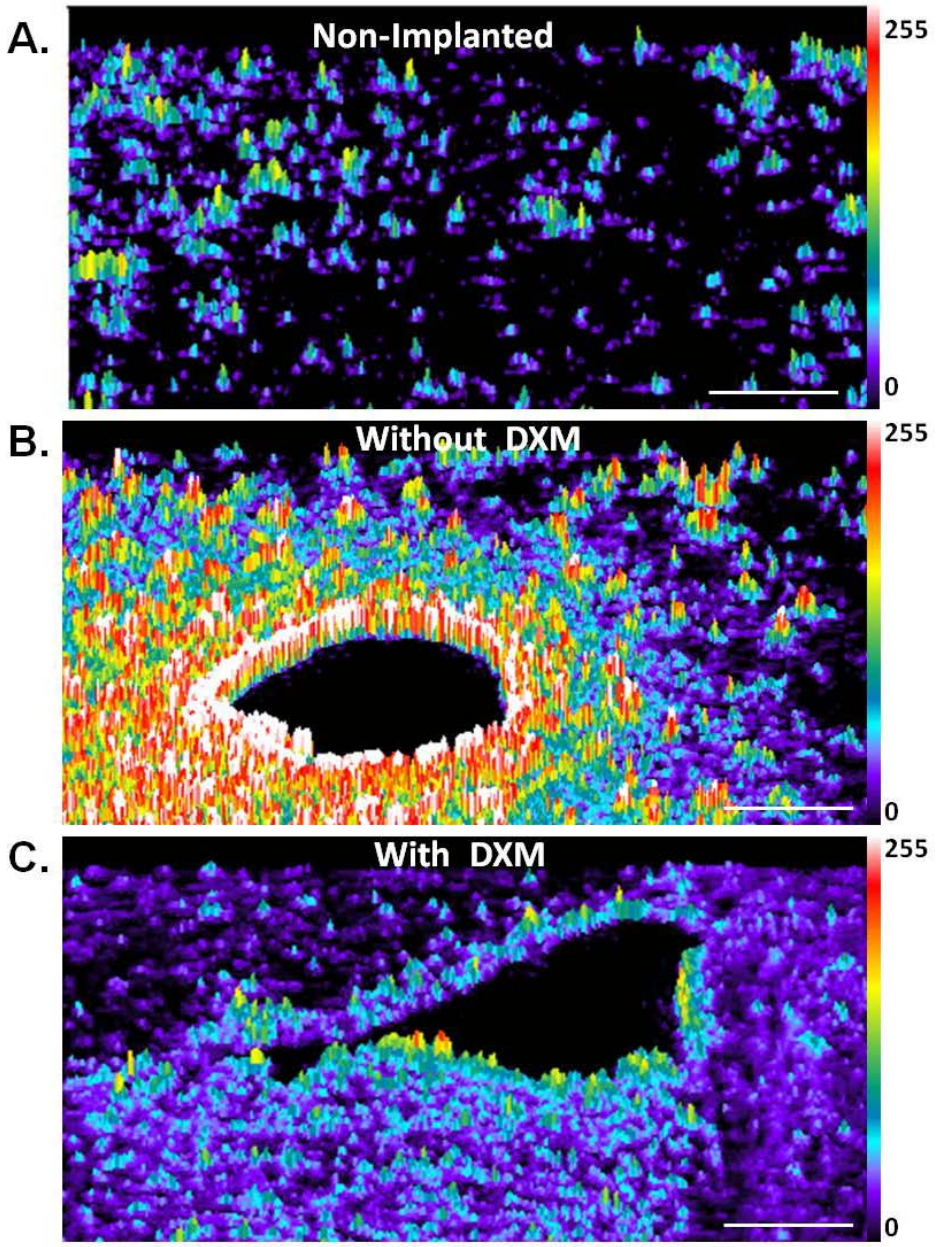

Figure I.10 A color-plot representation of the GFAP images of non-implanted striatal tissue (A) and striatal tissue dialyzed without (B) and with (C) dexamethasone. Pixel intensities are color coded from 0 to 255 as indicated on the color scales next to the images. Scale bars = 100 μm.

CHAPTER II. THE DOPAMINE PATCHWORK OF THE RAT NUCLEUS ACCUMBENS CORE

Adapted with revision from Zhan Shu, I. Mitch Taylor and Adrian C. Michael (2013) *European Journal of Neuroscience*, 38, 3221-3229.

A. INTRODUCTION

Dopamine (DA) is critically important in numerous aspects of normal CNS function (O'Donnell, 2003; Schultz, 2007) and the etiology of several CNS disorders, including Parkinson's disease (Schultz, 1982; Lotharius & Brundin, 2002), schizophrenia (Abi-Dargham et al., 2000), substance abuse (Phillips et al., 2003), and attention deficit hyperactivity disorder (Sagvolden et al., 2005). DA's diversity of function and dysfunction imparts deep significance to understanding the mechanisms that control extracellular DA concentrations and their spatiotemporal dynamics. Such mechanisms have been extensively studied in the subregions of the striatum (i.e. dorsal striatum and nucleus accumbens) that play central roles in motor control (Kish et al., 1988; Graybiel et al., 1994; Doya, 2000; Durieux et al., 2012) and the mediation of reward-related behaviors (Schultz, 1998; Ikemoto & Panksepp, 1999; Wise, 2004; Ariansen et al., 2012).

The kinetics of evoked DA release and DA clearance in the striatum are heterogeneous (May & Wightman, 1989; Garris et al., 1994b; Zachek et al., 2010). Consequently, it has become

common practice during voltammetric recording of extracellular DA to seek out “hot spots”, i.e. recording sites that produce maximally robust DA responses. The concept of hot spots, however, is inconsistent with the ultrastructure of the striatum, which contains a regular array of DA terminals arranged in a lattice-like formation (Moss & Bolam, 2008). Thus, a truly comprehensive understanding of dopaminergic mechanisms requires knowledge also of the properties and functions of sites that do not qualify as hot spots.

Voltammetric DA recordings in the dorsal portion of the rat striatum have revealed the presence of a patchwork of domains exhibiting significant differences in the kinetics and plasticity of evoked DA release, the kinetics of DA clearance, and the actions of several dopaminergic drugs (Moquin & Michael, 2009; Wang et al., 2010; Moquin & Michael, 2011, Taylor et al., 2012 & 2013). These differences derive, in part, from local variations in DA’s basal concentration, which establishes an autoinhibitory tone in the slow, but not the fast, domains. The objective of the present study was to address the hypothesis that a domain patchwork might exist also in the core of the nucleus accumbens (NAcc). Our findings confirm the existence of a domain patchwork in the NAcc but also show that the NAcc domains are substantially different from those in the dorsal striatum.

B. MATERIALS AND METHODS

1. Solutions, drugs, and reagents

All reagents were used as-received from their suppliers and all aqueous solutions were prepared in ultrapure water (NANOPure, Barnstead, Dubuque, IA, USA). Dopamine hydrochloride

(Sigma-Aldrich, St. Louis, MO, USA) standard solutions were prepared fresh just before use in N2-purged artificial cerebrospinal fluid (aCSF, 144 mM Na^+, 1.2 mM Ca^{2+}, 2.7 mM K^+, 149.1 mM Cl^-, 1.0 mM Mg^{2+}, 2.0 mM phosphate, pH 7.4). Raclopride tartrate (Sigma-Aldrich) was dissolved in phosphate buffered saline (PBS, 155 mM NaCl, 100 mM sodium phosphate, pH 7.4). Paraformaldehyde (PFA, 4% in PBS) was prepared from resin (Sigma-Aldrich) and stored at 4 °C.

2. Carbon fiber electrodes

Single carbon fibers (7-μm diameter T650, Cytec Carbon Fibers, LLC, Piedmont, SC, USA) were placed inside fire polished borosilicate glass capillaries (0.58 mm I.D., 1.0 mm O.D.; Sutter Instruments, Co., Novato, CA, USA). Each capillary was pulled to a fine tip (Narishige puller, Tokyo, Japan) and sealed with low-viscosity epoxy (Spurr Embedding Kit, Polysciences, Inc., Warrington, PA, USA). The exposed fiber was trimmed to 200 μm with a surgical blade and an electrical connection between the fiber and a Ag-coated copper wire (Squires Electronics, Inc., Cornelius, OR, USA) was formed with a droplet of mercury. The electrode tip was immersed in purified reagent-grade isopropyl alcohol (Sigma-Aldrich) for at least 20 min (Bath et al., 2000).

3. Fast-scan cyclic voltammetry (FSCV)

FSCV was performed with a custom-built potentiostat (electronics shop, Department of Chemistry, University of Pittsburgh) and a current amplifier (Keithley 428, Keithley Instruments, Inc., Cleveland, OH, USA) under software control (CVTarHeels 4.3, courtesy of Prof. Michael Heien, Department of Chemistry, University of Arizona (Heien et al., 2003)) running on a PC

equipped with analog interface boards (PCI-6052E and PCI-6711, National Instruments, Austin, TX, USA). The potential between scans was 0 V vs. Ag/AgCl. The triangular potential waveform (three linear sweeps to 1.0 V, then to -0.5 V, and back to 0 V at 400 V/s) was repeated at 10 Hz.

4. Electrode calibration

Electrodes were pre- and post-calibrated in DA standard solutions using a custom-built flow cell (University of Pittsburgh, Department of Chemistry Mechanics Shop) with gravity-fed aCSF. In vivo DA concentrations were determined by post-calibration.

5. Subjects

Protocols were in accordance with NIH guidelines (publication 86-23). The Institutional Animal Care and Use Committee of the University of Pittsburgh approved all procedures involving animals (male Male Sprague-Dawley rats, n = 38, 250-275 g, Hilltop Laboratories, Scottsdale, PA, USA).

6. Surgery

Rats were anesthetized with isoflurane (5% by vol. initially and 2.5% for maintenance) delivered via a ventilator (Harvard Apparatus, Holliston, MA, USA) and wrapped in a 37 °C homoeothermic blanket (Harvard Apparatus). A carbon fiber electrode was placed into the dorsal striatum (AP +1.2 mm, ML +1.4 mm, DV 5.0 mm below dura, (Paxinos & Watson, 1998)

and a Ag/AgCl reference electrode (Bioanalytical Systems Inc., West Lafayette, IN, USA) was placed in contact with the contralateral cortical surface via a salt bridge. A bipolar, stainless-steel stimulating electrode (MS303/B, Plastics One, Inc., Roanoke, VA, USA) was placed just above the ipsilateral medial forebrain bundle (MFB) (AP -4.3 mm, ML +1.2 mm, DV 7.5 below dura) and then slowly lowed until evoked DA release was detected in the striatum (Ewing et al., 1983; Kuhr et al., 1984; Michael et al., 1987). Thereafter, without moving the stimulating electrode the carbon fiber was slowly lowered into the NAcc (DV 6.6-7.6 mm below dura). Consistent with prior reports (Kuhr et al., 1986; Stamford et al., 1988; Garris et al., 1994b), electrical stimulation of the MFB evoked DA release in the dorsal striatum and NAcc.

In a separate group of rats, once the carbon fiber was positioned in the NAcc, stimulation (60 Hz, 250 μA, 3 s) was repeated at 5-min intervals. Between each stimulus the stimulating electrode was lowered slowly through the MFB in 100 μm vertical steps (results in Supplementary Figure II.13).

7. Electrical Stimulation

The electrical stimulus was a constant-current, biphasic square wave (duration 0.2-3 s, frequency 60 Hz, pulse intensity 150-550 μA, pulse width 2 ms) supplied by a pair of optical stimulus isolators (NL800A, Digitimer, Ltd., Letchworth Garden City, UK). When multiple consecutive trains were used, the four trains were 1-s long and separated by a 2-s interval.

8. Drug administration

Each rat received a series of pre-raclopride stimuli, a single dose of raclopride (2 mg/kg i.p.), and a final post-raclopride stimulus 30 min after drug administration.

9. Histology

A small lesion (12 V AC, 3-5 s) was used to identify the recording sites because carbon fiber tracks are otherwise not visible by light microscopy (Peters et al., 2004). Because the lesion procedure destroys the electrode, it was performed after electrode post-calibration: electrodes were retracted from the tissue, post-calibrated, and returned to their final stereotaxic coordinates for the lesion procedure. Every possible effort was made not to disturb the way the electrode was mounted on the carrier arm during post-calibration. After the lesion, rats were perfused via the heart with 160 mL PBS followed by 160 mL PFA. Brain tissue was removed from the skull, stored in cold PFA, cut into 30 μm coronal sections (Vibratome, St. Louis, MO, USA), stained with cresyl violet, cover-slipped, and examined with a light microscope (Leica Microsystems). All results reported herein are from recording sites in the NAcc (Supplementary Figure II.8).

10. Data analysis

The initial rate of evoked dopamine overflow was determined from the slope of the evoked responses during the first 300 ms of each electrical stimulus. The linear dopamine clearance rate was measured from the slope of the descending phase of the responses after the stimulus: linear segments were defined by at least three data points with an $r^2 > 0.96$. Overshoot duration was

defined by the time needed after the end of the stimulus for the evoked response to reach its maximum amplitude. The overshoot concentration was the amount by which the dopamine concentration continued to increase after the end of the stimulus. Statistical analyses were by t-test and two-way analysis of variance (ANOVA) with a repeated measures design (IBM SPSS Statistics 20).

C. RESULTS

1. DA shows two distinct kinetic profiles in NAcc

Electrically evoked DA release in the NAcc exhibits two distinct kinetic profiles, depending on the recording location, within individual animals (Figure II.1). During a brief stimulus (200 ms, 60 Hz, 250 μA) the fast kinetic profile (Figure II.1, solid line) exhibits evoked DA release without delay when the stimulus begins and short-term facilitation of release as the stimulus proceeds: short-term facilitation is evident in the greater increase in DA caused by the second 100 ms of the stimulus compared to the first 100 ms. When the stimulus ends, the DA signal continues to increase (overshoot) for an additional 200 ms before starting to return towards the baseline. In contrast, a slow recording location in the same animal exhibits no response (Figure II.1, dashed line). However, if the stimulus is extended to 1 s, the slow profile (Figure II.1, dash-dot line) exhibits robust DA release after a ~200-ms initial delay. The slow profile also exhibits short-term facilitation and overshoot. The presence or absence of the initial ~200-ms delay in evoked release provides an objective basis for classifying NAcc responses as fast or slow, respectively.

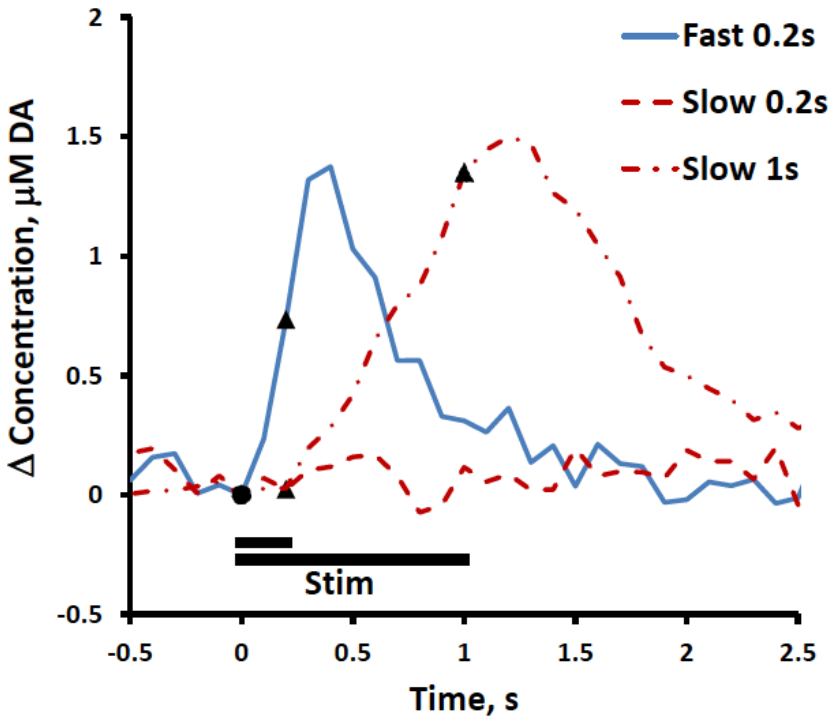

Figure II.1 Two types of evoked dopamine responses in NAcc. A brief stimulus (200 ms, 60 Hz, 250 µA) evokes both a fast (solid line) and slow (dashed line) profile at two recording sites within the NAcc of a single rat. A longer stimulus (1 s, 60 Hz, 250 µA) evokes a slow profile after a 200 ms initial delay (dash dot delay). In this and subsequent figures, solid circles and triangles mark the start and end of the stimulus, respectively.

The fast and slow NAcc profiles are consistent across multiple animals (Figure II.2: stimulus = 1 s, 60 Hz, 250 µA: solid lines are the average of multiple fast (n = 8) and slow (n = 8) profiles recorded in separate rats: the dotted lines are confidence intervals based on the SEMs: the same presentation format is used in subsequent figures). The responses are significantly different (see ANOVA results in the figure legend). These two profiles completely define evoked DA responses in the NAcc, i.e. no other profiles were detected. The maximum amplitude (Figure II.2b), initial rate of overflow (Figure II.2c), and rate of DA clearance after the stimulus (Figure II.2d) are significantly profile-dependent. However, the two profiles exhibit

similar overshoot duration (Figure II.2e). Whether a fast or slow profile is observed at any given recording location is not determined by the location of the stimulating electrode (Supplementary Figure II.13).

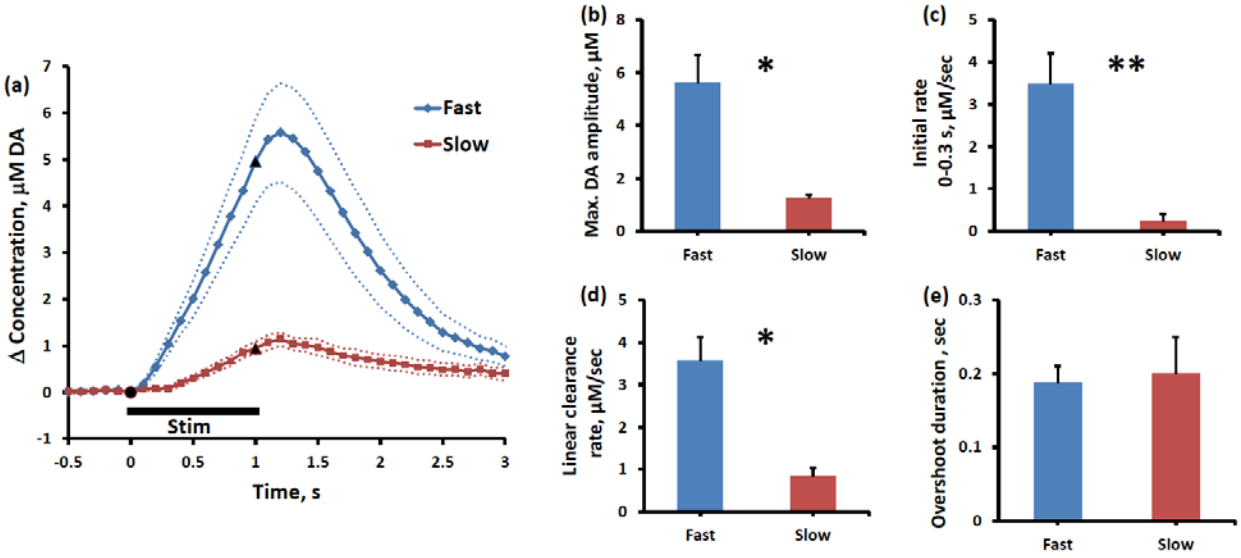

Figure II.2 Comparison of fast and slow responses during a 1-s stimulus. In this and subsequent figures, the solid lines and symbols report the average of profiles recorded in multiple animals and the dotted lines report the confidence interval based on the SEM of each data point. (a) The profiles are the average of 8 fast (diamond) and 8 slow (square) responses. The difference between fast and slow profiles is significant (all data from 0.1 to 2.9 s, two-way ANOVA with a repeated measures design: domains $F_{(1,14)} = 12.051$; n = 16; $p < 0.005$). The maximum amplitude (2b, independent-samples t-tests, $*p < 0.005$), initial rate of overflow (2c, independent-samples t-tests, $**p < 0.001$), and rate of DA clearance after the stimulus (2d, independent-samples t-tests, $*p < 0.005$) are significantly profile-dependent. The overshoot duration is not significantly (2e, independent-samples t-tests, $p > 0.5$) different between fast and slow profiles.

2. Effects of current intensity

Distinct fast and slow NAcc profiles are consistent over a broad range of stimulus current intensities (Figure II.3, stimulus = 3 s, 60 Hz, 150-550 μA: SEM ranges omitted for clarity). At intensities ≥300 μA and ≥450 μA the fast and slow profiles, respectively, exhibit a constant initial rate of DA clearance (see also Supplementary Figure II.9a): this indicates saturation of DA clearance and justifies the use of the observed clearance rates as the apparent V_{max} of DA uptake in each domain. The apparent V_{max} of the fast profile, 3.90 ± 0.57 μM/s (n = 4), is significantly ($p < 0.05$) higher than that of the slow profile, 2.24 ± 0.22 μM/s (n = 6).

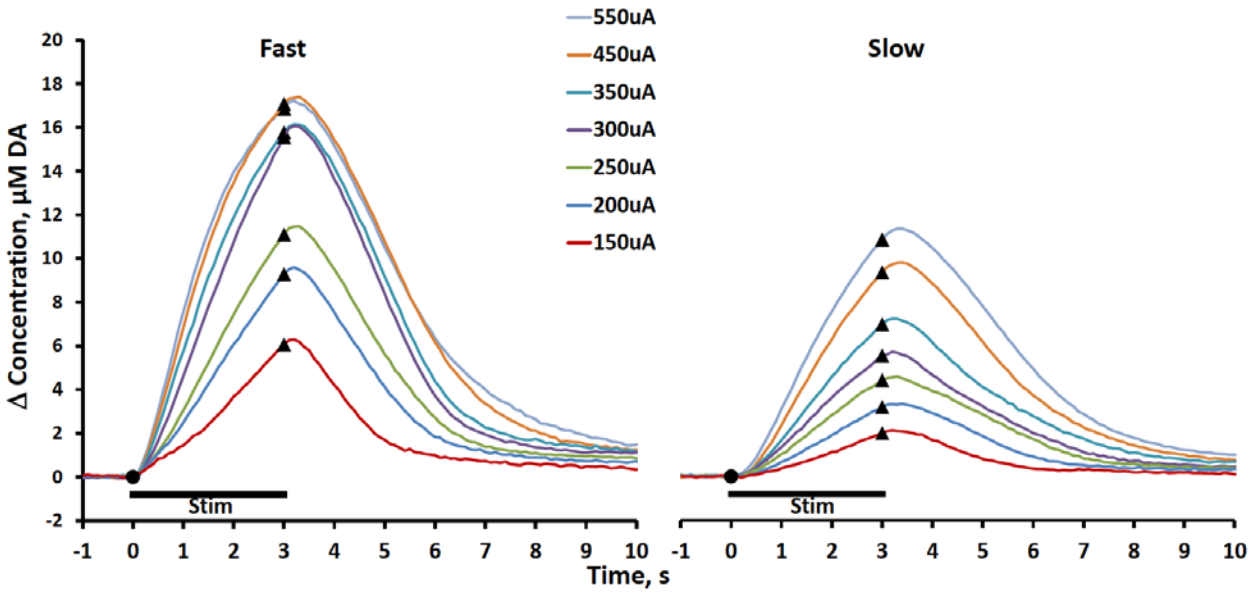

Figure II.3 Effects of current intensity on evoked DA overflow. Average fast (n=4) and slow (n=6) profiles as a function of stimulus intensity (3 s, 60 Hz, 150-550 μA). Error bars and symbols for individual data points omitted for clarity. The maximum DA amplitude (independent-samples t-test, $p < 0.05$) and initial rate (0-0.3 s, independent-samples t-test, $p < 0.05$) are significantly profile-dependent across all 150-550 μA intensities. See Supplementary Figure II.S9b for information on the rate of linear clearance after the stimulus.

3. Short-term facilitation of NAcc fast DA release

The NAcc fast profile exhibits short-term facilitation of DA release, whereas the dorsal-striatum fast profile exhibits short-term depression (Moquin & Michael, 2009). Since this is a unique aspect of the NAcc response, we examine it in more detail here (Figure II.4). During brief stimuli over a range of current intensities (200 ms, 60 Hz, 150-550 μA), the slow profiles exhibit either no or minimal evoked DA release but the fast profiles exhibit a steady increase in maximum response amplitude. However, after the first 100 ms of the stimulus, the amplitude of DA release in the fast profile is independent of the stimulus intensity (Supplementary Figure II.10). The amplitude increases steadily with stimulus intensity during the second 100 ms of the stimulus (short-term facilitation) and during the 100 ms after the stimulus ends (overshoot).

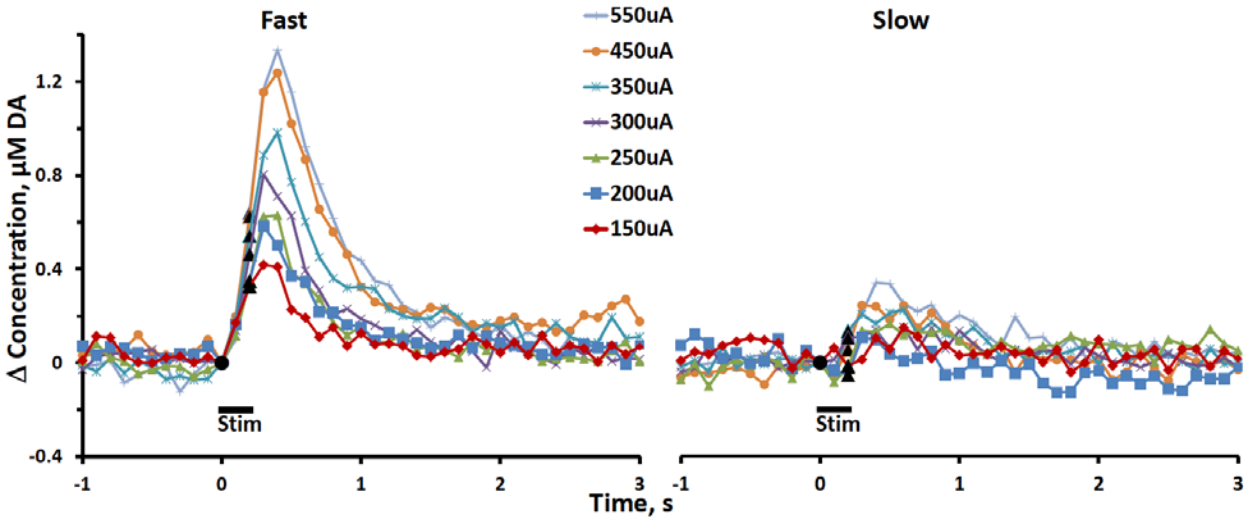

Figure II.4 Short-term facilitation in NAcc fast domains. Average profiles recorded in fast (n = 4) and slow (n = 6) domains during brief stimuli as a function of stimulus intensity (200 ms, 60 Hz, 150-550 μA). Error bars omitted for clarity. The difference between fast and slow response maximum DA amplitude at all current intensities is significant (one sample t-test, 150-300 μA, $p < 0.05$; independent-samples t-test, 350-550 μA, $p < 0.05$). See Supplementary Figure II.10 for information on the amplitude of release 100, 200, and 300 ms after the stimulus begins.

4. NAcc responses to multiple consecutive stimuli

The NAcc yields distinct fast and slow profiles during consecutive stimuli (stimuli = 1-s pulse trains with 2-s intervals, 60 Hz, 250 μA, Figure II.5a). The amplitudes of the fast and slow responses are significantly different (Fig 5b: two-way ANOVA with repeated measures $F_{(1,14)}$ = 17.058, n = 16, $^{**}p < 0.001$) but there are no significant train-to-train differences in amplitude in either domain. Each consecutive train returned the DA concentration to the same absolute level (Figure II.5b). When the response amplitudes were measured with respect to the signal at the beginning of each train, there was a slight but not significant decrease in the amplitudes normalized with respect to the first train (Figure II.5c). Both the fast and slow profiles exhibit a ~200 ms overshoot at the end of each consecutive train.

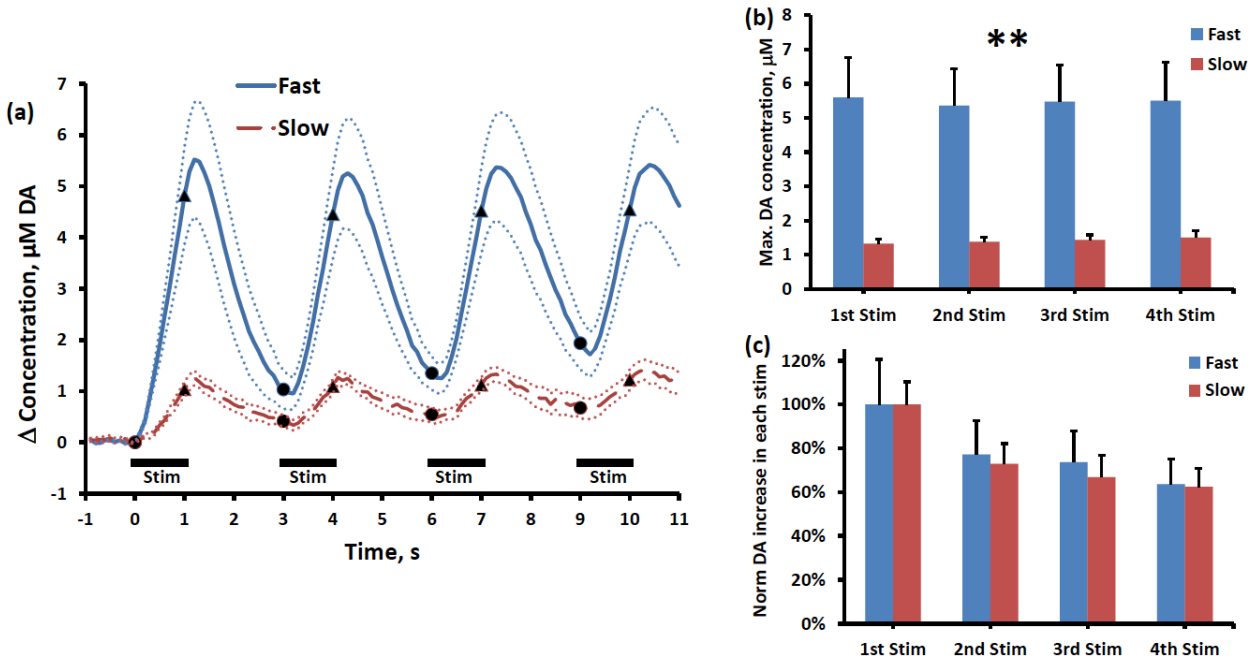

Figure II.5 Evoked dopamine overflow during multiple consecutive stimuli. (a) Average (± SEM) of individual responses: fast (solid line; n = 8 rats) and slow (dashed line; n = 8 rats) during four 1-s stimulus trains separated by 2-s intervals (60 Hz, 250 μA). (b) The difference between fast and slow response in maximum DA amplitude in multiple stimulus trains is significant (two-way ANOVA with a repeated measures design; $F_{(1,14)} = 17.058$; n = 16; $^{**}p < 0.001$). (c) When the response amplitudes were measured with respect to the signal at the beginning of each train, there was a slight but not significant decrease in the amplitudes normalized with respect to the amplitude during the first train (two-way ANOVA with a repeated measures design; stimulation sequence $p > 0.05$ and domains $p > 0.05$).

5. Effects of raclopride

Both the fast (Figure II.6) and slow (Figure II.7) NAcc profiles are sensitive to the D2 receptor antagonist, raclopride (2 mg/kg i.p.). In both domains, raclopride increased the overall amplitude of the responses but had no significant effect on the first 100 ms of the fast profile or the first 200 ms of the slow profile and had no significant effect on the rate of DA clearance after the end of the stimulus. Raclopride only significantly increased the overshoot duration of slow profiles (Figure II.7e, paired-samples t-test, $p < 0.0005$).

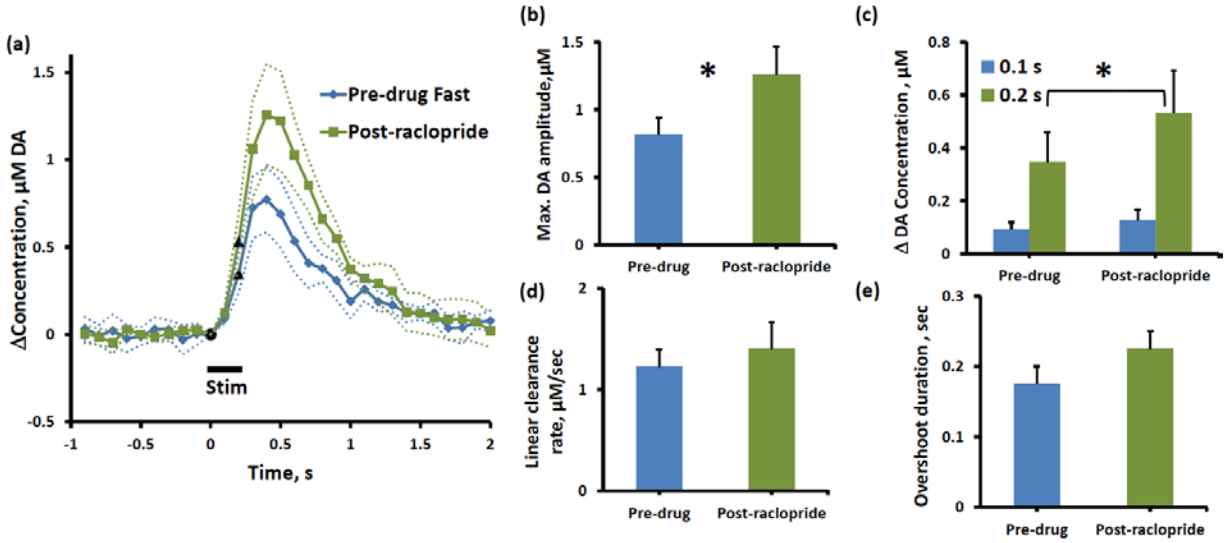

Figure II.6 Effects of raclopride on fast profiles. (a) Average (± SEM, n = 6) of individual responses during 0.2 s stimulus (60 Hz, 250 μA). (b) Raclopride significantly (paired samples t-test; $p < 0.05$) increased the maximum DA amplitude. (c) Raclopride had no significant effect on the first 100 ms of the fast profile (paired samples t-test; $p < 0.05$, only at 0.2 s). (d) Raclopride did not significantly affect the linear clearance rate or (e) overshoot duration of the fast profile.

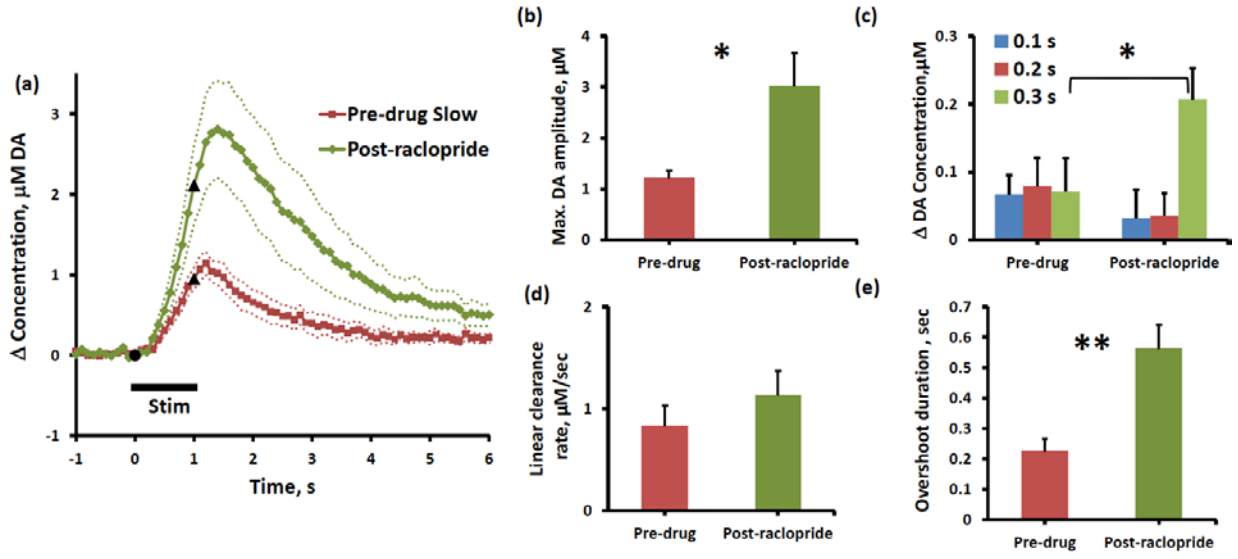

Figure II.7 Effects of raclopride on slow profiles. (a) Average (± SEM, n = 6) of individual responses during 1-s stimulus (60 Hz, 250 μA). (b) Raclopride significantly (paired samples test; $p < 0.05$) increased the maximum DA amplitude. (c) Raclopride had no significant effect on the first 200 ms of the slow profile (paired samples test; $p < 0.05$, only at 0.3 s). (d) Raclopride did not significantly affect the linear clearance rate. (e) Raclopride significantly (paired samples test; $p < 0.0005$) increased overshoot duration of the slow profile.

D. DISCUSSION

The findings presented herein confirm that the NAcc exhibits two distinct DA kinetic profiles. The nature, fast or slow, of evoked DA responses depends solely on the location of the recording electrode, so it appears that the DA terminal field of the NAcc is organized as a patchwork of fast and slow spatial domains, in similar fashion to the patchwork we have identified in the dorsal striatum (Moquin & Michael, 2009; Wang et al., 2010; Moquin & Michael, 2011, Taylor et al., 2012 & 2013). Nevertheless, the NAcc domains are substantially different from those in the dorsal striatum in terms of short-term plasticity and the role of autoinhibition.

1. Patchwork vs. long-range diffusional distortion of evoked DA responses

Prior studies of evoked DA release have tended to focus on "hot spots" and so the literature contains no prior reports of a DA patchwork in the NAcc. Low-amplitude, delayed responses might be diffusional distortions of the fast responses (discussed by Taylor et al. 2012 & 2013) but several observations support the alternative view that the slow profiles reflect a distinct kinetic phenomenon. For example, in the NAcc the fast and slow profiles exhibit no clear difference in the duration of the post-stimulus response overshoot (Figure II.2e). The overshoot of the slow profiles would be longer if the slow profiles were derived from diffusion of DA from of fast domains. Instead, we observe no domain difference in the time for the maximal DA concentration to reach the recording electrode. Also, we observe a narrow range of response amplitude in the slow domains: this also speaks against a diffusion process because, if diffusion were involved, intermediate response amplitudes would be observed based on the distance between the electrode and the fast domains serving as the diffusion source. Instead, our results show no evidence of a concentration gradient between NAcc fast and slow domains. Our findings are much more consistent with DA diffusing within rather between the respective domains, a similar conclusion we have reached in the dorsal striatum (Taylor et al., 2012).

2. Patchwork vs. short-range diffusional distortion

In past studies, optimizing the recording site did not necessarily eliminate all signs of distortion by diffusion or the electrode response. The response overshoot has been attributed to short-range diffusional distortion caused by a Nafion film on the electrode or possibility a distortion associated with DA absorption kinetics on the electrode surface (Engstrom et al., 1988;

Wightman et al., 1988; Kawagoe et al., 1992; Venton et al., 2002). Several approaches have been developed to correct these distortions to gain access to the intrinsic kinetics of DA release and clearance (Garris et al., 1994a; Garris & Wightman, 1995; Garris et al., 1997; Wu et al., 2001b; Addy et al., 2010). However, our findings suggest that overshoot may also be a consequence of DA kinetics. For example, we observe overshoots when recording brief responses (stimulus = 200 ms, 60 Hz, 250 μA) in the NAcc (Figure II.2) but not in the dorsal striatum (Moquin & Michael, 2009; Taylor et al., 2012). During the present study, we confirmed that the same electrodes and recording technique that produce overshoots in the NAcc did not do so in the dorsal striatum (Supplementary Figure II.11). Thus, the overshoot appears to be a feature of the NAcc rather than an inherent feature of the FSCV recording technique.

3. The origin of overshoot in the NAcc

The blockade of DA uptake with nomifensine dramatically increases overshoot duration and amplitude in the dorsal striatum (Taylor et al., 2012). This raises the possibility that overshoots in the NAcc might be due to DA uptake, which is inherently slower in the NAcc than the dorsal striatum (Cass et al., 1992; Cass et al., 1993; Cragg et al., 2000; Wu et al., 2001a). Although the apparent V_{max} values for DA clearance in the fast and slow domains of the NAcc were significantly different, they were not significantly different from the corresponding values reported by the same experiment conducted in the dorsal striatum (Taylor et al., 2013 and Supplementary Figure II.9b). However, in the NAcc, the domains did not exhibit any substantial difference in the time course of DA clearance (Supplementary Figure II.12): this is a stark contrast with the dorsal striatum, where the time course of DA clearance is domain-dependent (Moquin & Michael, 2011; Taylor et al., 2012). So, DA clearance in the NAcc appears to

operate under near pseudo-first order conditions, especially at stimulus intensities <500 μA. Thus, we attribute the consistent overshoots in the NAcc to a higher value of the apparent K_M of DA clearance.

Our findings agree with prior reports that DA clearance is slower overall in the NAcc than in the dorsal striatum (Garris & Wightman, 1994; Wu et al., 2001a; Wu et al., 2001b). However, there appears to be some controversy over exactly why the rates of DA clearance are different between these two brain regions. Prior studies have reported a regional difference in the V_{max}, rather than the K_M, of DA clearance (Jones et al., 1995; Wu et al. 2001a). So, we were surprised to find no significant differences between the regional apparent V_{max} values obtained during this study (Supplementary Figure II.9b). It may be important to note that the apparent V_{max} values reported herein were obtained by increasing the stimulus intensity until a constant rate of linear DA clearance was achieved (Supplementary Figure II.9), thereby confirming full saturation of the transporter. Our study is unique in this regard, as no other in vivo studies have compared the apparent V_{max} values in this exacting manner. It should also be emphasized that we are reporting apparent kinetic parameters, whereas the prior studies reported intrinsic parameters obtained by means of diffusional corrections. However, it remains to be seen if the corrections have fully accounted for the complex nature of diffusion in the brain extracellular space (Nicholson, 1995; Nicholson & Sykova, 1998; Sykova & Nicholson, 2008). In vitro studies involving radiochemical methods also found differences in V_{max} rather than K_M (Near et al., 1988; Marshall et al., 1990) but Andrews and coworkers (Perez et al., 2007) have pointed out a number of technical challenges with such kinetic determinations.

4. Short-term facilitation in the NAcc

In the dorsal striatum, the evoked DA release in the fast and slow domains exhibits marked short-term depression and facilitation, respectively, especially during multiple consecutive stimuli (Moquin & Michael, 2009). This did not occur in the NAcc, where neither domain exhibited obvious plasticity during multiple consecutive stimuli (Figure II.5). Thus, the short-term plasticity of evoked release in the NAcc is dramatically different from that in the dorsal striatum.

Short-term facilitation in the NAcc responses is apparent, however, during the rising phases of both the fast and slow profiles. The details of short-term facilitation of the fast profiles are most clearly evident in the responses to 200 ms stimuli (Figure II.4, 60 Hz, 150-550 μA). The response amplitude 100 ms after the stimulus begins is independent of stimulus intensity (Supplementary Figure II.10). But, the response amplitude at 200 and 300 ms after the stimulus begins increases steadily with the stimulus intensity. These details are highly consistent with the restricted diffusion model we previously proposed to explain DA profiles in the dorsal striatum (Taylor et al., 2012). According to this model, the diffusion of DA molecules in the extracellular space is restricted by dead space microdomains or binding sites (Nicholson, 1995; Nicholson & Sykova, 1998; Sykova & Nicholson, 2008). Conventional diffusion occurs once DA release exceeds the tissue's capacity to retain DA. This model explains the temporal features of the NAcc responses. For example, the longer initial delay in slow domains is due to the slow rate of evoked release, which causes a lower overall response amplitude but also increases the time needed to exceed the tissue's capacity to retain DA. The consistent overshoot duration in the fast and slow domains is due to DA exhibiting similar diffusion dynamics once the stimulus exceeds the tissue's retention capacity.

Our finding of differences in the short-term plasticity of evoked DA release in dorsal striatum and NAcc is consistent with the prior reports of Cragg (2003) and of Yavich and coworkers (Chadchankar & Yavich, 2011). Cragg (2003) reported short-term depression in tissue slices from the dorsal part of the primate striatum (putamen) and short-term facilitation in the nucleus accumbens. Using a different stimulus protocol, Yavich and coworkers reported short-term facilitation in the dorsal but not ventral striatum of the mouse.

5. On the role of tonic autoinhibition

Many of the distinctions between the fast and slow DA domains of the dorsal striatum appear related to the status of tonic autoinhibition, which is absent in the fast domains but dominant in the slow domains (Moquin & Michael, 2009). In contrast, tonic autoinhibition does not appear to play a similar role in the NAcc. Raclopride, the D2 antagonist, increased the overall amplitude of evoked responses in the both NAcc fast and slow domains but had no effect during the initial 200 ms or 300 ms, respectively, of the stimuli. Thus, in the NAcc autoinhibition is observed after, but not before, the onset of evoked DA release, so there is no sign of tonic autoinhibition even in the slow domain.

Moreover, there is no clear evidence that D2 antagonist affects the kinetics of DA clearance in the NAcc (Garris et al., 1994a; Benoit-Marand et al., 2001). There is a slight but non-significant tendency for raclopride to increase the linear clearance rate, but this cannot be taken as a sign that autoreceptors are modulating DA uptake. At the relatively low DA concentrations involved in these experiments, the dopamine transporter appears to be operating under pseudo-first order conditions and raclopride had no noticeable impact on the overall time

for needed for the DA signal to return to the baseline. So, raclopride did not affect the pseudo-first order kinetics of DA clearance.

E. CONCLUSION

Our findings confirm the presence of a patchwork of DA kinetics in the NAcc but also show substantial differences between the NAcc domains and those of the dorsal striatum. Diffusion effects are clearly evident in the various profiles, but these are due to diffusion within rather than between the domains. All the profiles exhibit the features of the restricted diffusion model, the mechanisms of which have been explored in detail by others (Nicholson, 1995; Nicholson & Sykova, 1998; Sykova & Nicholson, 2008). The various profiles are observed with the same FSCV technique, the same carbon fiber electrodes, and the same stimulus procedures, and so appear unlikely to be due to instrumental distortions. The regional and domain-dependence of the profiles appear, therefore, to reflect the distinct DA kinetics at the various recording locations.

Our findings reveal two substantial differences between the NAcc and dorsal striatum. First, we find no clear evidence of any autoinhibitory tone in the NAcc. Second, and likely a consequence of the first, there are no clear signs of short-term plasticity in the NAcc, where multiple consecutive stimuli evoked consistent DA release. The functional significance of the patchworks themselves, the short-term plasticity in the dorsal striatum, and the lack thereof in the NAcc, remains to be established.

F. SUPPORTING INFORMATION

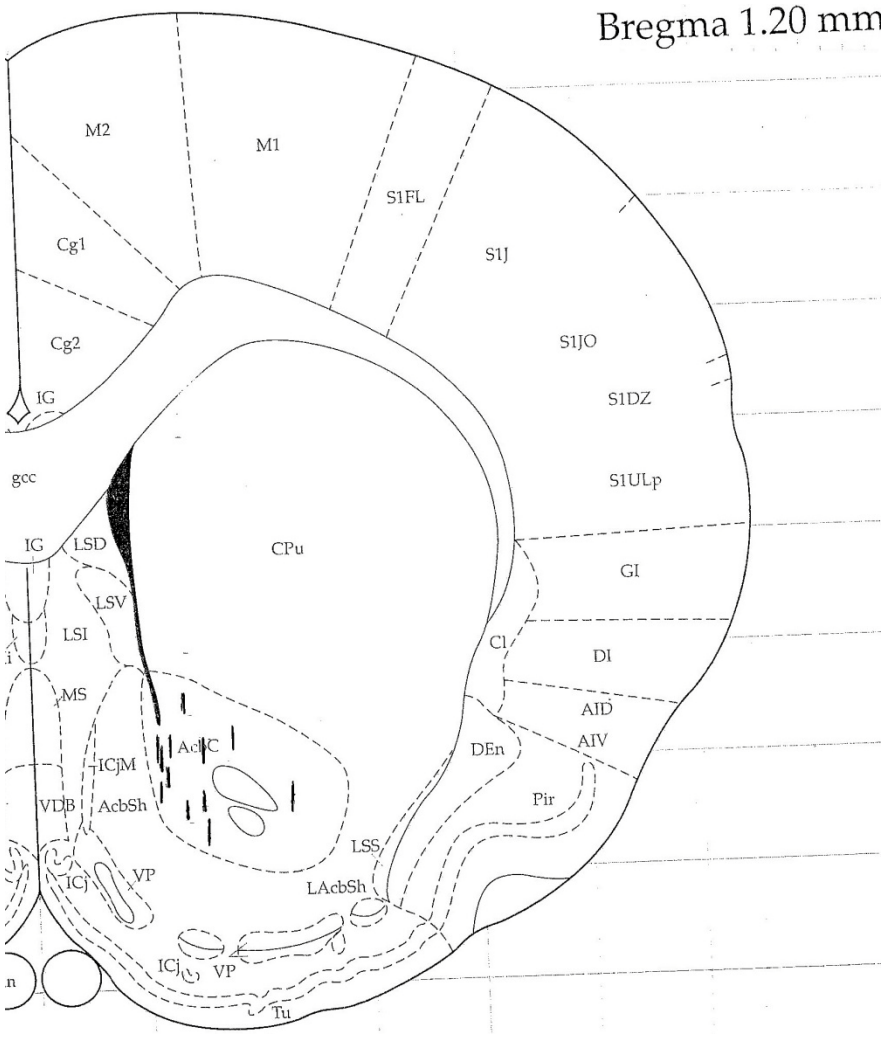

Figure II.8 Representative microelectrode placements in the NAcc.

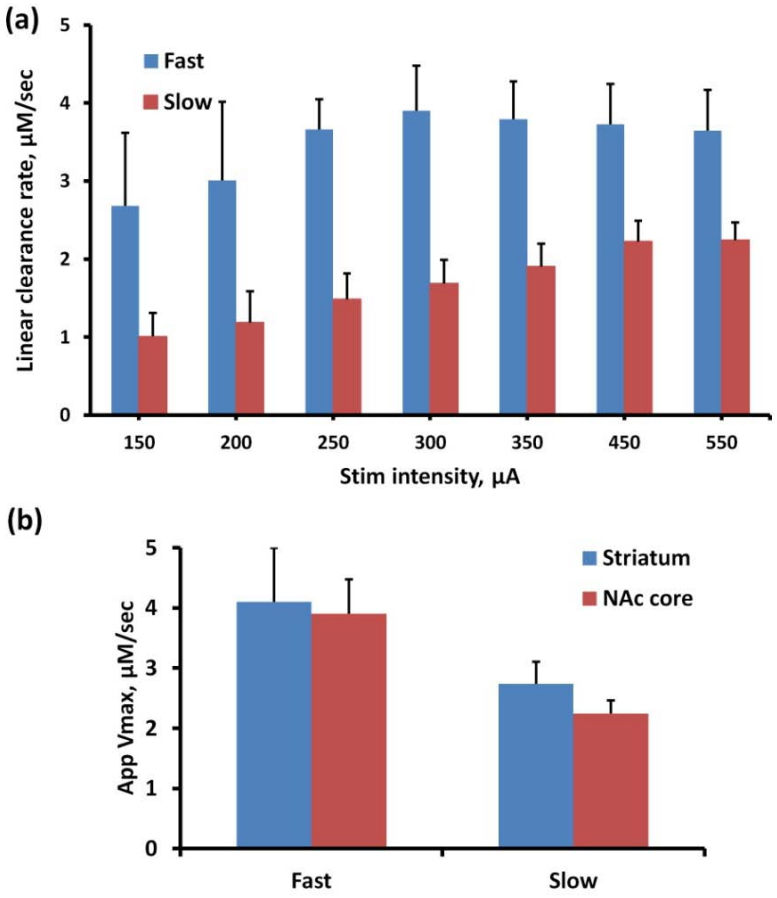

Figure II.9 Apparent V_{max} of DA clearance in fast and slow domains of the NAcc and dorsal striatum. (a) Linear DA clearance rates measured after stimulation at varying stimulus intensities (response profiles in Figure II.3: stimulus = 3 s, 60 Hz, 150-550 µA) in fast (red, n = 4 rats) and slow (blue, n = 6 rats) NAcc domains. The clearance rates reached a constant maximum value (apparent V_{max}) at stimulus intensities≥300 µA and ≥450 µA in fast and slow domains, respectively. (b) Neither of these apparent V_{max} values is significantly different from those obtained in the dorsal striatum using the same experimental design (independent-samples t-test, $p > 0.05$ in both fast and slow).

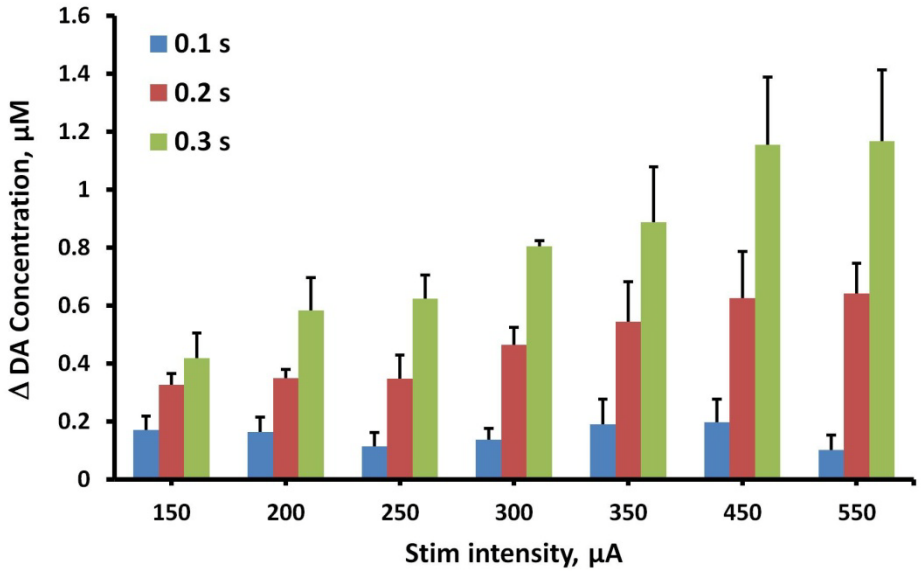

Figure II.10 Evoked DA concentrations in fast domains at first and second 100 ms of the stimulus and 100 ms after the end of the stimulus at different current intensities. Average (± SEM, n = 4 rats) of the evoked DA amplitude at 0.1-0.3 s after the start of the stimulus. The amplitude of DA release in the fast profile after the first 100 ms (blue) is independent of the stimulus intensity (one-way ANOVA with a repeated measures design, $F_{(6,18)} = 0.559$, $p > 0.5$). The amplitude increases steadily with stimulus intensity 200 ms (red) and 300 ms (green) after the stimulus begins (the data shown in green correspond to overshoot).

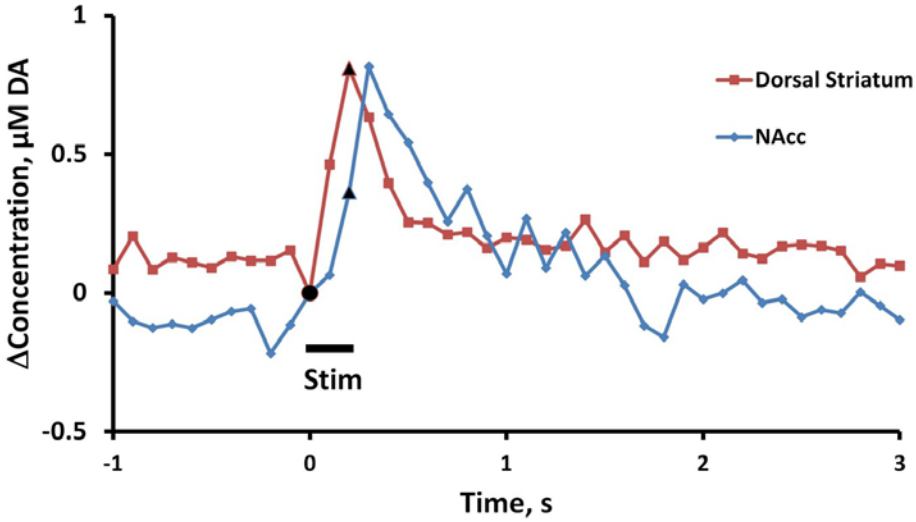

Figure II.11 Overshoot in dorsal striatum and NAcc. A representative example of a fast profile recorded in the dorsal striatum (red) and NAcc (blue) using the same carbon fiber electrode in a single rat. The symbols mark where the stimulus begins and ends. Overshoot was observed in the NAcc but not in the dorsal striatum.

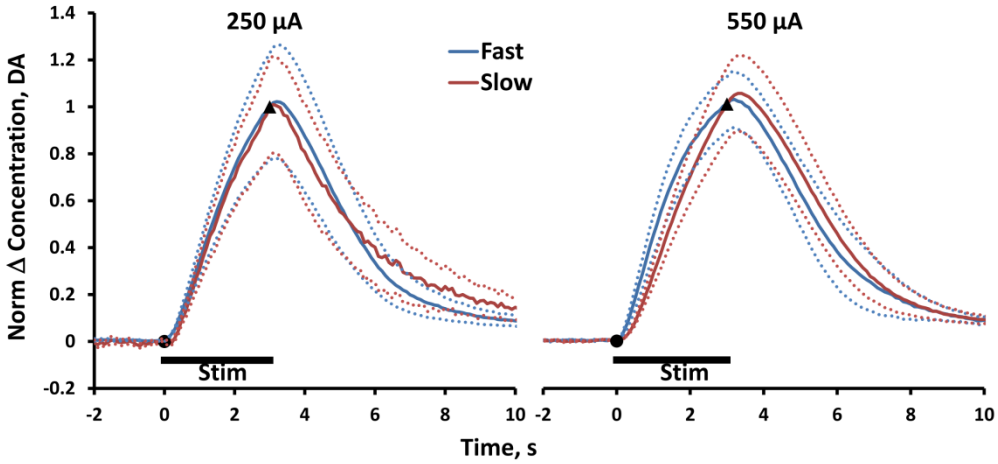

Figure II.12 Time course of DA clearance in the NAcc. The solid lines are the averages of fast (blue, n=4 rats) and slow (red, n=6 rats) profiles recorded at a stimulus intensity of 250 μA (left) and 550 μA (right). The profiles are normalized with respect to the DA amplitude recorded at the end of each 3-s stimulus. The dotted lines report the standard error of the means. This format of presentation demonstrates that the time course of DA clearance in the fast and slow domains is indistinguishable.

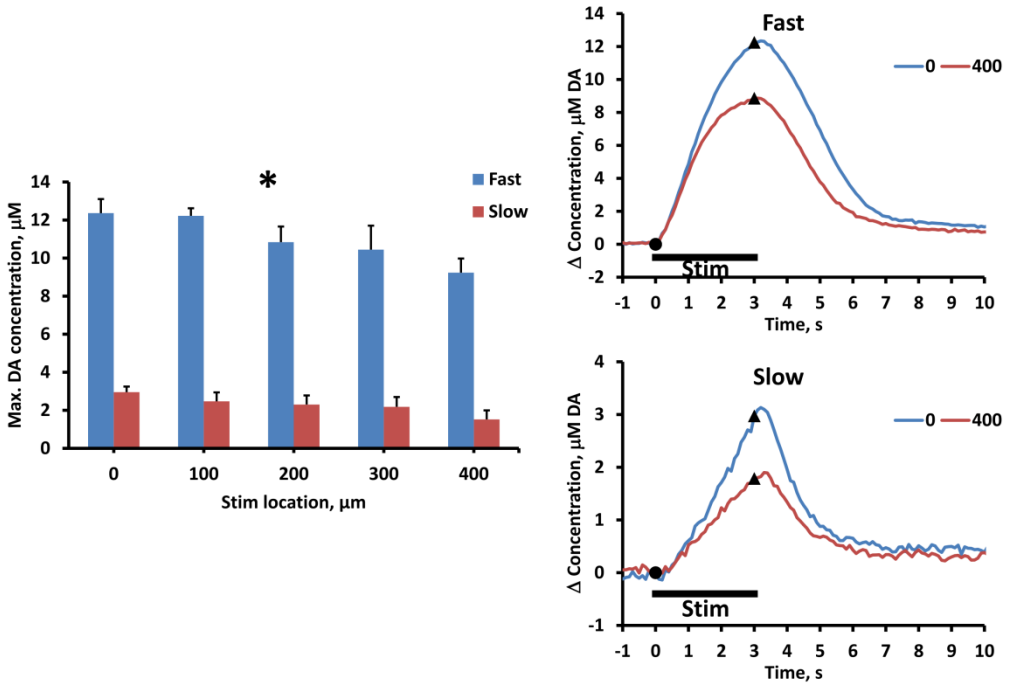

Figure II.13 The placement of the stimulating electrode does not determine whether recording sites exhibit fast or slow profiles. Evoked responses were recorded in the NAcc at 5-min intervals (60 Hz, 250 µA, 3-s). The stimulating electrode was lowered by 100 µm between each stimulus. The maximum DA amplitude observed in fast (n=3 rats) and slow (n=4 rats) domains (mean ± SEM) are plotted on the left: both the domain and the stimulus location were significant factors (two-way ANOVA with repeat measures design, domain factor $F_{(1,5)} = 144.572$; n = 7; $p = 0.00007$, stimulus location factor $F_{(4,20)} = 10.211$; $p = 0.0001$). The stimulus location was only a significant factor due to the lower amplitude observed when the stimulating electrode had been lowered by 400 µm from its original depth: this is most likely due to disruption of the MFB by the stimulating electrode. If results from the 400-µm location are omitted from the analysis, the stimulus location is not a significant factor. On the right, two representative profiles show the essential features of the fast and slow profiles are preserved when the stimulating electrode is lowered through the MFB.

CHAPTER III. REGION- AND DOMAIN-DEPENDENT ACTION OF NOMIFENSINE

Adapted with revision from Zhan Shu, I. Mitch Taylor, Seth H. Walters and Adrian C. Michael (2014) *European Journal of Neuroscience*, 40, 2320-2328.

A. INTRODUCTION

Dopamine (DA) is crucial to the motor, motivation, and reward related functions of the central nervous system (Johnson & Kenny, 2010; Jenkinson & Brown, 2011; Volkow et al., 2011). DA neurotransmission is initiated by the release of DA molecules and terminated by their reuptake via the dopamine transporter (DAT). The spatiotemporal dynamics of DA's extracellular concentration, and therefore the extent and duration of DA receptor stimulation, are intricately determined by the kinetics of DA release and clearance as well as the mass transport of DA through the extracellular space (Wightman et al., 1988; Garris et al., 1994; Cragg & Rice, 2004; Taylor et al., 2012; Taylor et al., 2013). Because numerous drugs that affect DA release and clearance have therapeutic value (Gottwald & Aminoff, 2011; Volkow et al., 2012) and/or abuse potential (Phillips et al., 2003; Hollander & Carelli, 2007), it is highly significant to know how such drugs alter the spatiotemporal dynamics of DA concentrations in the extracellular space.

The psychostimulants cocaine and nomifensine are competitive DAT inhibitors and thus alter DA's extracellular dynamics (Church et al., 1987; Koob & Bloom, 1988; Kuhar et al., 1991). That the actions of such drugs vary between brain regions has been a subject of intense interest. For example, their tendency to preferentially increase measures of extracellular DA in the nucleus accumbens (NAc) compared to the dorsal striatum (DS) conforms well with the central importance of the NAc in the mechanisms of substance abuse (Dichiara & Imperato, 1988; Carboni et al., 1989; Cass et al., 1992; Cass et al., 1993; Wu et al., 2001a). But, the present understanding of this preferential action remains somewhat incomplete because, first, the DS receives the densest dopaminergic innervation in the brain (Bjorklund & Dunnett, 2007), second, as yet there is no clear sign that DAT inhibitors exhibit greater potency in the NAc than DS (Boja & Kuhar, 1989; Izenwasser et al., 1990; Jones et al., 1995b) and, third, as yet there is no clear sign that competitive DAT inhibitors, such as cocaine and nomifensine, preferentially increase the DAT's apparent K_M in the NAc: rather, prior reports suggest that nomifensine acts preferentially in the DS and that cocaine acts non-preferentially (Wu et al., 2001a; Wu et al., 2001b).

We (Shu et al., 2013) have reported that the core of the NAc (NAcc), similarly to the DS (Moquin & Michael, 2009; Wang et al., 2010; Moquin & Michael, 2011), contains a patchwork of DA kinetic domains that respond in unique fashion to electrical stimulation of the medial forebrain bundle. The discovery of these domains leads us to hypothesize that the actions of nomifensine might be domain-dependent within the NAcc, as we previously found to be the case in the DS (Moquin & Michael, 2009; Taylor et al., 2012). So, the objectives of the present study were, first, to test the hypothesis that nomifensine exhibits domain-dependent actions in the NAcc and, second, to compare nomifensine's actions in the NAcc with those in the DS (Taylor et

al., 2013). We report herein for the first time a) that, within the NAcc, nomifensine preferentially promotes evoked DA release in the slow compared to the fast domains and b) that nomifensine preferentially increases the apparent K_M of DA clearance in the NAcc compared to the DS.

B. MATERIALS AND METHODS

1. Solutions, drugs, and reagents

Chemicals were used as-received from the indicated suppliers and solutions were prepared with ultrapure water (NANOPure, Barnstead, Dubuque, IA, USA). Nomifensine maleate (Sigma-Aldrich, St Louis, MO) was dissolved in phosphate buffered saline (137 mM NaCl, 2.7 mM KCl, 1.47 mM KH_2PO_4, 10 mM Na_2HPO_4, pH 7.4). Dopamine hydrochloride (Sigma-Aldrich) was dissolved just before use in artificial cerebrospinal fluid (aCSF, 144 mM NaCl, 1.2 mM $CaCl_2$, 2.7 mM KCl, 1.0 mM $MgCl_2$, 2.0 mM NaH_2PO_4, pH 7.4) and stored under N_2 to prevent DA oxidation. Paraformaldehyde (PFA, 4% in phosphate buffered saline) was prepared from resin (Sigma-Aldrich) and stored at 4 °C before use. Isoflurane was from Baxter Healthcare (Deerfield, IL, USA).

2. Carbon fiber electrodes

Carbon fiber microelectrodes were constructed with 7-μm diameter carbon fibers (T650, Cytec Carbon Fibers, LLC, Piedmont, SC, USA). The fibers were trimmed to a length of 200 μm and immersed in reagent grade isopropyl alcohol (Sigma) for 20 min before use (Bath et al., 2000).

3. Fast-scan cyclic voltammetry (FSCV)

Background subtracted fast-scan cyclic voltammetry (FSCV) was performed with a potentiostat (University of Pittsburgh, Department of Chemistry Electronics Shop), a current amplifier (Keithley 428, Keithley Instruments, Inc., Cleveland, OH, USA), and software (TarHeel CV v4, courtesy of Prof. Michael Heien, Department of Chemistry and Biochemistry, University of Arizona, Tucson, USA (Heien et al., 2003)). Between scans the applied potential was held at 0 V vs. Ag/AgCl. During the scans the voltage was swept linearly to 1.0 V, then to 0.5 V and back to 0 V at 400 V/s: the scan repetition frequency was 10 Hz.

4. Electrode calibration

Electrode calibration was performed using freshly prepared DA solutions before and after in vivo recordings. In vivo dopamine concentrations were determined by post-calibration.

5. Subjects

Subjects were male Sprague-Dawley rats (n = 37, 250-275 g, Hilltop Laboratories, Scottsdale, PA, USA). All procedures involving animals were in accordance with NIH guidelines (publication 86-23) and approved by The Institutional Animal Care and Use Committee of the University of Pittsburgh.

6. Surgery

Surgery was performed as described previously (Shu et al., 2013) under isoflurane anesthesia (5% by vol. initially and 2.5% for maintenance): isoflurane was vaporized (Cyprane Fortec, Fraser Harlake, Inc., Orchard Park, NY) in oxygen and delivered through a ventilator (Harvard Apparatus, Holliston, MA, USA). The anesthetized rats were maintained at 37 °C with a homoeothermic blanket (Harvard Apparatus). Carbon fiber electrodes were first placed into the striatum (A/P +1.2 mm, M/L +1.4 mm, D/V 5.0 mm below dura) (Paxinos & Watson, 1998) and bipolar, stainless-steel stimulating electrodes (MS303/B, Plastics One, Inc., Roanoke, VA, USA) were placed as described before (Ewing et al., 1983; Kuhr et al., 1984; Michael et al., 1987) in the medial forebrain bundle (A/P -4.3 mm, M/L +1.2 mm, D/V from 7.5 below dura: the vertical coordinate was adjusted until evoked release was observed). Finally, without moving the stimulating electrode, the carbon fiber electrodes were slowly lowered into the NAcc (D/V 6.6-7.6 mm below dura).

7. Electrical Stimulation

Electrical stimulation (constant current, biphasic square wave, pulse intensity 250 μA, pulse width 2 ms) was supplied by a pair of stimulus isolators (NL800A, Digitimer, Ltd., Hertfordshire, England). Stimulation was performed at 60, 30 and 15 Hz: details of the train duration are provided in the Results section.

8. Histology

Histological examination was performed as described previously (Peters et al., 2004; Shu et al., 2013) to verify that microelectrodes were correctly placed in the NAcc.

9. Experimental design

Once the recording and stimulating electrodes were in position, stimulus responses were recorded before and 30 min after a single dose of nomifensine (20 mg/kg i.p.) with no alterations in the electrodes, recording location, stimulating location, stimulation parameters, etc. As during our prior study in the DS (Taylor et al., 2012), we compared pre- and post-nomifensine responses in the same group of animals to assure the effect of the drug was established under the same recording and stimulating conditions.

10. Data analysis

Overshoot duration was defined by the time needed after the end of the stimulus for the evoked response to reach its maximum amplitude. The overshoot concentration was the amount by which the dopamine concentration continued to increase after the end of the stimulus. We quantified the apparent K_M of DA clearance by numerically evaluating the derivative of the descending phase of the response and finding the point at which the slope was one-half the corresponding apparent V_{max} reported by Shu et al., 2013. Statistical analyses were by the t-test, two-way analysis of variance (ANOVA) and two-way ANOVA with a repeated measures design (IBM SPSS Statistics 20).

C. RESULTS

Evoked responses reported recorded within the NAcc were objectively identified as fast or slow domains according to the criterion established by Shu et al., 2013 (see Figure II.1 of Chapter II: fast sites produce evoked DA within 200 ms of the start of a stimulus (60 Hz, 250 μA) but slow sites do not). The fast and slow profiles recorded during this study exhibit no statistically significant differences from those recorded in different animals and reported in Figure II.2 of Chapter II (Supplementary Information, Figure III.10). The sites of all NAcc recordings reported herein were confirmed by histology (Supplementary Information, Figure III.11).

1. Format of the presentation of evoked responses

Evoked responses are reported in Figures III.1-4, Figure III.6, and Supplementary Figures III.10 and III.12 in a consistent format (Figure III.7 is in a different format, which is explained below). The solid and dash lines are the averages of responses recorded in groups of rats: the n values, the number of rats per group, are stated in the figure legends. In the main text, solid lines are pre-nomifensine responses from fast and slow domains, and dash lines are post-nomifensine responses: the dotted lines are the ±SEM intervals: black symbols denote when the stimulus begins and ends. The stimulus frequency and duration are stated in the text and in the figure legends: the stimulus current was fixed at 250 μA.

2. Domain-dependent effects of nomifensine: fast domains

Nomifensine affects evoked responses in the NAcc fast domains (Figure III.1, stimulus = 0.2 s, 60 Hz: Figure III.2, stimulus = 1 s, 60 Hz). Nomifensine did not significantly affect the response during the 0.2-s stimulus (Figure III.1b, two-way ANOVA, repeated measures design: nomifensine $F_{(1,12)} = 0.220$, $p > 0.5$) but significantly increased both the duration (Figure III.1c, paired-samples t-test: $p < 0.00005$) and amplitude (Figure III.1d, paired-samples t-test: $p < 0.005$) of the overshoot. Nomifensine did not affect the response during the 1-s stimulus (Figure III.2b, time 0.1 to 1.0 s, two-way ANOVA, repeated measures design: nomifensine $F_{(1,12)} = 2.190$, $p > 0.1$) but significantly increased both the duration (Figure III.2c, paired-samples t-test: $p < 0.0005$) and amplitude (Figure III.2d paired-samples t-test: $p < 0.005$) of the overshoot. Thus, in the NAcc fast domains, nomifensine primarily acts on the overshoot portion of the response to brief stimuli.

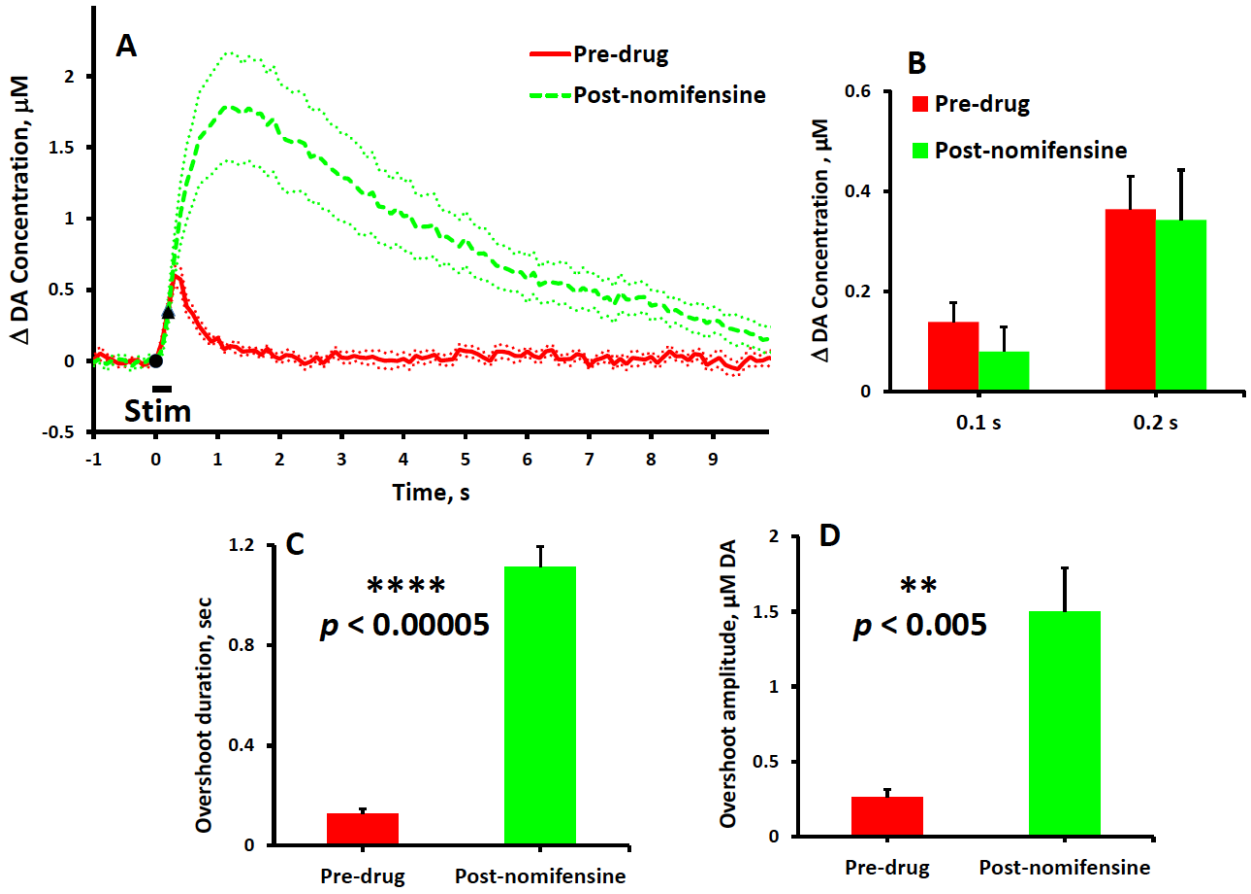

Figure III.1 The effects of nomifensine on evoked DA overflow in fast NAcc domains (stimulus = 0.2 s, 60 Hz, 250 µA). In this and subsequent figures, solid and dash lines show the average of responses recorded in a group of rats and dotted lines show the SEM. Black symbols denote when the stimulus starts and stops. (A) Evoked responses (n = 7) recorded before (solid) and after (dash) nomifensine administration. (B) Nomifensine did not significantly (two-way ANOVA, repeated measures design: nomifensine $F_{(1,12)} = 0.220$, $p > 0.5$) affect the DA overflow during the 0.2 s stimulus. (C & D) Nomifensine significantly increased the duration and amplitude (paired-samples t-tests: $^{**}p < 0.005$, **** $p < 0.00005$) of the stimulus overshoot.

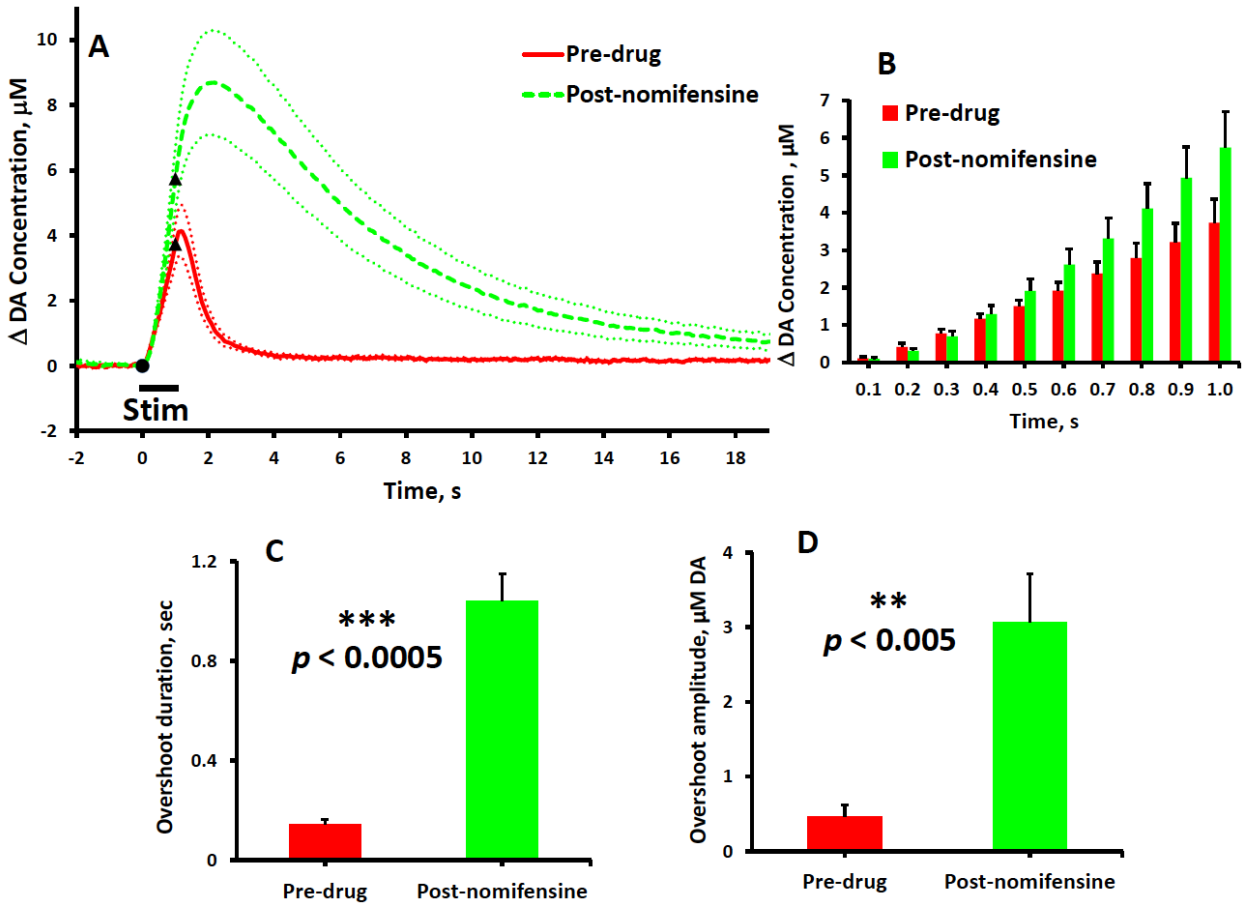

Figure III.2 The effects of nomifensine on evoked DA overflow in fast NAcc domains (stimulus = 1 s, 60 Hz, 250 µA). (A) Evoked responses (n = 7) recorded before (solid) and after (dash) nomifensine administration. (B) Nomifensine did not significantly (time 0.1 to 1.0 s, two-way ANOVA, repeated measures design: nomifensine $F_{(1,12)}$ = 2.190, $p > 0.1$) affect the rate of evoked DA overflow during the stimulus. (C & D) Nomifensine significantly increased the duration and amplitude (paired-samples t-tests: $^{**}p < 0.005$, $^{***}p < 0.0005$) of the stimulus overshoot.

3. Domain-dependent effects of nomifensine: slow domains

Nomifensine affects evoked responses in the NAcc slow domains (Figure III.3, stimulus = 0.2 s, 60 Hz; Figure III.4, stimulus = 1 s, 60 Hz). Before nomifensine, the 0.2-s stimulus evoked no detectable DA overflow. However, after nomifensine the response exhibited a maximal overflow of ~1 μM DA and a duration of ~10 s. The onset of these responses was delayed with respect to the start of the stimulus: in four out of eight cases, the onset of the overflow began after the end of the stimulus. Nomifensine significantly increased the responses during the 1 s stimulus (Figure III.4b, time 0.1 to 1.0 s, two-way ANOVA, repeated measures design: nomifensine $F_{(1,14)} = 6.738$, $p < 0.05$; time & nomifensine interaction $F_{(9,126)} = 8.451$, $p < 0.01$) and significantly increased both the duration (Figure III.4c, paired-samples t-test: $p < 0.0005$) and amplitude (Figure III.4d, paired-samples t-test: $p < 0.005$) of the response overshoot. Thus, nomifensine acts on both DA release during the stimulus and the overshoot of the response in NAcc slow domains.

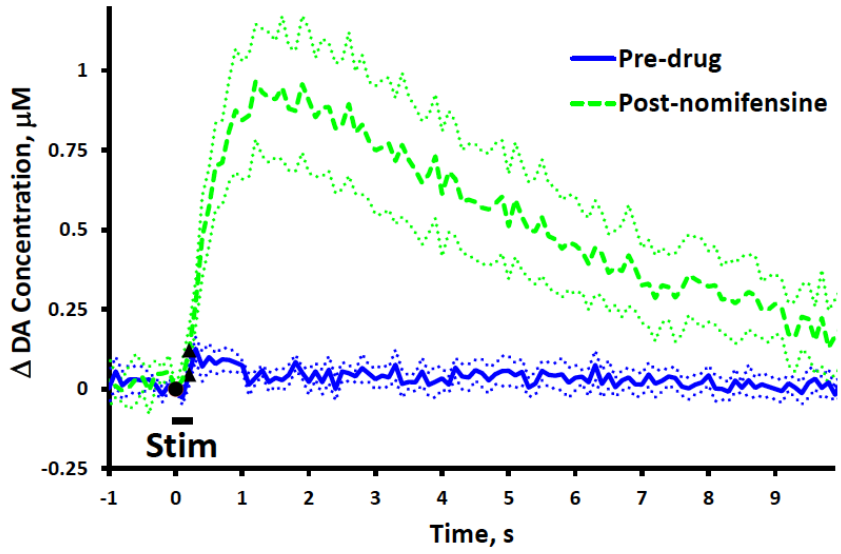

Figure III.3 Evoked responses (n = 8) recorded in slow NAcc domains (stimulus = 0.2 s, 60 Hz, 250 μA) before (solid) and after (dash) nomifensine administration.

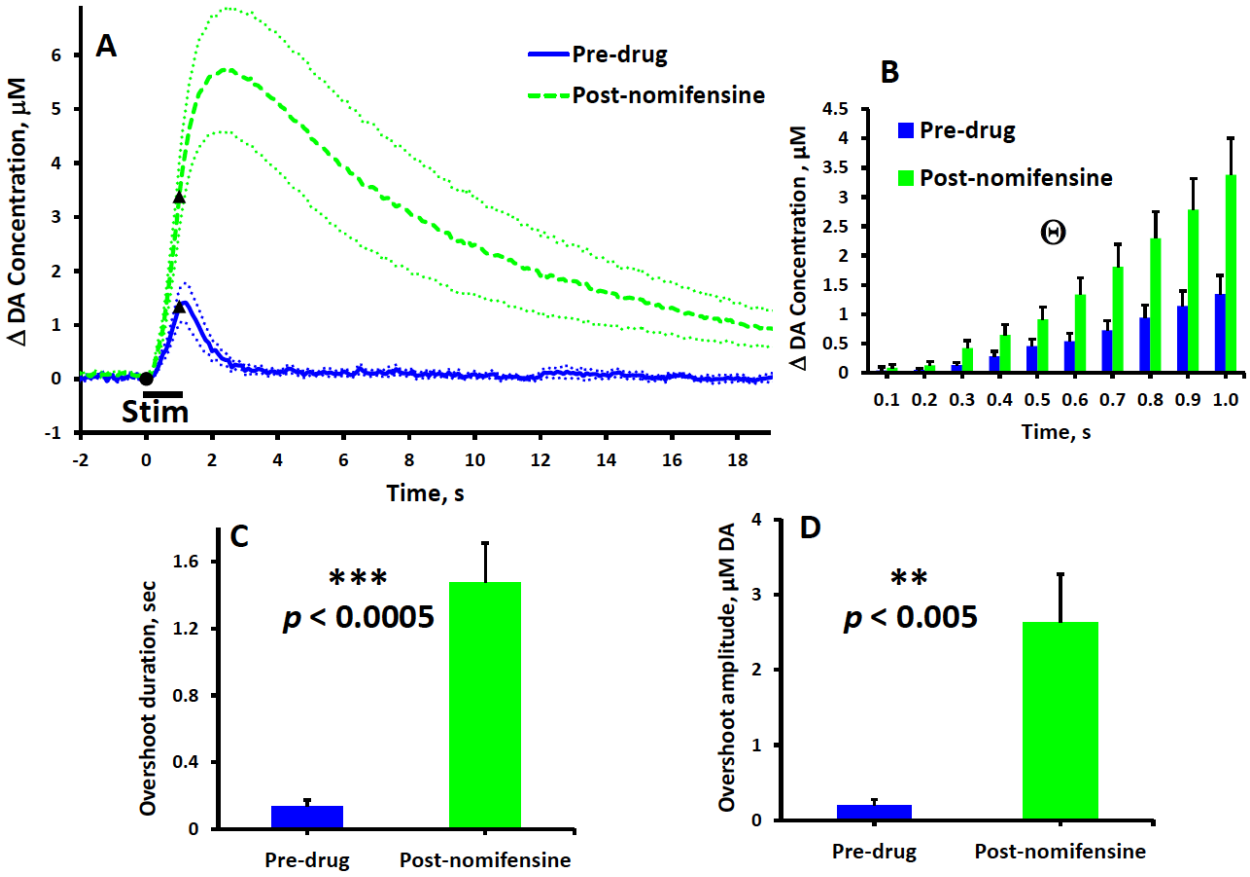

Figure III.4 Effect of nomifensine on evoked DA overflow in slow NAcc domains (stimulus = 1 s, 60 Hz, 250 µA). (A) Evoked responses (n = 8) recorded before (solid) and after (dash) nomifensine administration. (B) Nomifensine significantly (time 0.1 to 1.0 s, Θ two-way ANOVA, repeated measures design: nomifensine $F_{(1,14)} = 6.738$, $p < 0.05$; time & nomifensine interaction $F_{(9,126)} = 8.451$, $p < 0.01$) increased the rate of DA overflow during the stimulus. (C & D) Nomifensine significantly increased the duration and amplitude (paired-samples t-tests: $^{**}p < 0.005$, $^{***}p < 0.0005$) of the stimulus overshoot.

4. Domain-dependent effects of nomifensine: fast and slow comparisons

Within the NAcc, nomifensine preferentially increased three measures of evoked DA release in the slow compared to the fast domains (Figure III.5: the post-nomifensine values of initial rate of DA release and the duration and amplitude of the overshoot are normalized with respect to their pre-nomifensine values). Nomifensine preferentially increased the initial rate of DA release and the duration and amplitude of the overshoot in the slow (Figure III.5, blue bars) compared to the fast domains (Figure III.5, red bars) (Figure III.5a-c, independent-samples t-test: $p < 0.05$). Thus, nomifensine preferentially enhances evoked DA release in the slow NAcc domains.

5. The effects of nomifensine in slow domains during low frequency stimulations

We examined the effect of nomifensine on evoked responses in NAcc slow domains at lower stimulus frequency (Figure III.6). Upon stimulation at 15 Hz, a response was observed only after nomifensine administration (Figure III.6a). Hence, the NAcc slow domain exhibits the same "timing mismatch" phenomenon that we described previously in the slow domains of the DS (Taylor et al., 2013). Upon stimulation at 30 Hz, the pre-nomifensine response exhibited an initial delay of 1-2 s followed by short-term facilitation of evoked release, i.e. the response curved-upward as the stimulation continued (Figure III.6b, solid). Nomifensine eliminated the initial delay and the short-term facilitation but also increased the duration of the overshoot (Figure III.6b, dash). Thus, nomifensine exhibits an asymmetric effect on the temporal features of the DA response: nomifensine decreases the initial delay in the response when the stimulus begins but increases the overshoot when the stimulus ends.

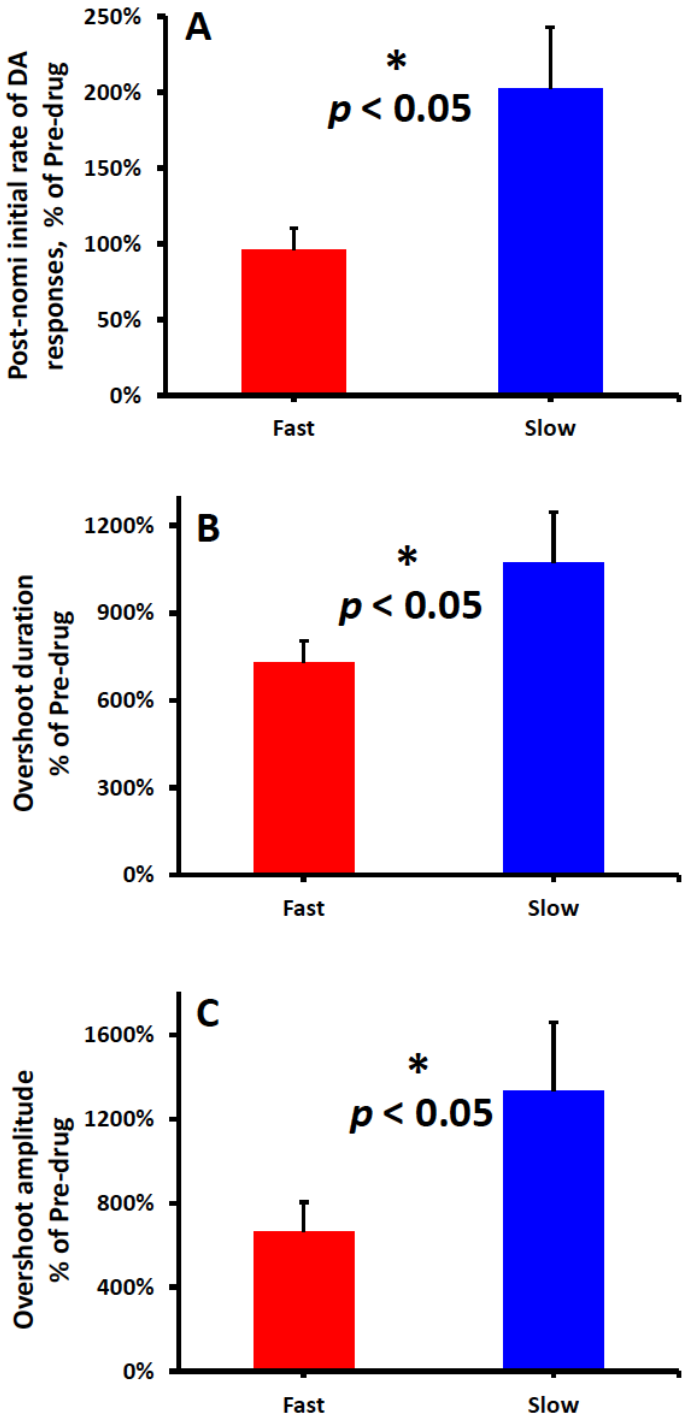

Figure III.5 The normalized effects of nomifensine on the evoked NAcc responses are domain-dependent (stimulus = 1 s, 60 Hz, 250 µA). (A) The initial rate of DA overflow (fast: 0-0.3s, slow: 0.3-0.5s), (B) the overshoot duration, and (C) the overshoot amplitude are reported here normalized with respect to their pre-nomifensine values. (A-C) Nomifensine preferentially increased the initial rate of DA release and the duration and amplitude of the overshoot in the slow (blue bars) compared to the fast domains (red bars) (independent-samples t-tests: *$p < 0.05$).

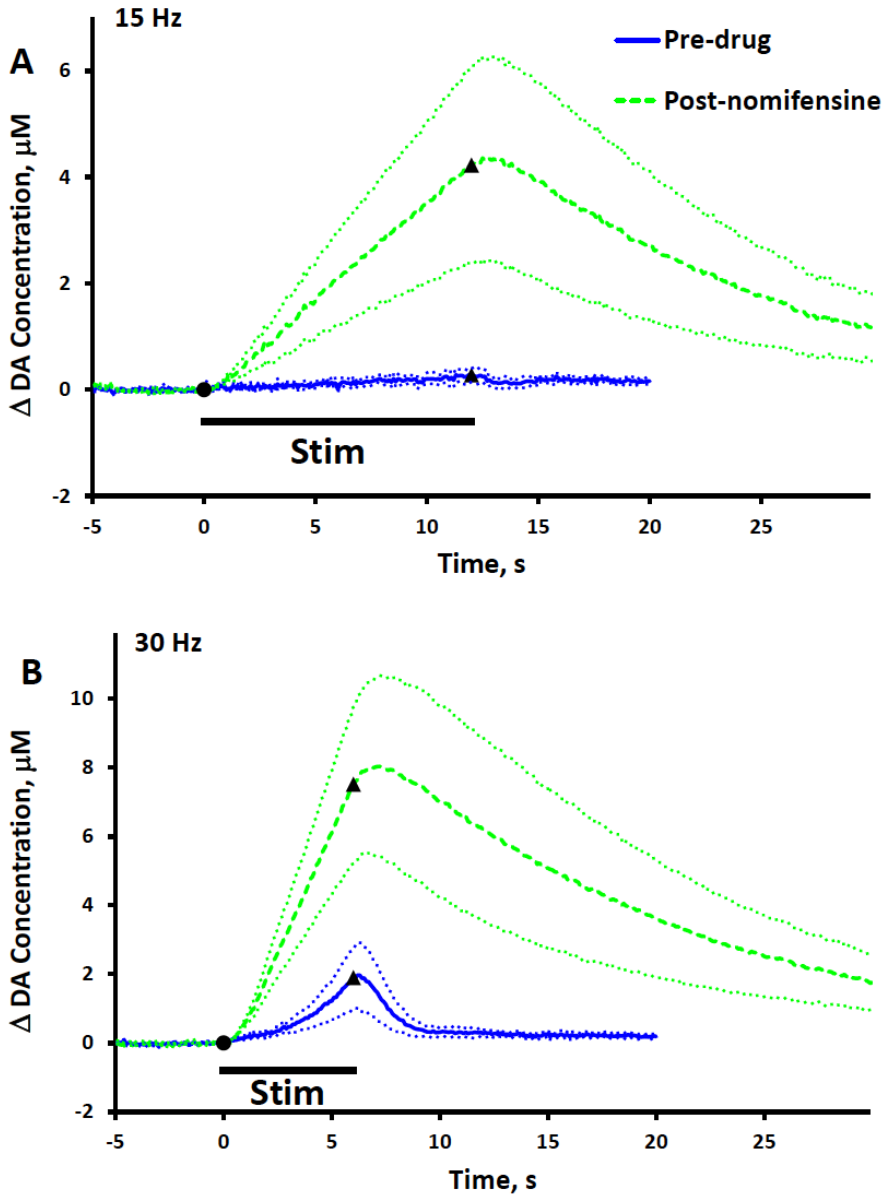

Figure III.6 Evoked responses (n = 5) recorded in NAcc slow domains before (solid) and after (dash) nomifensine administration (A, stimulus = 180 pulses, 15 Hz, 250 µA: B, stimulus = 180 pulses, 30 Hz, 250 µA).

6. Comparison of DA's NAcc dynamics after nomifensine: 0.2 s responses

It is relevant (see Discussion) to compare the dynamics of the post-nomifensine fast and slow responses (Figure III.7). Figure III.7 compares the 0.2 s slow post-nomifensine response (dash) to the 0.2 s fast post-nomifensine response after subtraction of the fast pre-nomifensine response (solid), both normalized to their respective maximum amplitude. The intention of subtracting the fast pre-response from the fast-post response is to isolate the nomifensine-induced overshoot component: this subtraction was not necessary in the case of the slow response because the pre-response was non-detectable. The nomifensine-induced overshoots observed in fast and slow domains are essentially identical (Figure III.7).

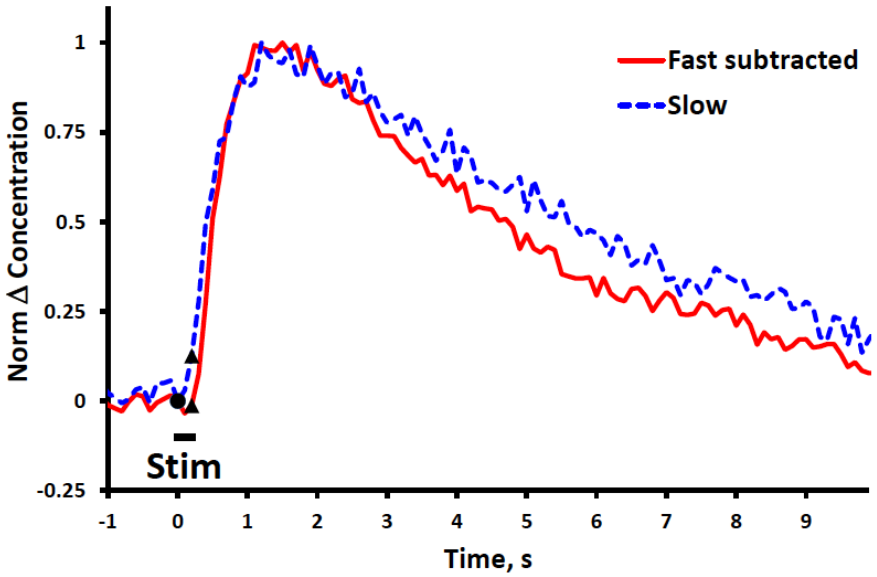

Figure III.7 Comparison of "pure overshoots" observed in fast (solid) and slow (dash) NAcc domains after nomifensine administration (stimulus = 0.2 s, 60 Hz, 250 μA). The blue line was obtained from Figure III.1a by subtracting the pre-drug response from the post-nomifensine response (see also Figure 9 of Taylor et al., 2012). The dash line is from Figure III.3. The two responses are normalized to their maximum amplitudes to enable comparison of their temporal features (SEMs omitted for clarity).

7. Nomifensine's impact on the apparent K_M of the DAT

We quantified the apparent K_M of DA clearance by numerically evaluating the derivative of the descending phase of the responses. For this purpose, we found it necessary to extend the stimulus duration to 3 s to ensure that the rate of clearance exceeded the one-half V_{max} values (see Supplementary Information: the 3-s responses are reported in Figure III.12 and the individual apparent K_M values are reported in Figure III.13). To gauge the effects of nomifensine, we normalized the post-nomifensine apparent K_M values with respect to their pre-nomifensine magnitude (Figure III.8). Nomifensine significantly increased all four apparent K_M values. The increase in apparent K_M was significantly larger in the NAcc (~500%) than in the DS (~200%) but was not domain-dependent (two-way ANOVA: regions $F_{(1,20)} = 13.213$, $p < 0.002$, domains $F_{(1,20)} = 0.932$, $p > 0.3$). To our knowledge, this is the first report of a preferential kinetic action of a DAT inhibitor in the NAcc compared to the DS.

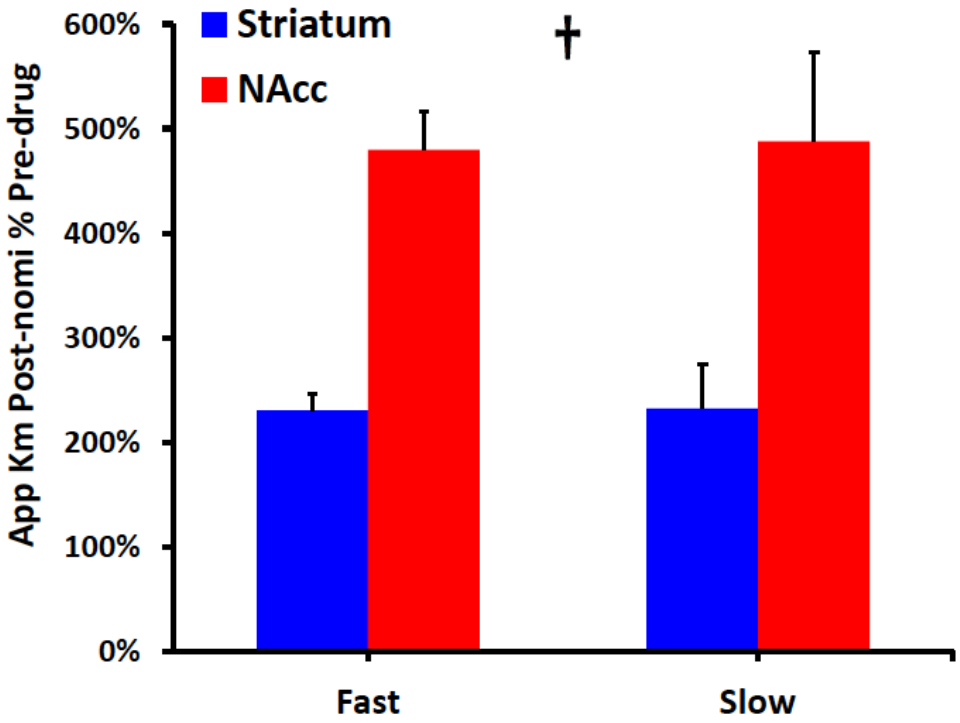

Figure III.8 Comparison of apparent K_M values obtained in fast and slow domains in the NAcc (red) and DS (blue). The post-nomifensine apparent K_M values are normalized with respect to the pre-drug values. The normalized values are region-dependent and domain-independent († two-way ANOVA: regions $F_{(1,20)} = 13.213$, $p < 0.002$; domains $F_{(1,20)} = 0.932$, $p > 0.3$).

8. Color plots

In order to acquiesce to the demands of two reviewers of this report, we provide 3-dimensional color plots of the FSCV data for the 1-s stimulus responses recorded before and after administration of nomifensine in the fast domains of the NAcc in Figure III.9 (more color plots see Supporting Information Figure III.14). These color plots, which provide no additional information over that which has already been stated above, show the FSCV data in a voltage-versus-time coordinate with current represented by a color scale. To prepare these plots, we normalized the background-subtracted FSCV currents with respect to each electrode's post-calibration sensitivity factor and averaged the results across the group of animals (n = 7). The plots show the dopamine oxidation peak, the quinone reduction peak, and background noise.

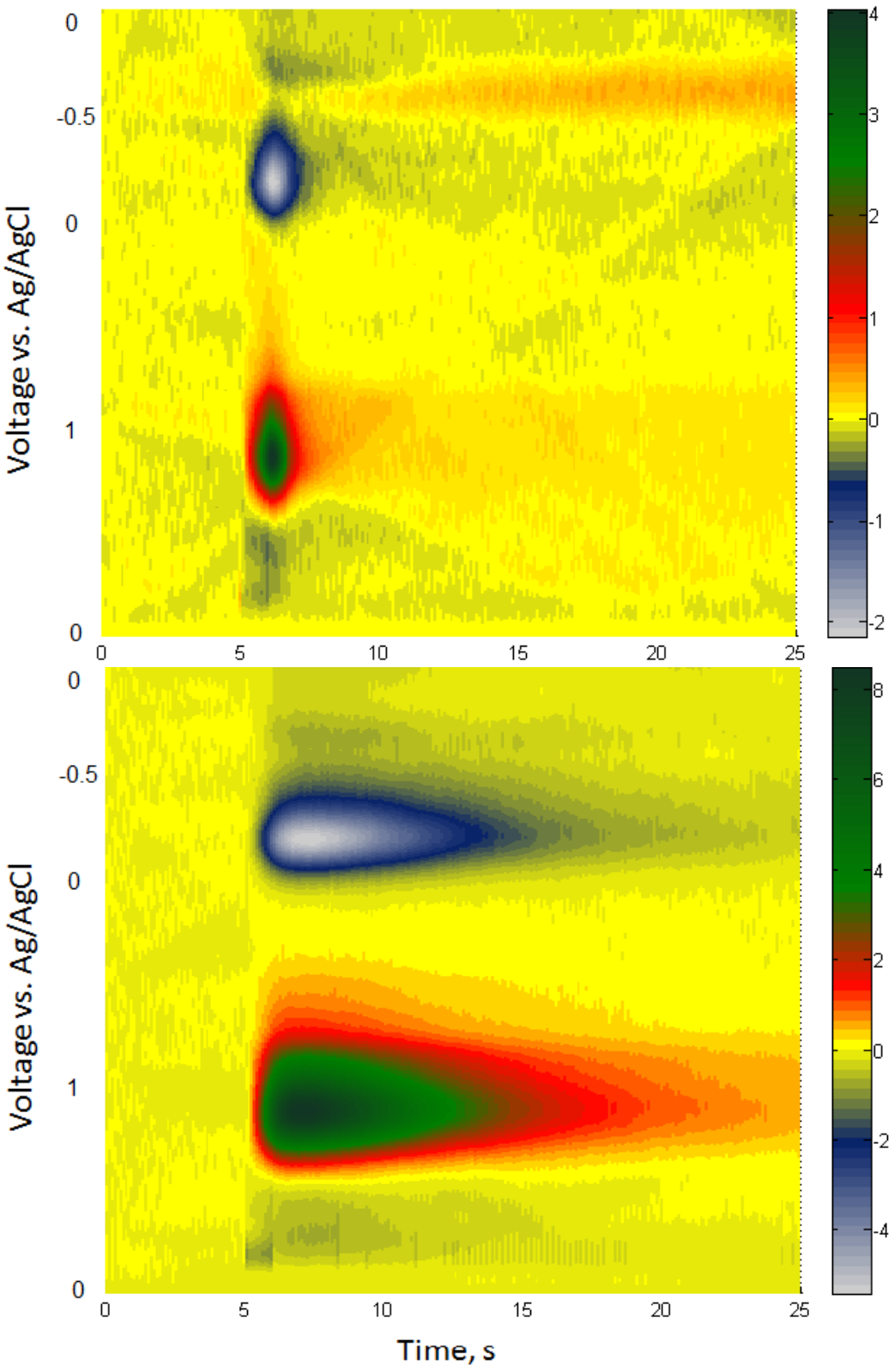

Figure III.9 Color plot (see text for explanation) of the FSCV data recorded during a 1-s stimulus (A) before and (B) after administration of nomifensine in fast NAcc domains.

D. DISCUSSION

The domain-dependent evoked DA responses (pre-nomifensine) recorded in the NAcc are not statistically different from those reported previously by Shu et al. (2013, see Supplementary Figure III.10), confirming that the NAcc domains are preserved across groups of animals. As in the DS (Taylor et al., 2012), nomifensine exerts robust and domain-dependent actions on evoked responses in the NAcc (Figures III.1-6). Together with our previous DS results (Taylor et al., 2012), the present study provides a comprehensive evaluation of both the region-dependent and domain-dependent actions of a DAT inhibitor, for the first time.

1. Summary of nomifensine's actions in the NAcc

When stimulation is delivered at 60 Hz in relatively brief trains (0.2 or 1 s, Figures III.1-4), nomifensine increases both the duration and amplitude of the response overshoot in both domains. In the case of the 0.2 s stimulus trains, the post-nomifensine maximum DA signal in the fast domain was more than 400% of the pre-nomifensine maximum amplitude and the overshoot duration was ~500% longer than the stimulus. In the slow domain, the pre-nomifensine response to the 0.2 s stimulus train was non-detectable (Figure III.3), so the post-nomifensine response is predominantly overshoot. Interestingly, the temporal features of the overshoots in the fast and slow domains are essentially identical (Figure III.7). Nomifensine significantly increased the DA concentrations observed during the 1-s stimulus trains in the slow domains, but not in the fast domains.

2. Nomifensine preferentially acts on NAcc slow domains compared to fast domains

With a 1-s stimulus, it was possible to quantify the initial rate of evoked DA release as well as the duration and amplitude of the overshoots in fast and slow domains under consistent experimental conditions. We normalized the post-nomifensine values with respect to their pre-nomifensine values (Figure III.5). All three measures of evoked DA release were significantly larger in the slow domain. We therefore conclude that nomifensine acts preferentially on evoked DA release in the NAcc slow domains compared to the NAcc fast domains. We report this phenomenon here for the first time.

Taylor et al. (2012) reported the domain-dependent actions of nomifensine on evoked DA release in the DS. There are notable differences between the NAcc and DS. First, nomifensine had a much larger effect on the initial rate of DA release in the DS slow domains (~800%) than the NAcc slow domains (~200%). In contrast with the NAcc, nomifensine's actions on the duration and amplitude of the DS overshoot were largest in the fast domains. Thus, we report here for the first time that the domain-dependent actions of nomifensine are also region-dependent. These findings add to the view that the domains of the NAcc and DS are truly distinct from one other, reinforcing the concept that DA kinetics are both region and domain dependent.

3. Nomifensine's actions on the apparent K_M of DA uptake: considerations

As a competitive DAT inhibitor, nomifensine's primary pharmacological action is to change the apparent K_M of DA uptake. However, DAT inhibitors have additional secondary actions. For example, in anesthetized animals, DAT inhibition decreases the firing rate of DA neurons via

indirect agonism of the D2 receptors (Studer & Schultz, 1987; Einhorn et al., 1988; Mercuri et al., 1991), while in non-anesthetized animals DAT inhibitors induce phasic DA events (Aragona et al., 2008) and burst firing of DA neurons (Koulchitsky et al., 2012). Here, however, we wish to evaluate nomifensine's primary action by determining the apparent K_M of DA clearance. To do so, however, requires consideration of how to go about extracting apparent K_M information from evoked responses.

In several previous reports, K_M values were quantified by means of a numerical model that simulates the evoked responses (Wightman et al., 1988; Jones et al., 1995a; Wu et al., 2001a; Wu et al., 2001b). The model assumes that a gap, or a physical space, is interposed between the recording electrode and nearby DA terminals: such a gap is expected to cause diffusional distortion of the evoked responses. However, as we have explained before (Moquin & Michael, 2009; Taylor et al., 2012), the observed features of evoked responses in the DS cast doubt on the diffusion gap distortion model, which in turn, casts doubt on the kinetic values obtained via simulation. We now report that the same issue arises in the NAcc.

A diffusion gap is predicted to cause two types of temporal distortion of the evoked responses; an initial lag in the DA signal when the stimulus begins and an overshoot of the DA signal after the stimulus ends. A diffusion gap would necessarily cause these distortions to go hand-in-hand: if there is an initial lag, there must also be an overshoot, and vice versa. However, in both the DS and NAcc, responses with overshoot but without initial lag are entirely commonplace. In fast domains, for example, DAT inhibition leads to prominent overshoot but no obvious lag. According to the diffusion gap model, this should not be.

A modified diffusion gap model described by Venton et al., (2003) hypothesized that DAT inhibition increases the apparent dimension of the diffusion gap, invoking the concept that

DAT inhibition extends DA's lifetime in the extracellular space and so enables it to diffuse further. The evoked responses do not support this hypothesis:

First, both in the DS and the NAcc, DAT inhibition diminishes the initial lag in slow domains, this effect being most obvious at low stimulus frequencies (Figure III.6; see also Figure 5 of Taylor et al., 2013). This observation directly contradicts the hypothesis that DAT inhibition increases the apparent diffusion gap. Moreover, the rapid onset of the post-nomifensine responses confirms the presence of DA terminals in close proximity to the recording electrode, which shows that there is no diffusion gap to cause diffusional distortion. Rather than diffusional distortion, we conclude that the temporal features of the evoked responses reflect the local activity of DA terminals in the immediate vicinity of the recording site.

Second, our findings do not provide clear evidence that DA's diffusion distance post-nomifensine is domain dependent (Figure III.7). Originally, responses with prominent initial lag were attributed to a poor choice of recording site with a large diffusion gap interposed between the electrode and its nearest-neighbor DA terminals (Kuhr et al., 1987; Engstrom et al., 1988; Wightman et al., 1988). Likewise, responses without lag were attributed to small gaps and minimal diffusional distortion. In that case, however, then the different gap sizes would necessarily produce distinct temporal profiles, regardless of experimental conditions. After nomifensine, however, this is simply not what is observed (see Figure III.7, above, and Figure 9 of Taylor et al., 2012): the essentially identical appearance of the post-nomifensine overshoots would be impossible if the fast and slow responses were caused by different gaps.

4. Nomifensine's actions on the apparent K_M of DA uptake: the analysis

Because our findings do not confirm the presence of a diffusion gap, we chose to quantify apparent K_M directly from the slope of the descending phase of the response. The advantage of slope analysis is that makes no mass transfer assumptions. However, the kinetic parameters obtained by slope analysis are clearly not the intrinsic, biophysical parameters of the DAT per se. Nevertheless, if it is to be assumed, as is generally the case, that the DA signal at the electrode is a useful analog of DA neurotransmission, then the apparent values are of great interest for the clear, simple, and logical reason that mass transport delivers DA molecules not only to the recording electrodes but also to their pre- and post-synaptic targets.

Nomifensine significantly increases the apparent K_M in both the fast and slow domains of both the NAcc and DS: this is an expected result because nomifensine is a competitive inhibitor. However, nomifensine preferentially increases the apparent K_M in the NAcc compared to the DS (Figure III.8), a phenomenon we report here for the first time. Interestingly, although the effect of nomifensine on apparent K_M is clearly region-dependent, it is not domain-dependent: the proportional increase in apparent K_M was similar in the fast and slow domains of each region (Figure III.8). Thus, the change in apparent K_M may not by itself explain all the region and domain dependent actions of nomifensine on DA release. But, as mentioned above, DAT inhibitors have secondary pharmacological effects.

E. CONCLUSION

This study reaffirms the presence of a patchwork of DA kinetic domains within the NAcc and establishes that nomifensine's actions within the NAcc are domain dependent. Nomifensine preferentially enhances three measures of DA release in the NAcc slow domains compared to the NAcc fast domains: the rate of initial release as well as the duration and amplitude of the overshoot. In this respect, the domain-dependent actions of nomifensine are distinct from those in the DS. Moreover, nomifensine preferentially increases the apparent K_M of DA clearance in the NAcc compared to the DS, and this preferential effect was domain-independent. This first report of a preferential kinetic effect of a DAT inhibitor in the NAcc is in good accord with prior literature showing that DAT inhibitors preferentially affect the NAc compared to the DS.

F. SUPPORTING INFORMATION

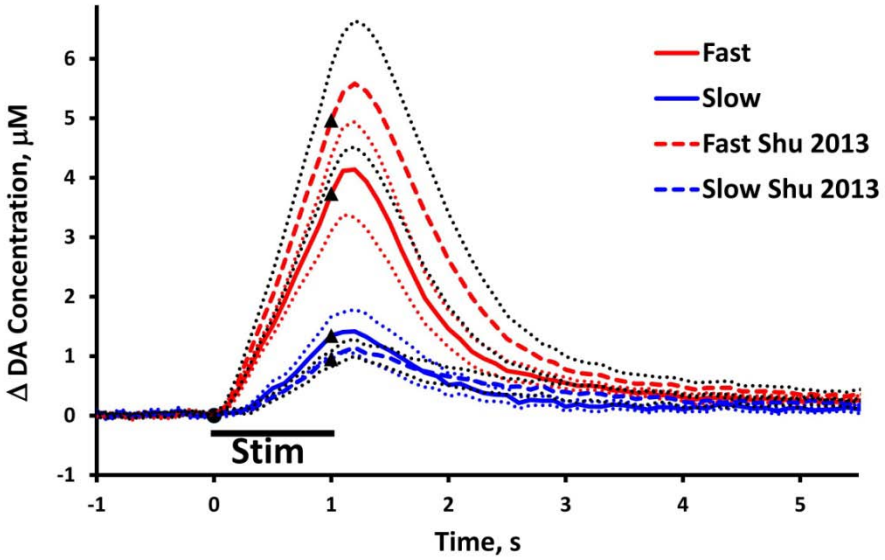

Figure III.10 The domain-dependent evoked DA responses are consistent across animals. Evoked DA responses recorded in the present group of subjects (solid lines) are not significantly different from those we reported previously (dash lines with black dots as SEM, Figure II.2 in Chapter II) in both fast (two-way ANOVA with a repeated measures design from 0.1 to 2.9s, $p > 0.3$) and slow (two-way ANOVA with a repeated measures design from 0.1 to 2.9s, $p > 0.5$) domains. The recording locations were objectively identified as corresponding to fast or slow domains on the basis of the amplitude of evoked DA release during the first 200 ms of the stimulus, as thoroughly explained in Chapter II.

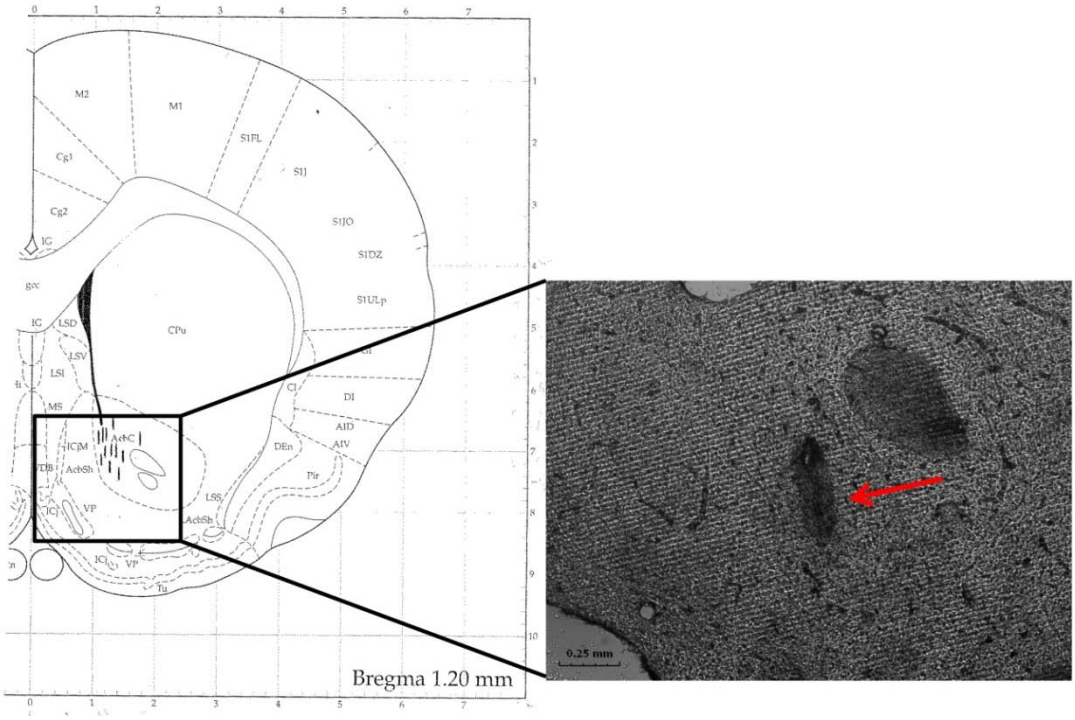

Figure III.11 Representative microelectrode placements in the NAcc. One representative electrical lesion (arrow) on the brain slice is enlarged on the right side. Scale bar: 250 µm.

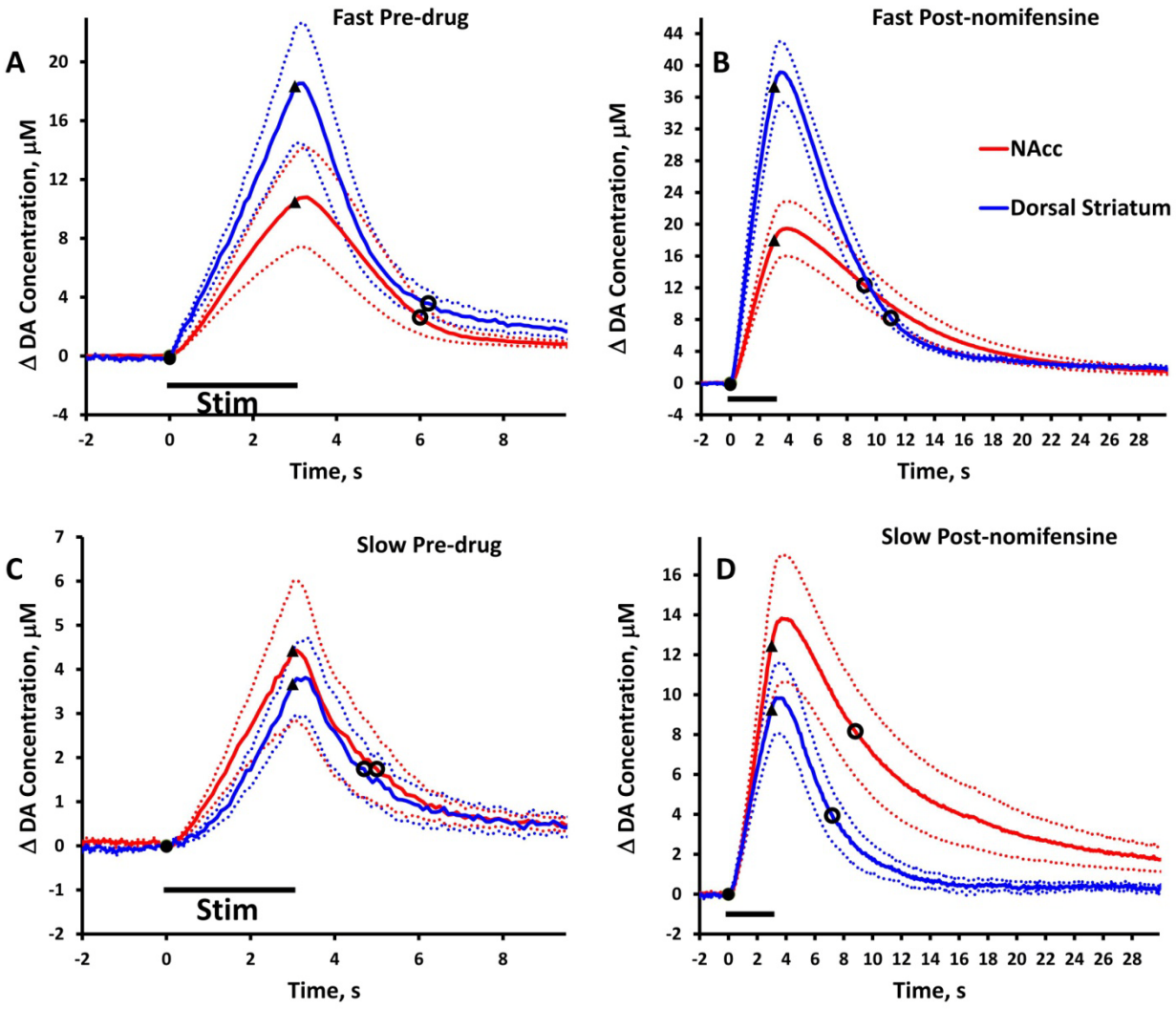

Figure III.12 Slope analysis to extract apparent K_M values. (A&B) Pre- and post-nomifensine responses recorded in fast domains (average ± SEM, NAcc n = 7, DS n = 6) and (C&D) slow domains (average ± SEM, NAcc n = 7, DS n = 8) in the NAcc (red) and DS (blue) (stimulus = 3 s, 60 Hz, 250 µA). The black circles indicate the average apparent K_M values of DA clearance (see details in Figure III.13, Discussion and Figure III.8).

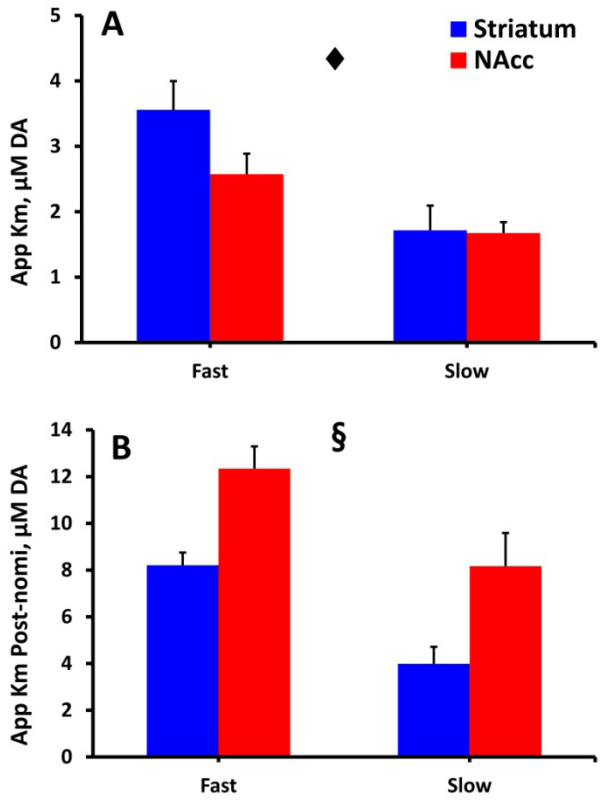

Figure III.13 Comparison of apparent K_M values obtained in fast and slow domains in the NAcc (red) and DS (blue). Apparent K_M values of DA clearance are measured from the responses in Figure III.12 and reported as the average ± SEM. (A) In the pre-drug condition, the apparent K_M of DA clearance is domain- but not region-dependent (◆ two-way ANOVA domains $F_{(1,20)} = 16.257$, $p < 0.001$, regions $F_{(1,20)} = 2.276$, $p > 0.14$). (B) Post-nomifensine, the apparent K_M of DA clearance is domain- and region-dependent (**§** two-way ANOVA domains $F_{(1,20)} = 18.989$, $p < 0.0005$, regions $F_{(1,20)} = 18.606$, $p < 0.0005$).

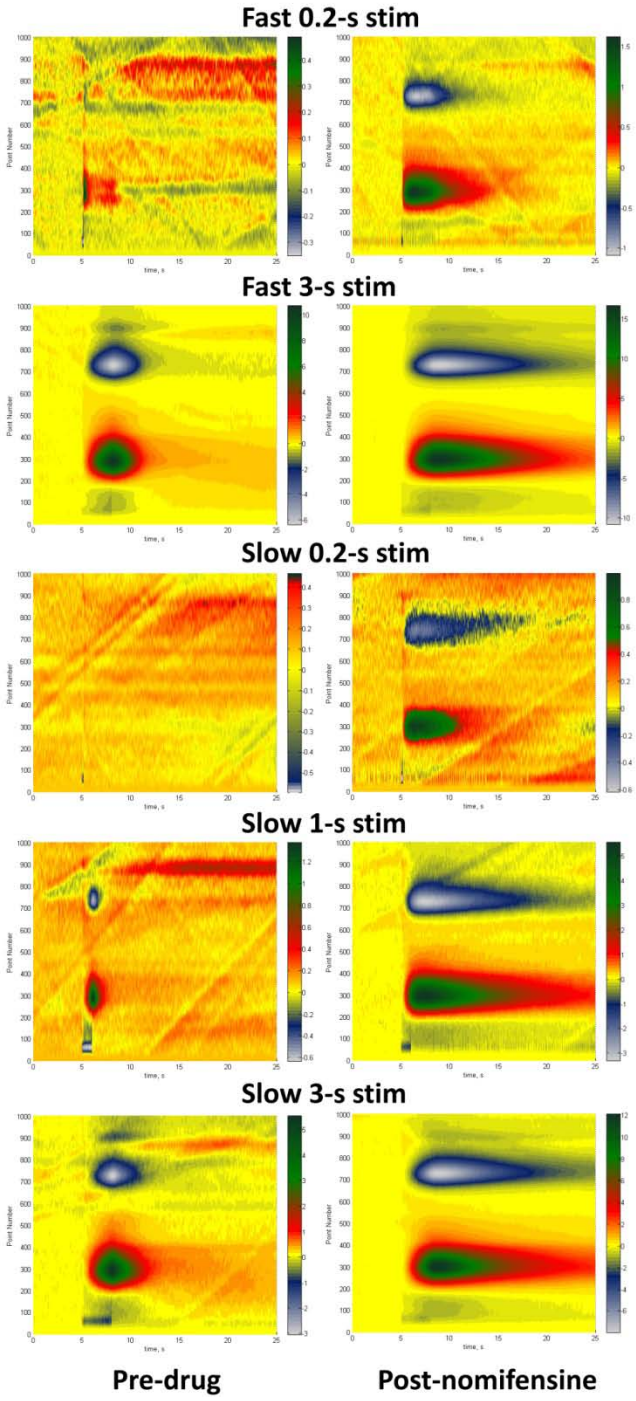

Figure III.14 3-dimensional color plots of the FSCV data. To prepare these plots, we normalized the background-subtracted FSCV currents collected before (left) and after (right) the administration of nomifensine with respect to each electrode's post-calibration sensitivity factor and averaged the results across the group of animals (Fast: n=7, Slow: n=8).

BIBLIOGRAPHY

Abi-Dargham, A., Rodenhiser, J., Printz, D., Zea-Ponce, Y., Gil, R., Kegeles, L.S., Weiss, R., Cooper, T.B., Mann, J.J., Van Heertum, R.L., Gorman, J.M. & Laruelle, M. (2000) Increased baseline occupancy of D-2 receptors by dopamine in schizophrenia. P. Natl. Acad. Sci. USA, 97, 8104-8109.

Addy, N.A., Daberkow, D.P., Ford, J.N., Garris, P.A. & Wightman, R.M. (2010) Sensitization of Rapid Dopamine Signaling in the Nucleus Accumbens Core and Shell After Repeated Cocaine in Rats. J. Neurophysiol., 104, 922-931.

Alderson, P. & Roberts, I. (1997) Corticosteroids in acute traumatic brain injury: systematic review of randomised controlled trials. BMJ, 314, 1855-1859.

Aragona, B.J., Cleaveland, N.A., Stuber, G.D., Day, J.J., Carelli, R.M. & Wightman, R.M. (2008) Preferential enhancement of dopamine transmission within the nucleus accumbens shell by cocaine is attributable to a direct increase in phasic dopamine release events. J Neurosci, 28, 8821-8831.

Arbuthnott, G. W. and Wickens, J. (2007) Space, time and dopamine. Trends Neurosci, 30, 62-69.

Ariansen, J.L., Heien, M.L., Hermans, A., Phillips, P.E., Hernadi, I., Bermudez, M.A., Schultz, W. & Wightman, R.M. (2012) Monitoring extracellular pH, oxygen, and dopamine during reward delivery in the striatum of primates. Front Behav. Neurosci., 6, 36.

Bath, B.D., Michael, D.J., Trafton, B.J., Joseph, J.D., Runnels, P.L. & Wightman, R.M. (2000) Subsecond adsorption and desorption of dopamine at carbon-fiber microelectrodes. Anal. Chem., 72, 5994-6002.

Baur, J.E., Kristensen, E.W., May, L.J., Wiedemann, D.J. & Wightman, R.M. (1988) Fast-Scan Voltammetry of Biogenic-Amines. Anal. Chem., 60, 1268-1272.

Becker, J.B. & Cha, J.H. (1989) Estrous cycle-dependent variation in amphetamine-induced behaviors and striatal dopamine release assessed with microdialysis. Behavioural Brain Research, 35, 117-125.

Benoit-Marand, M., Borrelli, E. & Gonon, F. (2001) Inhibition of dopamine release via presynaptic D2 receptors: time course and functional characteristics in vivo. J. Neurosci., 21, 9134-9141.

Benveniste, H. & Diemer, N.H. (1987) Cellular reactions to implantation of a microdialysis tube in the rat hippocampus. Acta. Neuropathol., 74, 234-238.

Benveniste, H., Hansen, A.J. & Ottosen, N.S. (1989) Determination of brain interstitial concentrations by microdialysis. J. Neurochem., 52, 1741-1750.

Berger, C., Schabitz, W.R., Georgiadis, D., Steiner, T., Aschoff, A. & Schwab, S. (2002) Effects of hypothermia on excitatory amino acids and metabolism in stroke patients: a microdialysis study. Stroke, 33, 519-524.

Bjorklund, A. & Dunnett, S.B. (2007) Dopamine neuron systems in the brain: an update. Trends Neurosci, 30, 194-202.

Boja, J.W. & Kuhar, M.J. (1989) [H-3] Cocaine Binding and Inhibition of [H-3] Dopamine Uptake Is Similar in Both the Rat Striatum and Nucleus Accumbens. Eur J Pharmacol, 173, 215-217.

Borland, L.M. & Michael, A.C. (2004) Voltammetric study of the control of striatal dopamine release by glutamate. J. Neurochem., 91, 220-229.

Borland, L.M. & Michael, A.C. (2007) An Introduction to Electrochemical Methods in Neuroscience. CRC Press. Boca Raton, FL.

Borland, L.M., Shi, G., Yang, H. & Michael, A.C. (2005) Voltammetric study of extracellular dopamine near microdialysis probes acutely implanted in the striatum of the anesthetized rat. J. Neurosci. Methods, 146, 149-158.

Bosche, B., Dohmen, C., Graf, R., Neveling, M., Staub, F., Kracht, L., Sobesky, J., Lehnhardt, F.G. & Heiss, W.D. (2003) Extracellular concentrations of non-transmitters amino acids in peri-infact tissue of patients predict malignant middle cerebral artery infarction. Stroke, 34, 2908-2915.

Bradberry, C.W., Barrett-Larimore, R., L.,, Jatlow, P. & Rubino, S., R. (2000) Impact of Self-Administered Cocaine and Cocaine Cues on Extracellular Dopamine in Mesolimbic and Sensorimotor Striatum in Rhesus Monkeys. J.Neurosci., 20, 3874-3883.

Bradberry, C.W., Nobiletti, J.B., Elsworth, J.D., Murphy, B., Jatlow, P. & Roth, R.H. (1993) Cocaine and Cocaethylene: Microdialysis Comparison of Brain Drug Levels and Effects on Dopamine and Serotonin. J. Neurochem., 60, 1429-1435.

Bungay, P.M., Morrison, P.F., Dedrick, R.L., Chefer, V.I. & Zapata, A. (2007) Principles of quantitative microdialysis. In Westerink, B.H.C., Cremers, T.I.F.H. (eds) Handbook of microdialysis: methods, applications, and perspectives. Elsevier, Amsterdam, 131-167.

Bungay, P.M., Newton-Vinson, P., Isele, W., Garris, P.A. & Justice, J.B. (2003) Microdialysis of dopamine interpreted with quantitative model incorporating probe implantation trauma. J. Neurochem., 86, 932-946.

Cahill, P.S., Walker, Q.D., Finnegan, J.M., Mickelson, G.E., Travis, E.R. & Wightman, R.M. (1996) Microelectrodes for the measurement of catecholamines in biological systems. Anal. Chem., 68, 3180-3186.

Carboni, E., Imperato, A., Perezzani, L. & Dichiara, G. (1989) Amphetamine, Cocaine, Phencyclidine and Nomifensine Increase Extracellular Dopamine Concentrations Preferentially in the Nucleus Accumbens of Freely Moving Rats. Neuroscience, 28, 653-661.

Cass, W.A., Gerhardt, G.A., Gillespie, K., Curella, P., Mayfield, R.D. & Zahniser, N.R. (1993) Reduced Clearance of Exogenous Dopamine in Rat Nucleus-Accumbens, but Not in Dorsal Striatum, Following Cocaine Challenge in Rats Withdrawn from Repeated Cocaine Administration. J Neurochem, 61, 273-283.

Cass, W.A., Gerhardt, G.A., Mayfield, R.D., Curella, P. & Zahniser, N.R. (1992) Differences in dopamine clearance and diffusion in rat striatum and nucleus accumbens following systemic cocaine administration. J. Neurochem., 59, 259-266.

Cass, W.A., Zahniser, N.R., Flach, K.A. & Gerhardt, G.A. (1993) Clearance of exogenous dopamine in rat dorsal striatum and nucleus accumbens: role of metabolism and effects of locally applied uptake inhibitors. J. Neurochem., 61, 2269-2278.

Castner, S.A., Xiao, L. & Becker, J.B. (1993) Sex differences in striatal dopamine:in vivo microdialysis and behavioral studies. Brain Research, 610 127-134.

Chadchankar, H. & Yavich, L. (2011) Sub-regional differences and mechanisms of the short-term plasticity of dopamine overflow in striatum in mice lacking alpha-synuclein. Brain Res., 1423, 67-76.

Chaurasia, C. S., Muller, M., Bashaw, E. D. et al. (2007) AAPS-FDA workshop white paper: Microdialysis principles, application, and regulatory perspectives. J Clin Pharmacol, 47, 589-603.

Chefer, V.I., Zapata, A., Shippenberg, T.S. & Bungay, P.M. (2006) Quantitative no-net-flux microdialysis permits detection of increases and decreases in dopamine uptake in mouse nucleus accumbens. J. Neurosci. Meth, 155, 187-193.

Church, W.H., Justice, J.B. & Byrd, L.D. (1987) Extracellular Dopamine in Rat Striatum Following Uptake Inhibition by Cocaine, Nomifensine and Benztropine. Eur J Pharmacol, 139, 345-348.

Clapp-Lilly, K.L., Roberts, R.C., Duffy, L.K., Irons, K.P., Hu, Y. & Drew, K.L. (1999) An ultrastructural analysis of tissue surrounding a microdialysis probe. J. Neurosci. Methods, 90, 129-142.

Cosford, R.J.O., Vinson, P., Kukoyi, S. & Justice, J.B.J. (1996) Quantitative microdialysis of serotonin and norepinephrine: Pharmacological influences on in vivo extraction fkaction. J. Neurosci. Meth., 68, 39-47.

Cragg, S.J. (2003) Variable dopamine release probability and short-term plasticity between functional domains of the primate striatum. J. Neurosci., 23, 4378-4385.

Cragg, S.J. & Rice, M.E. (2004) DAncing past the DAT at a DA synapse. Trends Neurosci, 27, 270-277.

Cragg, S.J., Hille, C.J. & Greenfield, S.A. (2000) Dopamine release and uptake dynamics within nonhuman primate striatum in vitro. J. Neurosci., 20, 8209-8217.

Dichiara, G. & Imperato, A. (1988) Drugs Abused by Humans Preferentially Increase Synaptic Dopamine Concentrations in the Mesolimbic System of Freely Moving Rats. P Natl Acad Sci USA, 85, 5274-5278.

Doya, K. (2000) Complementary roles of basal ganglia and cerebellum in learning and motor control. Curr. Opin. Neurobiol., 10, 732-739.

Dreier, J.P., Bhatia, R., Major, S., Drenckhahn, C., Lehmann, T.N., Sarrafzadeh, A., Willumsen, L., Hartings, J.A., Sakowitz, O.W., Seemann, J.H., Thieme, A., Lauritzen, M. & Strong, A.J. (2006) Delayed ischaemic neurological deficits after subarachnoid haemorrhage are associated with clusters of spreading depolarizations. Brain, 129, 3224-3237.

Dreier, J.P., Ebert, N., Priller, J., Megow, D., Lindauer, U., Klee, R., Reuter, U., Imai, Y., Einhaupl, K.M., Victorov, I. & Dirnagl, U. (2000) Products of hemolysis in the subarachnoid space inducing spreading ischemia in the cortex and focal necrosis in rats: a model for delayed ischemic neurological deficits after subarachnoid hemorrhage? J. Neurosurg., 93, 658-666.

Durieux, P.F., Schiffmann, S.N. & de Kerchove d'Exaerde, A. (2012) Differential regulation of motor control and response to dopaminergic drugs by D1R and D2R neurons in distinct dorsal striatum subregions. Embo J., 31, 640-653.

Einhorn, L.C., Johansen, P.A. & White, F.J. (1988) Electrophysiological Effects of Cocaine in the Mesoaccumbens Dopamine System - Studies in the Ventral Tegmental Area. J Neurosci, 8, 100-112.

Engstrom, R.C., Wightman, R.M. & Kristensen, E.W. (1988) Diffusional distortion in the monitoring of dynamic events. Anal. Chem., 60, 652-656.

Ewing, A.G., Bigelow, J.C. & Wightman, R.M. (1983) Direct in vivo monitoring of dopamine released from 2 striatal compartments in the rat. Science, 221, 169-171.

Fabricius, M., Fuhr S., Willumsen L., Dreier J.P., Bhatia R., Boutelle M.G., Hartings J.A., Bullock, R., Strong, A.J. & Lauritzen, M. (2008) Association of seizures with cortical

spreading depression and peri-infarct depolarisations in the acutely injured human brain. Clinical Neurophysiology, 119, 1973-1984.

Feuerstein, D., Manning, A., Hashemi, P., Bhatia, R., Fabricius, M., Ervine, M., Strong, A.J., & Boutelle, M.G. (2010) Dynamic metabolic response to multiple spreading depolarizations in patients with acute brain injury: an online microdialysis study. J. Cereb. Blood Flow and Metab., 30, 1343-1355.

Garris, P.A. & Wightman, R.M. (1994a) Different kinetics govern dopaminergic transmission in the amygdala, prefrontal cortex, and striatum - an in-vivo voltammetric study. J. Neurosci., 14, 442-450.

Garris, P.A. & Wightman, R.M. (1994b) In-Vivo Voltammetric Measurement of Evoked Extracellular Dopamine in the Rat Basolateral Amygdaloid Nucleus. J Physiol-London, 478, 239-249.

Garris, P.A. & Wightman, R.M. (1995) Regional differences in dopamine release, uptake, and diffusion measured by fast-scan cyclic voltammetry. In Boulton, A.A., Baker, G.B. & Adams, R.N. (eds) Voltammetric Methods in Brain Systems. Humana, Totowa, pp. 179-220.

Garris, P.A., Christensen, J.R., Rebec, G.V. & Wightman, R.M. (1997) Real-time measurement of electrically evoked extracellular dopamine in the striatum of freely moving rats. J. Neurochem., 68, 152-161.

Garris, P.A., Ciolkowski, E.L. & Wightman, R.M. (1994b) Heterogeneity of evoked dopamine overflow within the striatal and striatoamygdaloid regions. Neuroscience, 59, 417-427.

Garris, P.A., Ciolkowski, E.L., Pastore, P. & Wightman, R.M. (1994a) Efflux of dopamine from the synaptic cleft in the nucleus-accumbens of the rat-brain. J. Neurosci., 14, 6084-6093.

Goritz, C., Mauch, D.H., Nagler, K. & Pfrieger, F.W. (2002) Role of glia-derived cholesterol in synaptogenesis:new revelations in the synapse-glia affair. J. Physiology - Paris, 96, 257-263.

Gottwald, M.D. & Aminoff, M.J. (2011) Therapies for Dopaminergic-Induced Dyskinesias in Parkinson Disease. Ann Neurol, 69, 919-927.

Grace, A.A. (1991) Phasic Versus Tonic Dopamine Release and the Modulation of Dopamine System Responsivity - a Hypothesis for the Etiology of Schizophrenia. Neuroscience, 41, 1-24.

Grace, A.A. (2000) The tonic/phasic model of dopamine system regulation and its implications for understanding alcohol and psychostimulant craving. Addiction, 95, S119-S128.

Graybiel, A.M., Aosaki, T., Flaherty, A.W. & Kimura, M. (1994) The basal ganglia and adaptive motor control. Science, 265, 1826-1831.

Greco, P.G., Meisel, R.L., Heidenreich, B.A. and Garris, P.A. (2006) Voltammetric measurement of electrically evoked dopamine levels in the striatum of the anesthetized Syrian hamster. J Neurosci Meth, 152, 55-64.

Hascup, E.R., Bjerken, S., Hascup, K.N., Pomerleau, F., Huettl, P., Stromberg, I. & Gerhardt, G.A. (2009) Histological studies of the effects of chronic implantation of ceramic-based microelectrode arrays and microdialysis probes in rat prefrontal cortex. Brain Res., 1291, 12-20.

Hashemi, P., Bhatia, R., Nakamura, H., Dreier, J.P., Graf, R., Strong, A.J. & Boutelle, M.G. (2009) Persisting depletion of brain glucose following cortical spreading depression, despite apparent hyperaemia: evidence for risk of an adverse effect of Leao's spreading depression. J. Cereb. Blood Flow Metab., 29, 166-175.

Heien, M., Phillips, P.E., Stuber, G.D., Seipel, A.T. & Wightman, R.M. (2003) Overoxidation of carbon-fiber microelectrodes enhances dopamine adsorption and increases sensitivity. Analyst, 128, 1413-1419.

Hollander, J.A. & Carelli, R.M. (2007) Cocaine-associated stimuli increase cocaine seeking and activate accumbens core neurons after abstinence. J Neurosci, 27, 3535-3539.

Ikemoto, S. & Panksepp, J. (1999) The role of nucleus accumbens dopamine in motivated behavior: a unifying interpretation with special reference to reward-seeking. Brain Res. Brain Res. Rev., 31, 6-41.

Izenwasser, S., Werling, L.L. & Cox, B.M. (1990) Comparison of the Effects of Cocaine and Other Inhibitors of Dopamine Uptake in Rat Striatum, Nucleus-Accumbens, Olfactory Tubercle, and Medial Prefrontal Cortex. Brain Res, 520, 303-309.

Jaquins-Gerstl, A. & Michael, A.C. (2009) Comparison of the brain penetration injury associated with microdialysis and voltammetry. J. Neurosci Methods, 183, 127-135.

Jaquins-Gerstl, A., Shu, Z., Zhang, J., Liu, Y., Weber, S.G. & Michael, A.C. (2011) Effect of Dexamethasone on Gliosis, Ischemia, and Dopamine Extraction during Microdialysis Sampling in Brain Tissue. Anal. Chem., 83, 7662-7667.

Jenkinson, N. & Brown, P. (2011) New insights into the relationship between dopamine, beta oscillations and motor function. Trends Neurosci, 34, 611-618.

Johnson, P.M. & Kenny, P.J. (2010) Dopamine D2 receptors in addiction-like reward dysfunction and compulsive eating in obese rats. Nat Neurosci, 13, 635-U156.

Jones, S.R., Garris, P.A. & Wightman, R.M. (1995b) Different effects of cocaine and nomifensine on dopamine uptake in the caudate-putamen and nucleus accumbens. J Pharmacol Exp Ther, 274, 396-403.

Jones, S.R., Garris, P.A., Kilts, C.D. & Wightman, R.M. (1995a) Comparison of Dopamine Uptake in the Basolateral Amygdaloid Nucleus, Caudate-Putamen, and Nucleus-Accumbens of the Rat. J Neurochem, 64, 2581-2589.

Jung, M.C. & Weber, S.G. (2005) Influence of chemical kinetics on postcolumn reaction in a capillary Taylor reactor with catechol analytes and photoluminescence following electron transfer. Anal. Chem., 77, 974-982.

Justice, J.B., Jr. (1993) Quantitative microdialysis of neurotransmitters. J. Neurosci. Methods, 48, 263-276.

Kawagoe, K.T., Garris, P.A., Wiedemann, D.J. & Wightman, R.M. (1992) Regulation of transient dopamine concentration gradients in the microenvironment surrounding nerve terminals in the rat striatum. Neuroscience, 51, 55-64.

Kish, S.J., Shannak, K. & Hornykiewicz, O. (1988) Uneven pattern of dopamine loss in the striatum of patients with idiopathic Parkinson's disease. Pathophysiologic and clinical implications. N. Engl. J. Med., 318, 876-880.

Koob, G.F. & Bloom, F.E. (1988) Cellular and Molecular Mechanisms of Drug-Dependence. Science, 242, 715-723.

Koulchitsky, S., De Backer, B., Quertemont, E., Charlier C. & Seutin, C. (2012) Differential effects of cocaine on dopamine neuroon firing in awake and anesthetized rats. Neuropsycopharm, 37, 1559-1571.

Kuhar, M.J., Ritz, M.C. & Boja, J.W. (1991) The Dopamine Hypothesis of the Reinforcing Properties of Cocaine. Trends Neurosci, 14, 299-302.

Kuhr, W.G., Bigelow, J.C. & Wightman, R.M. (1986) In vivo comparison of the regulation of releasable dopamine in the caudate-nucleus and the nucleus-accumbens of the rat-brain. J. Neurosci., 6, 974-982.

Kuhr, W.G., Ewing, A.G., Caudill, W.L. & Wightman, R.M. (1984) Monitoring the stimulated release of dopamine with in vivo voltammetry .1. characterization of the response observed in the caudate-nucleus of the rat. J. Neurochem., 43, 560-569.

Kuhr, W.G., Wightman, R.M. & Rebec, G.V. (1987) Dopaminergic-Neurons - Simultaneous Measurements of Dopamine Release and Single-Unit Activity during Stimulation of the Medial Forebrain-Bundle. Brain Res, 418, 122-128.

Kulagina, N.V., Zigmond, M.J. & Michael, A.C. (2001) Glutamate regulates the spontaneous and evoked release of dopamine in the rat striatum. Neuroscience, 102, 121-128.

Laabs, T.L., Wang, H., Katagiri, Y., MaCann, T., Fawcett, J.W. & Geller, H.M. (2007) Inhibiting glycosaminoglycan chain polymerization decreases the inhibitory activity of astrocyte-derived chondroitin sulfate proteoglycans. J. Neurosci., 27, 14494-14501.

Liu, Y., Zhang, J., Xu, X., Zhao, M., Andrews, A.M. & Weber, S.G. (2010) Capillary Ultrahigh Performance Liquid Chromatography with Elevated Temperature for Sub-One Minute Separations of Basal Serotonin in Submicroliter Brain Microdialysate Samples. Anal. Chem., 82, 9611-9616.

Lotharius, J. & Brundin, P. (2002) Pathogenesis of Parkinson's disease: dopamine, vesicles and alpha-synuclein. Nat. Rev. Neurosci., 3, 932-942.

Marcus, H.J, Carpenter, K., Price, S.J., Hutchinson, P.J. (2010) In vivo assessment of high-grade glioma biochemistry using microdialysis: a study of energy-related molecules, growth factors and cytokines. J. Neurooncol., 97, 11-23.

Marshall, J.F., O'Dell, S.J., Navarrete, R. & Rosenstein A.J. (1990) Dopamine higg-affinity transport site topography in rat brain: major differences between dorsal and ventral striatum. Neuroscience., 37, 11-21.

May, L.J. & Wightman, R.M. (1989) Heterogeneity of stimulated dopamine overflow within rat striatum as observed with in vivo voltammetry. Brain Res., 487, 311-320.

Meixensberger, J., Kunze, E., Barcsay, E., Vaeth, A. & Roosen, K. (2001) Clinical cerebral microdialysis: brain metabolism and brain tissue oxygenation after acute brain injury. Neurol. Res., 23, 801-806.

Mercuri, N.B., Stratta, F., Calabresi, P. & Bernardi, G. (1991) Nomifensine but Not Amantadine Increases Dopamine-Induced Responses on Rat Substantia-Nigra Zona Compacta Neurons. Neurosci. Lett., 131, 145-148.

Michael, A.C., Borland, L.M., Mitala, J.J., Jr.,, Willoughby, B.M. & Motzko, C.M. (2005) Theory for the impact of basal turnover on dopamine clearance kinetics in the rat striatum after medial forebrain bundle stimulation and pressure ejection. J. Neurochem., 94, 1202-1211.

Michael, A.C., Ikeda, M. & Justice, J.B., Jr. (1987) Mechanisms contributing to the recovery of striatal releasable dopamine following MFB stimulation. Brain Res., 421, 325-335.

Mitala, C.M., Wang, Y., Borland, L.M., Jung, M., Shand, S., Watkins, S., Weber, S.G. & Michael, A.C. (2008) Impact of microdialysis probes on vasculature and dopamine in the rat striatum: a combined fluorescence and voltammetric study. J. Neurosci. Methods, 174, 177-185.

Moquin, K.F. & Michael, A.C. (2009) Tonic autoinhibition contributes to the heterogeneity of evoked dopamine release in the rat striatum. J. Neurochem., 110, 1491-1501.

Moquin, K.F. & Michael, A.C. (2011) An inverse correlation between the apparent rate of dopamine clearance and tonic autoinhibition in subdomains of the rat striatum: a possible role of transporter-mediated dopamine efflux. J. Neurochem., 117, 133-142.

Moss, J. & Bolam, J.P. (2008) A dopaminergic axon lattice in the striatum and its relationship with cortical and thalamic terminals. J. Neurosci., 28, 11221-11230.

Mou, X., Lennartz, M.R., Leoegering, D.J. & Stenken, J.A. (2011) Modulation of the forgein body reaction for implants in the subcutanteous space: microdialysis probes as localized drug delivery/sampling devices. J. diabetes science and technology, 5, 619-631.

Near, J.A., Bigelow, J.C. & Wightman, R.M. (1988) Comparison of uptake of dopamine in the rat striatal chooled tissue and synaptosomes. J. Pharmacol. Exp. Ther., 245, 921-927.

Nicholson, C. (1995) Interaction between diffusion and Michaelis-Menten uptake of dopamine after iontophoresis in striatum. Biophys. J., 68, 1699-1715.

Nicholson, C. & Sykova, E. (1998) Extracellular space structure revealed by diffusion analysis. Trends Neurosci., 21, 207-215.

Nordstrom, C.H. (2009) Cerebral energy metabolism and microdialysis in neurocritical care. Childs. Nerv. Syst., 26, 465-472.

O'Donnell, P. (2003) Dopamine gating of forebrain neural ensembles. Eur. J. Neurosci., 17, 429-435.

Pacak, K., Tjurmina, O., Palkovits, M., Goldstein, D.S., Koch, C.A., Hoff, T. & Chrousos, G.P. (2002) Chronic Hypercortisolemia Inhibits Dopamine Synthesis and Turnover in the Nucleus accumbens: An in vivo Microdialysis Study. Neuroendocrinology 76, 148-157.

Parkin, M.C., Hopwood, S.E., Jones, D.A., Hashemi, P., Landolt, H., Fabricius, M.F., Lauritizen, M., Boutelle, M.G. & Strong, A.J. (2005) Dynamic changes in brain glucose and lactate in pericontusional ares of the human cerebral cortex, monitored with rapid sampling on-line microdialysis: relationship with depolarization-like events. J. Cerebral Blood Flow and Metab., 25, 402-413.

Paxinos, G. & Watson, C. (1998) The rat brain in stereotaxic coordinates. Academic Press, San Diego.

Perez, X.A., Bressler, A.J. & Andrews, A.M. (2007) Determining serotonin and dopamine uptake rates in synaptosomes using high-speed chronoamperometry. In Michael, A.C. & Borland, L.M. (eds), Electrochemical Methods for Neuroscience, CRC Press Taylor and Francis Group, Boca Raton, pp 103-124.

Perry, M., Li, Q. & Kennedy, R.T. (2009) Review of recent advances in analytical techniques for the determination of neurotransmitters. Anal. Chim. Acta., 653, 1-22.

Peters, J.L. & Michael, A.C. (1998) Modeling voltammetry and microdialysis of striatal extracellular dopamine: the impact of dopamine uptake on extraction and recovery ratios. J. Neurochem., 70, 594-603.

Peters, J.L., Miner, L.H., Michael, A.C. & Sesack, S.R. (2004) Ultrastructure at carbon fiber microelectrode implantation sites after acute voltammetric measurements in the striatum of anesthetized rats. J. Neurosci. Methods, 137, 9-23.

Phillips, P.E., Stuber, G.D., Heien, M.L., Wightman, R.M. & Carelli, R.M. (2003) Subsecond dopamine release promotes cocaine seeking. Nature, 422, 614-618.

Porcerelli, J. H., Cogan, R., Markova, T., Miller, K. and Mickens, L. (2011) The Diagnostic and Statistical Manual of Mental Disorders, Fourth Edition Defensive Functioning Scale: a validity study. Compr Psychiat, 52, 225-230.

Rittenhouse, K.D. & Pollack, G., M. (2000) Microdialysis and drug delivery to the eye Advanced Drug Delivery Reviews 45, 229-241.

Robinson, D.L. & Wightman, R.M. (2004) Nomifensine amplifies subsecond dopamine signals in the ventral striatum of freely-moving rats. J. Neurochem., 90, 894-903.

Robinson, D.L., Heien, M. & Wightman, R.M. (2002) Frequency of dopamine concentration transients increases in dorsal and ventral striatum of male rats during introduction of conspecifics. J. Neurosci., 22, 10477-10486.

Sadri-Vakili, G., Johnson, D.W., Janis, G.C., Gibbs, T.T., Pierce, R.C. & Farb, D.H. (2003) Inhibition of NMDA-induced striatal dopamine release and behavioral activation by the neuroactive steroid 3alpha-hydroxy-5beta-pregnan-20-one hemisuccinate. . J. Neurochem., 86, 92-101.

Sagvolden, T., Johansen, E.B., Aase, H. & Russell, V.A. (2005) A dynamic developmental theory of attention-deficit/hyperactivity disorder (ADHD) predominantly hyperactive/impulsive and combined subtypes. Behav. Brain Sci., 28, 397-419; discussion 419-368.

Sakowitz, O.W. & Unterberg, A.W. (2006) Detecting and treating microvascualr ischemia after subarachnoid hemorrhage. Current Opinion in Critical Care, 12, 103-111.

Sakowitz, O.W., Sebastian, W., Sarrafzadeh, A.S., Stover, J.F., Drier, J.P., Dendorfer, A., Benndorf, G., Lanksch, W.R. & Unterberg, A.W. (2001) Relation of cerebral energy metabolism and extracellular nitrite and nitrate concentrations in patients after aneurismal subarachnoid hemorrhage. J. Cereb.Blood Flow and Metab. , 21, 1067-1076.

Sakowitz, O.W., Stover, J.F., Sarrafzadeh, A.S., Unterberg, A.W. & Kiening, K.L. (2007) Effects of mannitol bolus administration on intracranial pressure, cerebral extracellular metabolites, and tissue oxygenation in severely head-injured patients. J. Trauma, 62, 292-298.

Sarrafzadeh, A.S., Sakowitz, O.W., Kiening, K.L., Benndorf, G., Lanksch, W.R. & Unterberg, A.W. (2002) Bedside microdialysis: a tool to monitor cerebral metabolism in subarachnoid hemorrhage patients? Crit. Care Med., 30, 1062-1070.

Schlenk, F., Frieler, K., Nagel, A., Vajkoczy, P. & Sarrafzadeh, A.S. (2008) Cerebral microdialysis for detection of bacterial meningitis in aneurismal subarachnoid hemorrhage patients: a cohort study. Critical Care, 13, 1-9.

Schultz, W. (1982) Depletion of dopamine in the striatum as an experimental model of Parkinsonism: direct effects and adaptive mechanisms. Prog. Neurobiol., 18, 121-166.

Schultz, W. (1998) Predictive reward signal of dopamine neurons. J. Neurophysiol., 80, 1-27.

Schultz, W. (2007) Multiple dopamine functions at different time courses. Annu. Rev. Neurosci., 30, 259-288.

Sesack, S. R., Aoki, C. and Pickel, V. M. (1994) Ultrastructural-Localization of D-2 Receptor-Like Immunoreactivity in Midbrain Dopamine Neurons and Their Striatal Targets. Journal of Neuroscience, 14, 88-106.

Shain, W., Spataro, L., Dilgen, J., Haverstick, K., Retterer, S., Isaacson, M., Saltsman, M. & Turner, J.N. (2003) Controlling cellular reactive responses around neural prosthetic devices using peripheral and local intervention strategies. IEEE Transaction on Neural Systems and Rehabilitation Engineering, 11, 186-188.

Shu, Z., Taylor, I.M. & Michael, A.C. (2013) The dopamine patchwork of the rat nucleus accumbens core. Eur. J. Neurosci., 38, 3221-3229.

Shu, Z., Taylor, I.M., Walters, S.H., & Michael, A.C. (2014). Region- and domain-dependent action of nomifensine. Eur. J. Neurosci.,40, 2320-2328

Smith, A.D. & Justice, J.B.J. (1994) The effect of inhibition of synthesis, release, metabolism and uptake on the microdialysis extraction fraction of dopamine. J. Neurosci. Methods, 54, 75-82.

Spataro, L., Dilgen, J., Retterer, S., Spence, A.J., Isaacson, M., Turner, J.N. & Shain, W. (2005) Dexamethasone treatment reduces astroglia responses to inserted neuroprosthetic devices in rat neocortex. Exp. Neurol., 194, 289-300.

Stamford, J.A., Kruk, Z.L. & Millar, J. (1988) Stimulated Limbic and Striatal Dopamine Release Measured by Fast Cyclic Voltammetry - Anatomical, Electrochemical and Pharmacological Characterization. Brain Res., 454, 282-288.

Stroncek, J.D. & Reichert, W.M. (2008) Indwelling Neural Implants: Strategies for Contending with the In Vivo Environment. In Reichert, W.M. (ed) Overview of Wound Healing in Different Tissue Types. CRC Press, Boca Raton, FL.

Studer, A. & Schultz, W. (1987) The Catecholamine Uptake Inhibitor Nomifensine Depresses Impulse Activity of Dopamine Neurons in Mouse Substantia-Nigra. Neurosci Lett, 80, 207-212.

Swanson, J. M. (2000) Dopamine-transporter density in patients with ADHD. Lancet, 355, 1461-1461.

Sykova, E. & Nicholson, C. (2008) Diffusion in brain extracellular space. Physiol. Rev., 88, 1277-1340.

Taylor, I.M., Ilitchev, I. & Michael, A.C. (2013) Restricted diffusion of dopamine in the rat dorsal striatum. ACS Chem. Neurosci., 4, 870-878.

Taylor, I.M., Jaquins-Gerstl, A., Sesack, S.R. & Michael, A.C. (2012) Domain-dependent effects of DAT inhibition in the rat dorsal striatum. J. Neurochem., 122, 283-294.

Venton, B.J., Troyer, K.P. & Wightman, R.M. (2002) Response times of carbon fiber microelectrodes to dynamic changes in catecholamine concentration. Anal. Chem., 74, 539-546.

Venton, B.J., Zhang, H., Garris, P.A., Phillips, P.E., Sulzer, D. & Wightman, R.M. (2003) Real-time decoding of dopamine concentration changes in the caudate-putamen during tonic and phasic firing. J Neurochem, 87, 1284-1295.

Volkow, N.D., Wang, G.J., Newcorn, J.H., Kollins, S.H., Wigal, T.L., Telang, F., Fowler, J.S., Goldstein, R.Z., Klein, N., Logan, J., Wong, C. & Swanson, J.M. (2011) Motivation deficit in ADHD is associated with dysfunction of the dopamine reward pathway. Mol Psychiatr, 16, 1147-1154.

Volkow, N.D., Wang, G.J., Tomasi, D., Kollins, S.H., Wigal, T.L., Newcorn, J.H., Telang, F.W., Fowler, J.S., Logan, J., Wong, C.T. & Swanson, J.M. (2012) Methylphenidate-Elicited Dopamine Increases in Ventral Striatum Are Associated with Long-Term Symptom Improvement in Adults with Attention Deficit Hyperactivity Disorder. J Neurosci, 32, 841-849.

Walters, S.H., Taylor, I.M., Shu, Z., & Michael, A.C. (2014) A Novel Restricted Diffusion Model of Evoked Dopamine. ACS Chem. Neurosci.

Wang, Y., Moquin, K.F. & Michael, A.C. (2010) Evidence for coupling between steady-state and dynamic extracellular dopamine concentrations in the rat striatum. J. Neurochem., 114, 150-159.

Wender, P. H., Reimherr, F. W., Marchant, B. K., Sanford, M. E., Czajkowski, L. A. and Tomb, D. A. (2011) A One Year Trial of Methylphenidate in the Treatment of ADHD. J Atten Disord, 15, 36-45.

Westerink, B.H. & Cremers, T.I.F.H. (eds) (2007) Handbook of Microdilaysis: Methods, Applications and Perspectivies. Academic Press, London.

Wightman, R.M. and Wipf, D.O. (1988) Ultrafast Cyclic Voltammetry. J. Electrochem. Soc., 135, C152-C152.

Wightman, R.M., Amatore, C., Engstrom, R.C., Hale, P.D., Kristensen, E.W., Kuhr, W.G. & May, L.J. (1988a) Real-Time Characterization of Dopamine Overflow and Uptake in the Rat Striatum. Neuroscience, 25, 513-523.

Wightman, R.M., Heien, M., Wassum, K.M. (2007) Dopamine release is heterogeneous within microenvironments of the rat nucleus accumbens. Eur. J. Neurosci., 26, 2046-2054.

Wightman, R.M., May, L.J. and Michael, A.C. (1988b) Detection of Dopamine Dynamics in the Brain. Anal Chem, 60, A769-A779.

Wise, R.A. (2004) Dopamine, learning and motivation. Nat. Rev. Neurosci., 5, 483-494.

Wu, Q., Reith, M.E., Kuhar, M.J., Carroll, F.I. & Garris, P.A. (2001a) Preferential increases in nucleus accumbens dopamine after systemic cocaine administration are caused by unique characteristics of dopamine neurotransmission. J. Neurosci., 21, 6338-6347.

Wu, Q., Reith, M.E., Walker, Q.D., Kuhn, C.M., Carroll, F.I. & Garris, P.A. (2002) Concurrent autoreceptor-mediated control of dopamine release and uptake during neurotransmission: An in vivo voltammetric study. J. Neurosci., 22, 6272-6281.

Wu, Q., Reith, M.E., Wightman, R.M., Kawagoe, K.T. & Garris, P.A. (2001b) Determination of release and uptake parameters from electrically evoked dopamine dynamics measured by real-time voltammetry. J. Neurosci. Methods, 112, 119-133.

Yang, H., Peters, J.L. & Michael, A.C. (1998) Coupled effects of mass transfer and uptake kinetics on in vivo microdialysis of dopamine. J. Neurochem., 71, 684-692.

Zachek, M.K., Takmakov, P., Park, J., Wightman, R.M. & McCarty, G.S. (2010) Simultaneous monitoring of dopamine concentration at spatially different brain locations in vivo. Biosens. Bioelectron., 25, 1179-1185.

Zhong, Y. & Bellamkonda, R.V. (2007) Dexamethasone-coated neural probes elicit attenuated inflammatory response and neuronal loss compared to uncoated neural probes. Brain Res., 1148, 15-27.

Zhou, F., Braddock, J.F., Hu, Y., Zhu, X., Castellani, R.J., Smith, M.A. & Drew, K.L. (2002) Microbial origin of glutamate, hibernation and tissue trauma: an in vivo microdialysis study. J. Neurosci. Methods, 119, 121-128.